Inaugural dissertation

for

obtaining the doctoral degree

of the

Combined Faculty of Mathematics, Engineering and Natural Sciences

of the

Ruprecht - Karls - University

Heidelberg

Presented by

Ali Haider Utsho (M.Sc. Biosciences)

Born in Pabna, Bangladesh

Date of Oral Examination: 05.07.2022

Depletion of Insulin Receptors leads to Metabolic alteration and Microvascular complications in zebrafish

Referees:

Prof. Dr. Marc Freichel

Prof. Dr. Jens Kroll

Hiermit erkläre ich an Eides statt, dass ich die vorliegende Arbeit ohne unzulässige Hilfe Dritter und nur unter Verwendung der angegebenen Quellen und Hilfsmittel verfasst habe. Jegliche Ausführungen, die wörtlich oder sinngemäß übernommen wurden, sind als solche kenntlich gemacht. Ich habe diese Arbeit bisher an keinem anderen in- oder ausländischen Naturwissenschaftlich-Mathematischen Fachbereich als Prüfungsarbeit verwendet oder als Dissertation eingereicht.

Kaiserslautern, den 18.03.2022

Ali Haider Utsho

To Baba and Ma

This one for you two

Acknowledgment

This Ph.D. thesis is the output of the effort and support of several people to whom I am extremely grateful. In the beginning, I would say thanks to my supervisor Prof. Dr. Jens Kroll to guide me well throughout the research work from the title's selection to finding the results. Conducting this study on a difficult topic couldn't be as simple as he made this for me. He has been my mentor and a better advisor for my doctorate study beyond the imagination.

I would like to bid my special thanks to Prof. Dr. Marc Freichel who accepted to be my supervisor and to Prof. Jan-Luuk Hillebrands and Prof. Dr. Harry Van Goor from Groningen for their continued support. Thank you Prof. Karen Bieback, who was always helpful. I want to specially mention and thank Dr. Sidney Cambridge, for being such a nice mentor and encouraging me in doing science. I would like to mention Dr. Thomas Fleming for the help with experiments and Dr. Gernot Poschet for the metabolomics measurements. One person has been influential and inspiring, thank you Prof. Hans-Peter Hammes for being such a guide. I would like to add the whole DIAMICOM graduate program for providing us with such an amazing opportunity to work on interesting topics.

Elisabeth and Felix, we shared some good times in the lab. Sara and Dajana, it was also nice to start sharing the fly lab. Katrin Bennewitz, Lucas Wiggenhauser, Lisa Walter, Bowen Lou, Xiaogang Li, David Wohlfart, Nitin Patil and everyone else from our institute, Thank you all. Thanks to Christoph Tabler for performing the EM imaging for this project and Prof. Dr. Harry Van Goor from UMCG for the help in staining the kidneys and Dr. Sandra Cramer-Stoll for generating mutants.

I would also like to thank Agnese Fiori, you have been a good friend be it about DIAMICOM or light talk, and those Groningen days were awesome. Tariqul, thanks for your motivation while writing. T., Po, Baki, Gul thanks man for being there in the biochemistry department and see, it's already been 15 years since we started studying biology.

Special thanks to my wife Shazia who has always been supportive no matter what I do. The inspiration she has provided has been tremendously helpful, without those I do not think I could carry on. I would like to thank my younger sister Orchi, for all those light and funny talks and have faith in me.

Two persons have shaped my life, my father and my mother. No thanks would be enough for you two. All I try is to make you two proud. I know you have never lost faith in me, no matter what condition I have been through. I dedicate my thesis to you two.

I. Contents

Summary

Diabetes is a major metabolic disorder and type 2 diabetes (T2D) is the most prevalent form of diabetes where insulin resistance serves as the reason for hyperglycemia. Insulin receptors are a crucial part of the insulin signaling pathway that mediates glucose uptake in skeletal muscles and adipose tissues as well as in other organs. Insulin signaling promotes glycogen and protein synthesis, cell growth, inhibits apoptosis through several downstream pathways. Different aspects of Insulin receptor depletion have been conducted in mice and zebrafish yet the implication with microvascular complications in zebrafish has not been carried out. Thus, this study was directed towards finding the abnormalities caused by insulin receptor knockout in zebrafish.

My study was conducted in zebrafish where I have taken advantage of zebrafish as a model organism and the availability of *Tg(fli1:EGFP)* and *Tg(wt1b:EGFP)* transgenic zebrafish. Zebrafish depleted of Insulin receptors (insulin receptor a: *insra*$^{-/-}$ and insulin receptor b: *insrb*$^{-/-}$) were generated using CRISPR/Cas9 gene-editing technology and then I characterized the morphology of the mutants during the early and adult stages. I have found that the larvae showed no hyperglycemia, however, overfeeding can lead to fasting high glucose in *insra*$^{-/-}$ fish. I also observed that while trunk vasculature is affected only in *insra*$^{-/-}$ larvae, retinal hyaloid vasculature is affected in both *insra*$^{-/-}$ and *insrb*$^{-/-}$ larvae. Furthermore, abnormalities in retinal vasculature were also found in over-fed *insra*$^{-/-}$ fish and in normal-fed *insrb*$^{-/-}$ fish. I have observed metabolic shift in those mutants as saturated & unsaturated fatty acids and cholesterol increased in *insra*$^{-/-}$ and *insrb*$^{-/-}$ larvae. Also in adult fish, we found a higher amount of fatty acids in skeletal muscle.

Altogether, the data acquired from this study show that despite maintaining a euglycemic state, microvascular complications can arise when insulin receptors are knocked out in zebrafish. Therefore it can be said that high glucose is not the only factor behind the development of microvascular complications in zebrafish.

Zusammenfassung

Diabetes ist eine wichtige metabolische Krankheit und Typ-2-Diabetes (T2D) ist die häufigste Form von Diabetes, bei welcher Insulinresistenz der Grund für Hyperglykämie ist. Insulin-Rezeptoren (Insr) spielen eine entscheidende Rolle im Insulin-Signalweg, welcher die Glukoseaufnahme in die Skelettmuskulatur, das Fettgewebe und in andere Organe steuert. Der Insulin-Signalweg fördert die Glykogen- und Proteinsynthese, das Zellwachstum und hemmt die Apoptose durch mehrere nachgeschaltete Signalwege. Verschiedene Aspekte der Insr-Depletion wurden bei Mäusen und Zebrafischen untersucht, aber die Wirkung der Insr-Depletion auf mikrovaskuläre Komplikationen wurde bis dato noch nicht erforscht. Daher lag das Hauptaugenmerk dieser Arbeit auf der Entdeckung dieser Anomalien.

Der Stellenwert von Zebrafischen als Modellorganismus und die Verfügbarkeit von *Tg(fli1:EGFP)* und *Tg(wt1b:EGFP)* transgenen Zebrafischen machten ihn zu einem geeigneten Forschungsobjekt für meine Arbeit. Der Zebrafisch hat zwei Insr (*insra* und *insrb*), von denen mit Hilfe der CRISPR/Cas9 Methode Deletionsmutanten (*insra*$^{-/-}$ und *insrb*$^{-/-}$) generiert wurden. Anschließend habe ich die Morphologie der *insr*-Mutanten im Larven- und Erwachsenenstadium untersucht. Dabei fand ich heraus, dass die Larven zwar keine Hyperglykämie zeigten, die nüchternen *insra*$^{-/-}$ Zebrafische, welche vorher über einen Zeitraum von acht Wochen überfüttert wurden, allerdings einen hohen Glukosespiegel hatten. Desweiteren konnte ich beobachten, dass während die Rumpfblutgefäße nur bei *insra*$^{-/-}$ Larven betroffen waren, die Hyloidblutgefäße in beiden Mutanten betroffen waren. Außerdem konnte ich Anomalien in den Retinablutgefäßen bei überfütterten *insra*$^{-/-}$ und normal gefütterten *insrb*$^{-/-}$ Erwachsenentieren feststellen. Neben den bereits erwähnten Veränderungen konnte ich eine erhöhte Konzentration von Fettsäuren (gesättigte und ungesättigte) und Cholesterin in den Larven beider Mutanten nachweisen. In adulten Tieren konnte ich stattdessen nur eine erhöhte Fettsäurekonzentration in der Skelettmuskulatur beobachten.

Insgesamt zeigen die aus dieser Studie gewonnenen Daten, dass in Zebrafischen selbst bei einem normalen Glukosespiegel mikrovaskuläre Komplikationen auftreten können, wenn die Insulinrezeptoren deletiert sind. Schlussfolgernd kann gesagt werden, dass ein hoher Glukosespiegel nicht der einzige Faktor für die Entstehung von mikrovaskulären Komplikationen in Zebrafisch ist.

1. Introduction

1.1 Diabetes mellitus

Diabetes Mellitus (DM) is a major metabolic disorder, and it is growing at an alarming rate worldwide. Currently, half a billion (463 million) people are suffering from it. In the last two decades, the number of patients suffering from Diabetes among 20-79 years old adults has risen from 151 million in 2000 to 463 million in 2019. Along with this, it is projected that in 2030, there will be 578 million and in 2045 there will be 700 million patients suffering from Diabetes around the world. These numbers are higher than projected earlier as in 2009 it was projected that within 2030, we would see 438 million diabetic people. This number indicates that right now 8.3% of the world population is suffering, while in 2045, we would find almost 1 in every 10 people a diabetic (Fig 1.1) (IDF, 2019).

Diabetes is a chronic metabolic disorder that is characterized by a raised blood glucose level as a result of low insulin production or reduced insulin sensitivity. Majorly Diabetes can be classified into three types. Type 1 Diabetes (T1D), Type 2 Diabetes (T2D), and Gestational Diabetes (GD). American diabetes association categorizes Neonatal Diabetes, disease of the exocrine pancreas, and drug or chemical induced diabetes as the 4th type of diabetes (ADA; Diabetes Care, 2020:43). There are other types of classification such as (maturity-onset diabetes in the young (MODY), latent autoimmune diabetes in adults (LADA), Ketosis-prone diabetes in adults (IDF, 2019; Tuomi *et al*. 2014).

T1D which is often called insulin-dependent diabetes or juvenile-onset diabetes occurs when pancreatic beta-cells (β-cells) are destroyed by the cellular-mediated autoimmune response. T1D patients make up around 5-10% of all patients with diabetes. T1D is also referred to as early-onset diabetes as per traditional classification but up to 50% of cases are seen during adulthood (Thomas *et al.* 2018). Half the number of T1D are misdiagnosed as T2D in adults (Hope *et al*. 2016). Genetic predisposition influences the risk of getting T1D but many environmental or behavioral factors such as diet, early-life exposure to viruses associated with islet inflammation (eg, enteroviruses), decreased gut-microbiome diversity, and vitamin-D insufficiency can also increase the probability (Rewers *et al.* 2016).

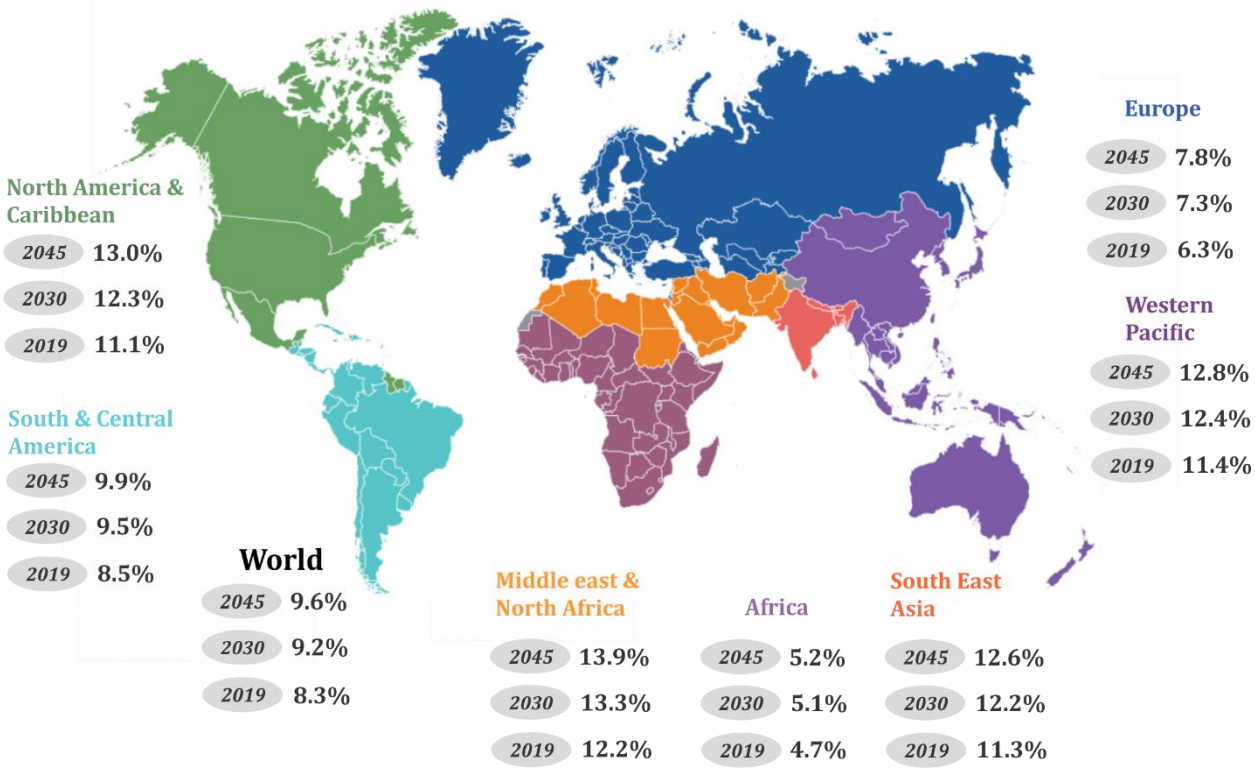

Fig 1.1: Diabetes Mellitus: an ever-growing threat. The figure shows the percentage of the population (20-79 years old adults) suffering from DM and the projected percentage in the year 2030 and 2045 in different demographic regions. The figure was taken and modified from IDF Atlas 9th edition. International Diabetes Federation (IDF). International Diabetes Federation. IDF Diabetes Atlas, 9th edition. Brussels, Belgium: 2019. Available at: https://www.diabetesatlas.org.

Contrary to T1D, T2D is characterized by insulin resistance in organs and is also termed idiopathic hyperglycemia (Chatterjee, Khunti, & Davies, 2017, Gale E. 2013). T2D was previously called noninsulin-dependent diabetes mellitus (NIDDM) or adult-onset diabetes. It occurs due to insulin insensitivity or insulin resistance in the muscle cells, adipose tissues, and hepatocytes (Artunc *et al*., 2016) and is seen in 90-95% of diabetic patients. Obesity has been a major contributing factor behind insulin resistance, insulin signaling pathway in key insulin-sensitive organs can be changed due to obesity-related accumulation of ectopic fat (Petersen *et al*. 2007). In addition to that, age, lack of physical exercise, and genetic predisposition in presence of the history of diabetes in first-degree relatives might be factors for T2D too (Chatterjee *et al*., 2017).

Gestational diabetes is seen during pregnancy but is resolved after the birth of the child. There are two reasons for Gestational diabetes which include insulin resistance caused by tumor necrosis factor-alpha (TNF-α) or human placental lactogen and lower insulin secretion (Thomas and Philipson, 2015). Mutation in genes necessary for β-cell development, regulation, or function or in the insulin gene can cause MODY.

Apart from the traditional classification of 3 types of diabetes as well as other specific types of diabetes, a new classification based on six variables was proposed by Ahlqvist and her colleagues. The six variables are insulin resistance, BMI, age at diagnosis, HbA1c values, glutamate decarboxylase antibodies, and homoeostatic model assessment 2 estimates of β-cell function. According to this classification, diabetes patients are clustered into five groups. The first cluster labeled as severe autoimmune diabetes (SAID) takes up 6.4% of all patients. The second cluster consists of 17.5% of all diabetes patients are named severe insulin-deficient diabetes (SIDD). 15.3% of the diabetes patients fall into the third cluster labeled as severe insulin resistant diabetes (SIRD). Cluster 4 is categorized as mild obesity related diabetes (MOD) includes 21.6% of all patients. The 5th cluster is labeled as mild age related diabetes (MARD) and 39.1% of patients fall in this cluster (Ahlqvist *et al*. 2018). Furthermore, this new classification based on multiple criteria rather than just the glucose values would eventually help diagnose diabetes and treat it properly.

1.2 Diabetic complications

The detection of diabetes in a patient is clinically identified by the presence of hyperglycemia and it can be detected by measurement of glucose (fasting and postprandial) directly in blood or the value of HbA1c. While severe acute metabolic complications like ketoacidosis occur because of extreme hyperglycemia or coma as a result of hypoglycemia, long-term hyperglycemia leads to vascular and nervous system dysfunction (Fig 1.2).

Diabetic complications can be distinguished into two segments, macrovascular and microvascular. Macrovascular complications include cardiovascular disease, ischemic stroke, and peripheral arterial diseases. Nephropathy or kidney diseases, retinopathy or eye diseases, and neuropathy or neural damages are considered microvascular complications.

Here, despite being physiologically not responsive to insulin, sensory neurons and endothelial cells are damaged by hyperglycemia like insulin-responsive cells such as macrophages, podocytes, or Schwann cells. (Filla & Edwards, 2016; Forbes & Cooper, 2013). Although, T1D and T2D both have one common symptom that is hyperglycemia, when it comes to diabetic complications, the underlying mechanisms in the development of complications are sometimes different in T1D and T2D patients (Wolf *et al*. 2007).

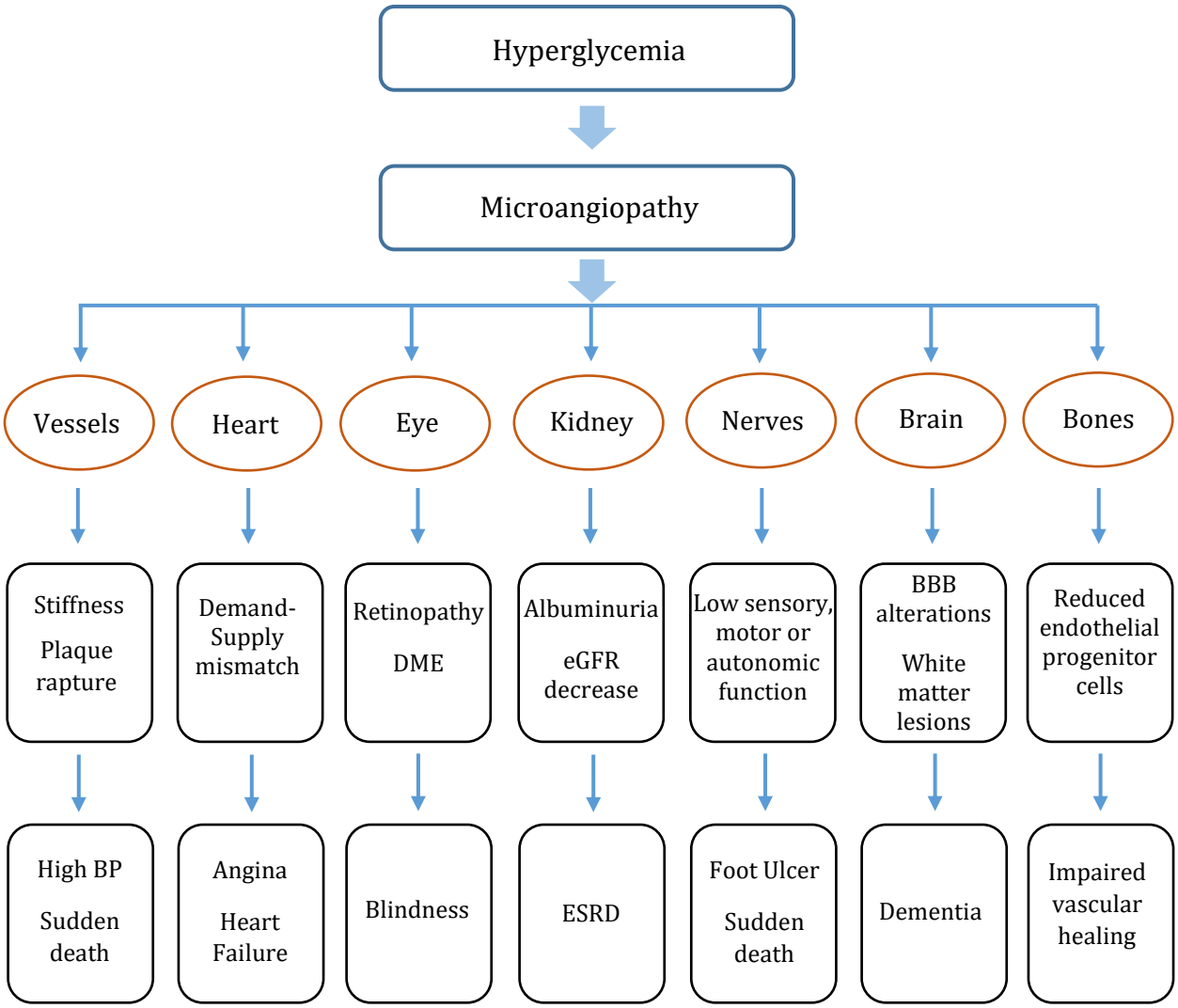

Fig 1.2: Systemic consequences of microvascular diseases caused by diabetes. DME = Diabetic Macular Edema, eGFR = estimated glomerular filtration rate, BP = blood pressure, BBB = blood-brain barrier, ESRD = end-stage renal disease. The figure is taken and modified with the permission from the publisher. Avogaro & Fadini, 2019; https://doi.org/10.1016/j.ijcard.2019.02.030.

Diabetic nephropathy

Diabetic nephropathy (DN) is the major reason for end-stage renal failure and affects almost 30% of all patients with diabetes at any stage of life. The term DN is now replaced as Diabetic kidney disease (DKD) according to the new guidelines and terminology (National Kidney Foundation, 2007, Mora-Fernández *et al*., 2014). DKD is also a major risk factor for the development of macrovascular complications (Chronic Kidney Disease Prognosis Consortium, 2010). Patients who have hypertension and poor control over blood glucose are seen to be mostly affected by DKD but a group of patients also develop nephropathy despite normal blood pressure and good glycemic control. Genetic predisposition plays a role in getting DKD as prevalence among African Americans, Asians and Native Americans are higher (US renal data system: USRDS 2003, Young BA *et al*. 2003).

DKD is characterized by several changes in renal structure and functions. Mesangial expansion in glomeruli, the basement membrane is thickened, nodular glomerulosclerosis is seen in DKD patients (Lim, 2014, Dronavalli *et al.* 2008). Development of proteinuria and glomerular hyperfiltration is seen during the early stage of DN but is followed by a progressive decline of glomerular filtration rate (GFR) which is the best marker of renal function (Currie, 2014). If persistent albumin excretion is higher than 200µg/min in at least two from three consecutive urine collections, it is clinically considered as DKD when the patient does not have any other type of kidney or renal tract disease (Hovind *et al*., 2001). Serum creatinine is the most common index for assessment of GFR but sensitivity is not very high (Currie *et al*., 2014). Five steps have been identified in diabetic nephropathy: those start with glomerular hyperfiltration > the silent stage > incipient nephropathy > overt nephropathy > end-stage renal disease. These stages are classified based on urinary albumin excretion and glomerular filtration rate (Gnudi, Coward, & Long, 2016).

Adequate control of metabolic and hemodynamic abnormalities is the first and foremost step in treating DKD or delaying the progression of DKD. Metabolic control includes glycemic and hypertension control. Several drugs like rosiglitazone with metformin or SGLT-2 inhibitor like empagliflozin have been proven effective in glycemic control leading to reduce disease

progression (Zhang *et al*. 2008, Chua & Bakris, 2006). Metformin is effective in reducing glucose levels in T2D patients and has nephroprotective effects too (Salpeter *et al.* 2008, Eisenreich & Leppert. 2017, Kawanami, Takashi, & Tanabe, 2020). Metformin reduces glucose levels in T2D patients by multiple mechanisms such as reducing gluconeogenesis, improving the function of glucagon-like peptide-1, increasing glucose uptake in muscle and liver, and reducing the function of glucagon (Pernicova & Korbonits, 2014). Sodium-Glucose Co-Transporter 2 (SGLT-2) is found in the renal proximal tubule and is a high capacity, low-affinity transporter. It is one of the two co-transporters (SGLT-1 and SGLT-2) with the function to reabsorb glucose in the kidney and is responsible for 90% of the glucose reabsorption. Blocking of SGLT-2 decreases glucose reabsorption thus increasing urinary excretion of glucose resulting in lower plasma glucose. Supporting the theory, the clinical trial also shows that SGLT-2 is effective in reducing disease progression (Weir. 2016, Wanner C *et al*. 2016, Toto. 2017). Angiotensin receptor blockers, aldosterone antagonists, calcium channel blockers, hypertensive drugs like angiotensin-converting enzyme (ACE) inhibitors also have been effective to various degrees in reducing the progress of diabetic kidney disease (Jorge L. Gross *et al*. 2005, Lewis *et al*. 2001, Brenner *et al*. 2001, Schojedt *et al*. 2005, Rossing *et al*. 2005, Lim, 2014).

Diabetic Retinopathy

Another common complication of diabetes where plasma glucose is closely related to its onset and progression is diabetic retinopathy (DR). Early clinical features of DR are intraretinal microvascular anomalies, dot and blot hemorrhages, microaneurysms, cotton wool spots (Lois *et al*. 2014), changes in vascular permeability, capillary degeneration, and neovascularization is often seen. The major risk factors for this disease are the duration of diabetes, elevated levels of hemoglobin HbA_{1c}, poor glycemic control, blood pressure, high lipid profile (Yau *et al*. 2012). DR is another comorbidity most apparent in patients suffering from DKD. The prevalence of DR is many-fold higher among T2D patients with albuminuria compared to diabetic patients without renal issues (Drury *et al*. 2011; Groop *et al*. 2009).

Diabetic retinopathy is sometimes considered a late-onset complication for diabetes as the loss of vision or impaired vision is generally diagnosed in the later stage. DR takes a long time to develop as most T2D patients and almost all T1D patients have retinal lesions after 20 years of diabetes (Hirai *et al*. 2011, Kempen *et al*. 2004). Clinically DR can be distinguished into two stages. Non-proliferative diabetic retinopathy (NPDR) is the early stage of DR where capillary occlusion and vascular permeability are observed in the retinal vasculature. During this stage, most people do not notice any visual impairment. But proliferative diabetic retinopathy (PDR) is the more advanced stage of DR, and the main pathogenesis is the neovascularization in the retina. T2D patients often suffer from diabetic macula edema (DME) which is one of the most common reasons for vision loss and occurs when the blood-retinal barrier is broken, and the macula is swelled or thickened because of sub- and intra-retinal accumulation of fluid (Romero-Aroca *et al*. 2016). 6% of the T2D patients suffer from diabetic maculopathy and symptoms include disorder in color sensing, difficulties with reading, floaters in front of the eye, etc (Hammes, Lemmen, & Bertram, 2020).

Hyperglycemia initiates several chains of functions which causes the development of DR therefore strong control over blood glucose reduces the possibility of getting retinopathy as it does with nephropathy. Control over blood pressure is also particularly important as hypertension increases blood flow and mechanical damage of vascular endothelial cells or stimulates the release of vascular endothelial growth factors (Klein R 2008, Suzuma *et al*. 2001, Cheung, Mitchell, & Wong, 2010). Benfotiamine which is a lipid soluble thiamine derivative has also been seen to block the pathways behind the damage caused by hyperglycemia and prevent the development of experimental diabetic retinopathy (Hammes et al., 2003). Lipid-lowering drugs have been effective in T2D patients in reducing the risk of retinopathy despite no measurable change in lipid profile (Cheung and Wong, 2008). In addition to these physiological controls, treatment like Laser photocoagulation, Vitrectomy, anti-VEGF agents, cataract surgery as well as intraocular administration of corticosteroid has also been used against DME and DR (Cheung et al., 2010; Heng et al., 2013, Kim *et al*. 2007, Yilmaz *et al*. 2009, Aiello *et al*. 2005).

Diabetic Neuropathy

Alongside nephropathy and retinopathy, patients with diabetes suffer from another microvascular complication, diabetic neuropathy which affects both the somatic and autonomic divisions of the peripheral nervous system (Forbes & Cooper, 2013). Neuropathy can be a major factor behind erectile dysfunction, impaired wound healing, and cardiovascular dysfunction in diabetic patients. More than 50% of diabetic patients eventually have neuropathy at some time in their life and the lifetime risk of foot lesions such as gangrene lies at 15% to 25% (Avogaro & Fadini, 2019). DN can be distinguished, depending on their anatomical distribution such as proximal or distal, symmetric or asymmetric. It can also be divided according to the clinical course like acute or chronic and based on characteristics like hypersensitive or hyposensitive. The most common form of DN is the chronic distal symmetrical polyneuropathy (DSP) which is seen for almost 75% of DN patients (Albers & Pop-Busui, 2014, Bansal *et al*. 2006). Diagnosis of DSP requires testing of signs like symmetric decrease of distal sensation, burning or aching pain, asleep numbness or unequivocally abnormal ankle reflexes, and abnormal nerve conduction study (Tesfaye *et al*. 2010). Several other types of subacute onset neuropathies are also identified. Those are diabetic radiculoplexus neuropathy, acute painful small fiber neuropathy, diabetic focal peripheral neuropathies, chronic inflammatory demyelinating polyradiculoneuropathy, etc. (Chan *et al*. 2012, Tesfaye and Kempler. 2005, Sinnreich *et al*. 2005).

Like other microvascular complications, prevention and treatment of diabetic neuropathy depend heavily on glycemic control and lifestyle interventions (Kluding *et al*. 2012, Albers *et al*. 2010). Some treatments like acetylcarnitine, recombinant nerve growth factors, α-lipoic acid, actovegin have also been effective (Ziegler D. 2008, Ziegler et al. 2009, Sima *et al*. 2005, Ziegler *et al*. 2011).

Cardiovascular disease

Cardiovascular disease (CVD) is considered a macrovascular complication whose onset and progression are determined by combined negative effects of several risk factors. The reason behind the death of 52% of T2D patients and the death of 44% of T1D patients is CVD (Morrish *et al*. 2001, Huang *et al*. 2017) and patients who have no prior history of myocardial

infarction (MI) has 20.2% chance of getting another MI while compared to them, non-diabetic patients has only 3.5%. The risk of ischemic and hemorrhagic stroke is respectively 2.3 and 1.6 times higher in diabetic patients compared to non-diabetic ones as well as the risk of death and functional dependency. (Sarwar *et al*. 2010, Jia *et al*. 2011, O'Donnell *et al*. 2010). In addition to that, CVD is also enlisted as a comorbidity with DKD and DR as CKD influences cardiovascular outcome through calcium/phosphate abnormalities, sodium overload, uremic toxins, and vascular abnormalities (Di Lullo *et al*. 2015, Duh *et al*. 1999).

Among diabetes patients, CVD comprehends a large series of diseases such as peripheral arterial disease, coronary artery disease, ischemic stroke, premature atherosclerosis, and impaired cardiac function. Like other microvascular complications, glycemic control is the center of the treatments against macrovascular complications. Anti-platelet agents such as aspirin, lipid-lowering drugs with statins and fibrates, anti-hypertensive agents, glucagon-like peptide-1 receptor agonist, metformin, sulfonylurea have been used to treat or reduce risks of CVD in patients with diabetes (Forbes and Cooper. 2013, Holman *et al*. 2008, Muskiet *et al*. 2018). SGLT-2 inhibitors, which have been very effective in treating T2D and DKD patients have also been effective in reducing all-cause mortality by 32% in cardiovascular patients (Cowie & Fisher, 2020; Verma & McMurray, 2018). Among several proposed mechanism, SGLT-2 exert the action via inhibiting the Na+/H+ exchanger (NHE-1) in the myocardium, increasing the activation of M2 macrophages and inhibiting myofibroblast differentiation which results in antifibrotic effects, improving the ventricular loading conditions, are notable (Lee, Chang, & Lin, 2017; Uthman et al., 2018; Verma & McMurray, 2018).

1.3 Pathophysiology of Diabetic complication

Hyperglycemia is central to the complications of diabetes and there are several factors alongside hyperglycemia that plays the role. Patients often suffer from late-onset diseases despite maintaining the proper glycemic level. Several factors such as hemodynamic, metabolic, growth factors, inflammation, cell signaling, and transcription factors contribute to the development of a complication. Hemodynamic factors include activation of the renin-

angiotensin system or high levels of endothelin-I and urotensin-II (Huang *et al*. 2001, Rudberg *et al*. 2000). Multiple metabolic pathways such as the polyol pathway, advanced glycation end-products accumulation, hexosamine pathway, protein kinase C pathways are implicated in hyperglycemia-induced vascular damage (Brownlee, 2005).

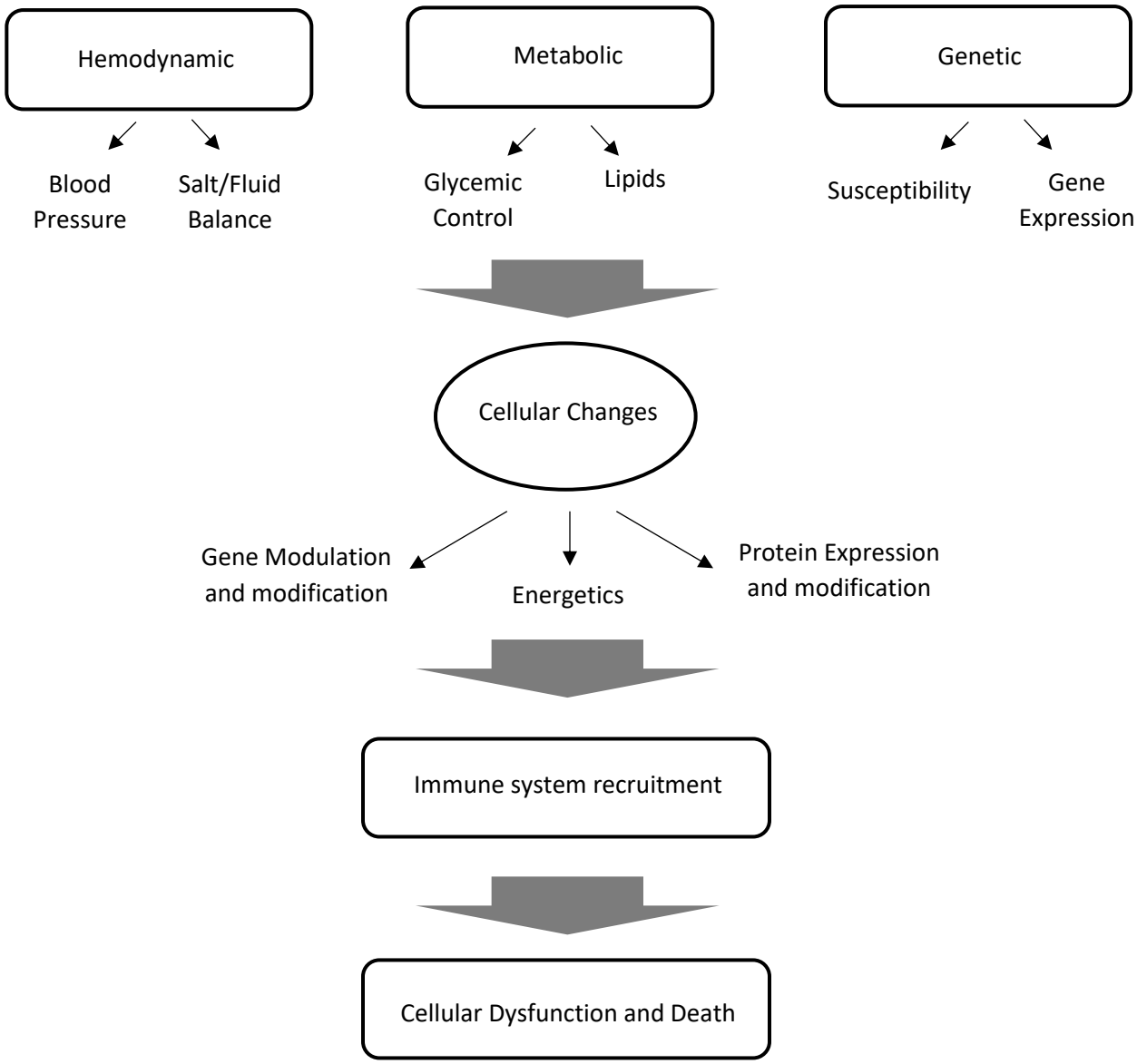

Fig 1.3: Overview of major areas responsible for the diabetes-mediated complication. Hemodynamic, metabolic, and genetic factors are responsible for cellular changes which in turn leads to complications seen in diabetes patients. The scheme was taken and modified with the permission from the publisher. Forbes & Cooper, 2013; doi:10.1152/physrev.00045.2011.

Sorbitol/Polyol pathway is one of the several pathways involved in microvascular complications. Aldose reductase is an enzyme that detoxifies aldehyde into inert alcohols, specifically converting glucose to sorbitol. During high glucose, aldose reductase uses the necessary co-factor NAD(P)H thus reducing the extent of antioxidant functions by reducing glutathione peroxidase activity. Accumulation of sorbitol in the cell is also detrimental because it can damage proteins through oxidations (Chung *et al*., 2003; Filla & Edwards, 2016).

Hyperglycemia can also cause damage through the production of reactive oxygen species (ROS). Mitochondrial oxidative phosphorylation leads to the generation of free radicals which are then neutralized by intracellular enzymes. Within mitochondria, 90% of oxygen is metabolized while sometimes 1% oxygen is reduced to O_2^-. In the case of hyperglycemia, mitochondria are affected and excess production of O_2^-leads to the production of H_2O_2 which is very detrimental to the cells. But higher glucose flux leads to higher ROS which in turn damages cellular proteins, mitochondrial DNA, reduces nitric oxide generation (Nishikawa *et al*. 2000, Fong, 2004, Lum and Roebuck. 2001, Sheetz & King, 2002).

The formation of reactive metabolites can damage intracellular components and can activate pathogenic pathways. The advanced glycation end products (AGE) are one of such compounds. The amount of AGEs is higher In diabetic renal glomeruli and retinal vessels (Brownlee, 2001). The damage is done by the AGE precursors by the following three mechanisms. First, extracellular matrix components are modified by AGE precursors that do not interact with other matrix components normally. Secondly, plasma proteins are modified by AGE precursors. Third, intracellular proteins are modified too. AGEs can also activate the nuclear factor-kappa B which can modify gene expressions (Brownlee, 2001, 2005; Giacco & Brownlee, 2010; Sheetz & King, 2002). Glyoxal, methylglyoxal (MG), and 3-deoxyglucosone are 3 molecules produced from glucose that forms AGEs by reacting with amino groups of cells. Glyoxal is formed from auto-oxidation of glucose, 3-deoxyglucosone is produced by the decomposition of amadori products and MG is produced from the fragmentation of glyceraldehyde-3-phosphate and dihydroxyacetone phosphate during glycolysis (Brownlee, 2001; Kristina Jörgens *et al*., 2015). Out of these three reactive metabolites, MG is the most reactive and can induce posttranslational modification of proteins by interacting with side

chains of amino acids such as arginine, lysine, and cysteine (Malmberg *et al*., 2005). MG has recently gained interest from diabetes researchers because of its specific involvement in retinopathy (Hammes, 2018) as well as can also contribute to the development of cardiovascular complications (Rabbani N *et al*., 2011, Wang X *et al*., 2005, Guo Q *et al*., 2009). MG generated from high glucose also modifies the VEGF signaling cascade pathway to alter small blood vessels (Jörgens *et al*., 2015). Moreover, MG can induce insulin resistance and glucose intolerance which can eventually lead to microvascular complications (Lodd *et al*., 2019).

Activation of protein kinase C (PKC) and hexosamine pathway by hyperglycemia is also involved in diabetes mediated complications. PKC can decrease the production of nitric oxides or induce expression of vascular endothelial growth factor (VEGF) which eventually lead to microvascular complications (Giacco & Brownlee, 2010).

Heritability of diabetic complications is a big factor in determining the susceptibility for instance susceptibility to DKD has a familial basis. Diabetic siblings with kidney disease possess three times the risk of DKD when compared to siblings of no kidney disease patients (Brownlee, 2001, Reidy *et al.* 2014). Ethnicity plays a big role too in determining the risk. It has also been reported that the risk of diabetic nephropathy is higher among African-Americans, Asians, and Native Americans (US renal data system: USRDS 2003, Young BA *et al*. 2003). In the case of CVD, 40-50% of indicators of atherosclerosis can be attributed to familial factors among individuals with diabetes (Langle *et al*, 2002). 25 to 50% of retinopathy cases among diabetic patients can be related to heritability (Arar *et al*, 2008, Hietala *et al*, 2008).

1.4 Insulin receptors and insulin signaling

Cells need glucose for energy generation and the glucose uptake mechanism varies depending on cell types. It can be insulin-independent that does not require any action of insulin or insulin-dependent where glucose update is mediated by complex pathways where glucose transporters (GLUT) take part. Insulin, an anabolic hormone one of the most potent hormones is needed for growth, tissue development, and glucose homeostasis. It is produced

in the β cells of the pancreas and produced as preproinsulin which is made up of proinsulin and a 24 amino acid peptide in the cytosol. This preproinsulin is then translocated into the endoplasmic reticulum where signal peptidase cleaves it and produces proinsulin with 9.4 KDa molecular weight. Insulin comes from this proinsulin peptide upon processing in the ER and the Golgi bodies (S. Liu et al., 2019; Mario, Thomas, & Wilhelm, 2010). The action of insulin is initiated after binding to the insulin receptor (IR) which consists of two α and two β subunits. These two subunits are linked by a disulfide bond and create an $\alpha_2\beta_2$ heterotetrameric complex. Insulin binds to the extracellular α subunit that eventually activates the tyrosine kinase domain of the β subunit by transmitting a signal across the plasma membrane.

Insulin signaling is very crucial for metabolic function which involves insulin, insulin related growth factors 1 and 2 (igf1 and igf2) as well as the receptors: IR, igf1 receptor, igf2 receptor, and IR like receptor (Saltiel and Kahn. 2001, Kitamura *et al*. 2003). Upon binding of the insulin to the cognate IRs on the cell surface, receptors are autophosphorylated, and their tyrosine kinase activities are increased. This leads the activated insulin to react with IR substrate 1 & 2 (IRS-1 & IRS-2) that influence the phosphatidylinositol-3 Kinase (PI3K) to convert phosphatidylinositol 3, 4 bisphosphate (PIP_2) to phosphatidylinositol 3, 4, 5 triphosphate (PIP3) (Kadowaki *et al*. 2012, Kadowaki *et al*. 2012). After the conversion of PIP_2 to PIP_3 serine threonine kinases phosphoinositide-dependent protein kinase 1 (PDPK1) and Akt1/ Akt2 binds to PIP_3 by their PH domains. This PDPK1 phosphorylates the Threonine at the 308 position in Akt and activates the Akt. Phosphorylation and activation of the Akt then mediate the vesicles containing Glucose transporter 4 (GLUT4) to be translocated to the plasma membrane, as a result, glucose is transported inside the cell (Pessin and Saltiel. 2000, Riehle and Abel. 2016). There are 13 different GLUT encoded in human that catalyzes glucose transportation. Those are named as GLUT 1-12 and HMIT (Joost & Thorens, 2009; Wood & Trayhurn, 2003). GLUT4 is highly expressed in skeletal muscle & adipose tissue and contributes significantly to glucose transportation. During an unstimulated state, GLUT4 is usually deposited in the intracellular region but in response to insulin stimulation, they are redistributed to the plasma membrane (Bryant *et al*. 2002,

Czech and Corvera, 1999). This transportation process is categorized as ATP-independent and facilitative diffusion mechanisms (Hruz and Mueckler, 2001).

Insulin signaling is very important not just for cellular glucose uptake, insulin signaling leads to various functions to be carried out by AKT (also known as protein kinase B) mediated phosphorylation (Riehle and Abel. 2014). Phosphorylation of B-cell leukemia/lymphoma 2 (BCL 2) inhibits apoptosis of cells, tuberous sclerosis complex (TSC) 1 or 2 phosphorylation increases mRNA translation and protein synthesis as well as promotes cell growth and mitochondrial fusion by activating mechanistic target of Rapamycin (mTOR) (Cho *et al*. 2001, DeBosch *et al*. 2006, Wullschleger *et al*. 2006). Phosphorylation of glycogen synthase kinase promotes glycogen synthesis and endothelial nitric oxide synthase induces vasodilation by increasing nitric oxide synthesis. Fatty acid translocase CD36 is also mediated by Akt. Extracellular regulated kinase 1/2 is also activated by the insulin signaling pathway to increase the expression of several genes. Insulin also activates mitogen activated protein (MAP) kinase which results in nuclear translocation of kinase and phosphorylation of transcription factors leading to cellular differentiation and proliferation (Kim *et al.* 2002, Saltiel & Kahn, 2012). All those pathways are activated by insulin signaling either through activation of Akt or independent of Akt activation.

As insulin signaling plays role in a variety of cellular functions, the depletion of insulin signaling has several detrimental effects on the physiology of the animals. As noted before, insulin resistance is the underlying reason for T2D, and diagnosis of diabetes has been done based on the level of glucose in the blood or the A1C criteria. The resistance against insulin is also called resistance syndrome or syndrome X. Humans who lack Insulin receptors suffer from intrauterine growth retardation, fasting hypoglycemia, postprandial hyperglycemia (Biddinger and Kahn, 2006; Taylor and Arioglu, 1999, Jospe *et al.* 1996, Krook *et al*. 1993). In 1993, Wertheimer and his colleagues reported an infant who had a homozygous deletion of the insulin receptor gene which resulted in the disease of Leprechaunism or Donohue syndrome. The same disease was reported by Rojek *et al.* in 2021 about an infant suffering from insulin resistance. in both cases, the infant was suffering from growth retardation and several physiological abnormalities (Rojek, *et al*., 2021).

The research on insulin resistance animals has started long before through the generation of insulin receptor knockout animals. *insr* knockout mice are born without any metabolic defects and look normal when compared to their littermates (~10% smaller) but glucose levels rise up to 1000 fold above normal after feeding, then die within 48-72 hours because of ketoacidosis (Kitamura, Kahn, & Accili, 2003b; L.Joshi et al., 1996). Tissue-specific *insr* KO mice have been generated using Cre-Lox technology and showed varied physiological conditions. Hepatocyte-specific insulin receptor knockout or Liver insulin receptor knockout (LIRCO) mice exhibit mild hyperglycemia in the fasting state and strong hyperglycemia in the postprandial state by the age of two months. Muscle insulin receptor knockout (MIRCO) mice were generated using the same technology with a different promoter which results in deletion of >90% of the insulin receptor in skeletal muscles and heart. These mice do not have hyperglycemia as well as hyperinsulinemia and show no abnormal response to glucose tolerance test. Interestingly these mice have high-fat content in the body. Adipocyte or fat cells specific knockout (FIRCO) have slightly improved lipid and glucose homeostasis. They have unaltered fasting and postprandial glycemic levels as well as no hyperinsulinemia (Bluher M *et al*., 2002). Local Insulin action on β-cell is very important for the survival of β-cell (Kitamotoa *et al*., 2017; Rhodes *et al*., 2013). B-cell specific insulin receptor knockout mice (βIRCO) show abnormal response when glucose tolerance test is performed at the age of two months. In the basal state, the highest glucose utilization is done in the brain but most of the glucose uptake into the brain is not mediated through insulin. Despite this fact, female neuron-specific insulin receptor knockout (NIRCO) mice show increased food intake rate, higher body weight, and double fat pad weight. Interestingly, male NIRCO mice exhibit different properties compared to their female counterpart in these three aspects (Biddinger & Kahn, 2006). These data suggest that action of insulin varies from organ to organ and the depletion of insulin receptors can be severely detrimental for animals.

1.5 Zebrafish as a model in diabetes research

Zebrafish (*Danio rerio*), a freshwater teleost fish commonly found in south Asian tropical water is a model organism extensively used in biological and medical research since the 1960s (B. E. Drummond & Wingert, 2016; Phillips & Westerfield, 2014). Zebrafish have been used as a model in developmental biology for a longer period, however, the resemblance of

several disease phenotypes and the emergence of new tools has also made it an attractive model for disease research (Lieschke & Currie, 2007; Morales & Wingert, 2017).

The Zebrafish genome has similarities with the human genome as 69% of the genes in the zebrafish genome have at least one ortholog from humans which provides advantages in gene function research (Howe *et al*., 2013). Temporary reverse genetics approach such as using anti-sense morpholino oligos which blocks the complementary RNA sequence and creates a transient knockdown of genes has been used to investigate the loss of function studies for orthologous genes (Heckler & Kroll, 2017; Lieschke & Currie, 2007; Peng, 2019). In addition to transient knockdown, using permanent mutagenesis techniques such as TALEN and CRISPR-Cas has given a wide idea about the gene functions and genetic background of diseases (P. Huang, Zhu, Lin, & Zhang, 2012; Hwang et al., 2013; Peng, 2019).

Zebrafish offers several benefits as a model organism such as cheap and easy maintenance, ease of genome editing, the possibility of keeping transparent for a few days which makes screening easier, short generation time, etc. Zebrafish embryos can develop functional early-stage organs within 48 hours of fertilization which gives an advantage in screening. Many transgenic lines of zebrafish are available and organs can be tagged with fluorescent proteins facilitating organ detection and monitoring (Kimmel *et al*., 1995). These properties make zebrafish a very convenient and good model for disease research (Heckler & Kroll, 2017; K Jörgens & Kroll, 2012; Morales & Wingert, 2017).

Zebrafish is an excellent model also for obesity, diabetes, and metabolic disease research (Seth, Stemple, & Barroso, 2013; Zang, Maddison, & Chen, 2018) as well as microvascular complications research. Exposure to high glucose such as incubation in glucose solution has traditionally been used as a method to induce hyperglycemia in zebrafish embryos. For experimental purposes, incubation in other metabolites has been used as well. Incubation of zebrafish embryos in glucose and MG solution led to increased hyperbranching in zebrafish embryos (Kristina Jörgens *et al*., 2015). Repeated incubation in glucose during the early stage can also create a thickening of retinal hyaloid vessels (Jung, Kim, Lee, & Kim, 2016) and high patterning in zebrafish embryos which can also be carried in adult stages (Singh *et al*., 2019).

Although incubation is an easy method to check the effect of hyperglycemia on zebrafish embryos, transient knockdown using morpholino provides an advantage over incubation. Injection of *insra* and *insrb* morpholinos have been shown to increase the whole body glucose of zebrafish embryos (Qi *et al*., 2021). Transient knockdown of *pdx1* can lead to hyperglycemia in the zebrafish embryo and hyperglycemia induced kidney morphology alteration can be seen in those *pdx1* devoid zebrafish embryos (Sharma *et al*. 2016). Knockout of *pdx1* can create hyperglycemia too in zebrafish and initiate retinal angiogenesis which can be used for hyperglycemia induced retinopathy research (Wiggenhauser *et al.,* 2020). Loss of glyoxalase1 (*glo1*) enzyme in zebrafish can lead to postprandial high blood glucose and upon overfeeding, can create fasting high glucose level (Lodd *et al.*, 2019). Mutation in Leptin receptors can lead to altered glucose tolerance in adult zebrafish (Michel *et al*. 2016).

Like mammals, zebrafish also have an insulin and insulin receptor mediated glucose transport system, and insulin mediated signaling activates several downstream physiological pathways (Caruso & Sheridan, 2011). However, unlike mammals, zebrafish have two insulin genes and two insulin receptors (Papasani *et al*. 2006). *insra* and *insrb* are implicated in zebrafish embryogenesis, blood glucose homeostasis, and nutrient metabolism. Knockdown of insulin receptors affects embryogenesis while depletion of insulin receptors leads to β-cell hyperplasia. The *insra*$^{-/-}$ and *insrb*$^{-/-}$ embryos have high glucose content in the whole body as well as downregulation of rate-limiting enzymes for glycolysis. But the enzymes involved in gluconeogenesis are upregulated only in *insra*$^{-/-}$ but not in *insrb*$^{-/-}$ (Gong *et al.*, 2018; Toyoshima *et al*., 2008). Aberration in nutrient metabolism is also seen in insulin receptor knockout zebrafish (B. Y. Yang *et al*., 2018). These data on *insra*$^{-/-}$ and *insrb*$^{-/-}$ shows that the roles of *insra* and *insrb* in blood glucose homeostasis and physiology in zebrafish are not the same. the primary act of Insra is to promote lipid synthesis whereas Insrb is more likely to promote protein synthesis and lipid catabolism. All these data show that zebrafish is an excellent model in diabetes and metabolism research. In this thesis, the name of the genes is written in small letters and italic fonts while the name of the proteins is written as the standard font with the first letter as capital.

1.6 Aim of the thesis

This research work was aimed at observing the pathological and metabolic effect of insr knockout in zebrafish. Previously *insra*$^{-/-}$ and *insrb*$^{-/-}$ mutants have been generated, physiological roles in glucose homeostasis and nutrient metabolism have been reported but microvascular complications have not been examined yet. With the availability of transgenic lines of zebrafish, I have analyzed how the loss of Insr affects vascular formation, kidney functions, and metabolic pathways. Using my study on zebrafish, I have tried to answer the following questions.

1. does the loss of IRs lead to any vascular malformation in zebrafish during the developmental stage? Is there any difference in effects between the trunk and retinal vasculature?

2. how does the depletion of IR affect the kidney in early stage and adult stage zebrafish? is there any effect on the function of the kidney of adult zebrafish too?

3. insulin signaling is central to various metabolic pathways in the cell. How does the knockout of *insr* affect or alter the metabolic pathways? How does the effect vary during the early and adult stage? What are the effects on different organs in zebrafish?

4. while looking at the above objectives, I also investigated: is there any difference between the two insulin receptors? If there is any, what are the differences that arise by the loss of specific insulin receptors?

2. Materials and methods

2.1 Materials

2.1.1 Chemicals

Unless specifically indicated, all chemicals used during the experiments were purchased from the following companies:

AppliChem GmbH

Carl Roth GmbH&Co.KG

Merck KGaA

Polysciences Europe GmbH

Roche Diagnostics GmbH

SERVA Electrophoresis GmbH

Sigma Aldrich Chemie GmbH

Thermo Fisher Scientific Inc.

AbCam PLC.

2.1.2 Animals

2.1.2.1 Zebrafish lines

All experimental procedures on animals were approved by the local government authority, Regierungspräsidium Karlsruhe (license no.: 35-9185.81/G-98/15) and carried out following the approved guidelines. Embryos of the lines *Tg(fli1:EGFP)* (Lawson and Weinstein, 2002) and *Tg(wt1b:EGFP)* (Perner *et* al., 2007) were utilized during this study for zebrafish (*Danio rerio*) experiments.

2.1.3 Equipment

Agarose gel chamber: Peqlab Biotechnologie GmbH

Bench top centrifuge: Rotina 420R Hettich

BioPhotometer 6131: Eppendorf

BioPhotometer D30: Eppendorf

Electronic balance: Kern & Sohn GmbH

Heating/Shaking block: HLC

Light Cycler 480: Roche/ Thermo Fisher Scientific Inc.

Microcentrifuge Mikro 200R: Hettich

Micropipette Puller: Sutter instruments Co.

NanoDrop ND-8000: Peqlab Biotechnologie GmbH

PCR cycler: BioRad

Ph-meter ProfiLine 197i: WTW

Pneumatic PicoPump PV 820: WPI

Protein gel electrophoresis system: BioRad

Table centrifuge: Carl Roth GmbH

Water Bath: Seelbach

Western Blot detection: Peqlab Biotechnologie GmbH

Western Blot system BioRad/Peqlab Biotechnologie GmbH

UV transilluminator: INTAS GmbH

2.1.4 Consumables

0.22 µm syringe filter: Millex

AceGlow chemiluminescence: Peqlab

Conical tubes (15 ml, 50 ml): Falcon (BD)

Dumont Tweezers No. 5: NeoLabs

Electrophoresis power supply: Consort

FACS tubes: Falcon (BD)

Filters (30 µm): Partec Cell Trics

Needle: 20G x 1 ½" nr.1: BD Microlance/ 30G x 1½

Nitrile Gloves: Semperguard
Nitrocellulose membrane 0.22 µm: Whatman
PCR tubes (0.2 ml): Star Labs
Petri dishes (10cm and quadratic): Greiner bio one
Pipettes (P1000, P200, P20 and P2): Gilson
Pipette tip refills (1000, 200, 10 µl): TipOne Star Labs
Pipette filter tips (1000, 100, 20 and 10 µl): Nerbe plus GmbH
Quantitative PCR 96-well reaction plate: Axon
Syringes (1 ml, 30 ml): BD Plastipak
Syringes for homogenization: Becton Dickinson
Tissue culture plate, 6 well: Becton Dickinson Labware; Falcon
Whatman filter paper: Sigma Aldrich

2.1.5 Buffers and solutions

2.1.5.1 Gel electrophoresis

Agarose gel sample laoding buffer:
10 mM Tris-HCl (pH 7.6)
0.03% bromophenol blue,
0.03% xylene cyanol FF,
60% glycerol
60 mM EDTA

TAE Buffer (50X)
Tris 242 g
Disodium EDTA 18.61 g
Glacial Acetic Acid 57.1 ml
DDI H_2O to 1 l

TAE buffer (1X)
20mL 50X TAE Buffer
980mL Distill H_2O

2.1.5.2 Western blotting

Electrophoresis/Running Buffer (10X)

Tris base	30.3 g
Glycine	144.4 g
SDS	10 g
ddH_2O	1L

Blotting/Transfer Buffer

Tris	30.28 g
Glycine	106.6
ddH_2O	10L

5X Laemmli Buffer

1.5M Tris/HCl, pH 6.8	8.34 ml
SDS	5 g
Bromophenol blue	0.25 g
Glycerol	5 ml
DTT	3.45 g
ddH_2O	50 ml

NP40 lysis buffer 0.87 g NaCl

1 M Tris/HCl, pH 7.4	5 ml
0.5 M Na2EDTA, pH 8	1.8 ml
Proteinase inhibitor cocktail	1 bottle
10% Nonidet P40 solution	10 ml
Glycerin	10 ml
ddH_2O	100 ml

10X PBS

$Na_2HPO4 \cdot 7H_2O$	25.6 g

NaCl	80 g
KCl	2 g
KH_2PO_4	2 g
ddH_20	1L

PBST	
TweenT20	500µL
ddH_20	1L

2.1.5.3 Solutions for Zebrafish

Eggwater	
Red sea Salt	3g
ddH_2O	
	3L

PTU (1-phenyl-2-thiourea) 10x stock	
PTU	608g
ddH_2O	1L

Tricaine" for anesthetization 10X	
3-amino benzoic acidethylester	2g
Tris base (pH 9)	20mL
ddH_2O	1L

2.1.5.3 antibodies

Primary antibodies

Antibody	Source	company	Dilution
Anti-Actin (I-19)	Goat	Santa Cruz Biotehnology	1:1000

Anti Insra/b	Rabbit	GeneTex Ltd	1:500

Secondary antibodies

Antibody	Source	company	Dilution
Rabbit anti goat HRP	Rabbit	DAKO	1:2000
Goat anti Rabbit HRP	Goat	Dako	1:2000

2.1.5.4 Kits

Name	Function	Producer
Illustra plasmidPrep mini spin Kit	Plasmid DNA extraction	GE Healthcare
MiRNeasy Mini Kit	RNA extraction and purificaton	Qiagen
mMessage machine Kit	In vitro RNA transcription	Invitrogen
QIAQuick PCR purification kit	PCR purification	Qiagen
RNeasy Mini Kit	RNA extraction and purification	Qiagen
SP6 mMessage mMachine Kit	In vitro RNA transcription	Ambion
SuperScript™- First Strand Kit	cDNA synthesis	Invitrogen
T7 MEGAshortscript Kit	In vitro RNA transcription	Ambion

2.1.5.5 Oligonucleotide

All oligonucleotide used during the project was purchased from and supplied by SigmaAldrich.

2.1.5.6 Oligos used for cloning in plasmid

Insra_CRISPR1_Fwd: TAGGTTGGGGAACAGGTCACTG

Insra_CRISPR1_Rev: AAACCAGTGACCTGTTCCCCAA

Insrb_CRISPR3_Fwd: TAGGAGTTGACGGTGGTGTATC

Insrb_CRISPR3_Rev: AAACGATACACCACCGTCAACT

2.1.5.7 Oligos used for genotyping zebrafishes

Insra_CRISPR1_gen_for: CTGCACTGTTATCGAAGGCC

Insra_CRISPR1_gen_rev: GCTGAAGTCGCCGTTGATAG

Insrb_CRISPR3_gen_for: CTGCCGCAACTTCCTGTAC

Insrb_CRISPR3_gen_rev: TAAACCTCACTCCCATCCCG

2.1.5.8 Oligos used for qPCR analysis

Insra_for_1: agaggccagcgagctctac

Insra_rev_1: cacttgtgtgggggctct

Insrb_for_1: gcctctgcggatcactacat

Insrb_rev_1: ctcctgcgtggtcttgaac

β-actin_for_1: ACGGTCAGGTCATCACCATC

β-actin_rev_1: TGGATACCGCAAGATTCCAT

2.1.5.9 DNA and protein markers

Name	Producer
Generuler DNA ladder Mix	Thermofischer Scientific
PageRuler Plus Prestained Protein Ladder	Thermofischer Scientific

2.1.6.0 Plasmids

Name	Source
pUC19	Addgene
pT3TS	Addgene

2.2 Method

2.2.1 Experiments with animals

2.2.1.1 Zebrafish maintenance

Zebrafish lines were raised and kept under standard animal husbandry conditions at the zebrafish lab in the CBTM, Mannheim. The protocol described in (Kimmel *et al.,* 1995) has been followed. Fishes were mated for fertilized eggs on special separate boxes. The next morning they were allowed to mate and the eggs were collected on Petri dishes. The eggs were washed and kept in an incubator at 28.5°C with or without.003% 1-phenyl-2-thiourea (PTU) to suppress pigmentation.

2.2.1.2 Determination of glucose at the larval stage

Glucose concentration was measured with the zebrafish larvae at 96 hpf. For this, zebrafish larvae were at first anesthetized using .003% Tricaine and ~50 larvae were collected in a 1.5mL microcentrifuge tube. Embryos were lysed in Sodium Phosphate buffer (100mM; 0.1% Triton X) and sonicated 20 times each time 30 sec. Samples were centrifuged at 4°C with a rotation speed of 14000 rpm for 5 minutes. The supernatant was collected and de-proteinated. Later on, glucose measurement was performed with Amplex™ Red Glucose/Glucose oxidase Assay Kit. Supplied protocol by the manufacturer was followed for the procedure. These experiments were done with the help of Dr. Thomas Fleming.

2.2.1.3 Blood Glucose measurement

Blood glucose level was measured using Accu-Check blood glucose monitor. For this measurement, the fish were anesthetized in tricaine solution for 1 minute. After that, the fish were taken under binos and a previously prepared apparatus with a glass needle was inserted into the anterior artery of the zebrafish (Zang *et al,* 2013). 2/3 drops of blood are then sucked out and put on the strip of the glucose monitor.

2.2.1.4 Generation of mutants

Using CRISPR/Cas technology, Dr. Sandra Cramer-Stoll has generated *insra* and *insrb* mutants. With this method, a gRNA targeting the gene (separate for *insra*/*insrb* in this case) along with mRNA for translation of Cas9 endonuclease was injected into the fertilized egg of zebrafish at the single cell stage. The gRNA leads the Cas9 endonuclease to break the double strand at a desired specific sequence in the genome, finally, the repair system tries to repair the breakage but during the process, some unwanted change like insertion or deletion is added. If the insertion or deletion is not equal to 3 or multiplier of 3 bases, it leads to premature stop codon thus generating mutated genetic sequence. The CRISPR gRNA was designed using the sequence available for *insra* and *insrb* genes on ensemble [http://www.ensembl.org/index.html] (*insra*: ENSDART00000008302.6 and *insrb*: ENSDART00000105823.6). The gRNA was injected at a single-cell stage to get F0 generation. Confirmed F0 generation carrying the mutation was then backcrossed with wild type to get heterozygous F1 which then was intercrossed to get homozygous F2 generation. In this study, 0-72 hours post fertilization (hpf) old zebrafish are considered as the embryo and 4dpf-1month old are as larvae (Parichy *et al*., 2009).

2.2.1.5 Overfeeding of Zebrafish

Wild type and mutant fishes were overfed while keeping them in specific boxes. Fish were separated by genotype and kept in two boxes for each genotype. The overfeeding protocol was run for 8 weeks. The protocol was designed according to Oka *et al*., 2010.

Normal Feeding: for normal feeding, each fish was fed with 5mg of hatched artemia in the morning and once dry flakes in the afternoon.

Overfeeding: each fish was fed with artemia 3 times and a total of 60mg of artemia and once dry food in the afternoon per day. For artemia, 2 hours gap was maintained between each feeds.

2.2.1.6 Imaging with bright field and fluorescence microscope

Images of zebrafish larvae and isolated organs were taken using an inverted microscope (Leica DMI 6000B with Leica DFC420 C and Leica LAS application suite 3.58 software).
Imaging of fluorescent larvae, the vasculature of transgenic line Tg*(fli1:EGFP)* larvae was taken using an inverted microscope (Leica DMI 6000B) fitted with Leica DFC420C camera.
Images of pronephros from Tg*(wt1b: EGFP*) were taken using Leica MZ10F microscope fitted with Leica DFC420C camera.

2.2.1.7 Imaging with Confocal microscopes

Images of the larval and adult retina, as well as vasculature of Tg(*fli1:EGFP*), were taken using a Leica TCS SP5 confocal microscope system. Images were taken at a 600Hz scanner while excited with a 488nm laser.

2.2.1.8 Quantification of vasculature in zebrafish larvae

Zebrafish have been established as an excellent model for vasculature and angiogenesis analysis because trunk axial vessel formation in different developing vertebrates is resembled by zebrafish vasculogenesis. The development of vasculature starts at a very early stage. In zebrafish, vascular endothelial cells arise from angioblasts from the lateral mesoderm.
These endothelial cells get specified when the gastrulation comes to an end which is approximately 10 hours post fertilization (Reischauer S *et al*, 2016; Stainier DY *et al*, 1995). A known endothelial cell marker in mouse friend leukemia integration 1 written as *fli1* (Melet *et al*, 1996; Lawson and Weinstein, 2002, Gore *et al*, 2012) which is also expressed during vascular development in zebrafish embryos can work as a promoter for *EGFP* in zebrafish: As a result, the whole vasculature can be seen in the transgenic zebrafish Tg(*fli1:EGFP*) during early stages (until 5 days post fertilization and kept transparent using PTU) when illuminated. The zebrafish larvae were anesthetized in 0.003% tricaine and then mounted in 2.5% agarose gel in a glass ring on a cover slip. After that, they were taken under a confocal microscope or fluorescent microscope, and the intersegmental vessel (ISV) numbers 5 to 22 are analyzed. The number of changes in the ISV and the DLAV is counted.

2.2.2 Biochemical experiments

2.2.2.1 Cloning of CRISPR oligos into plasmid

For CRISPR mediated gene knockout, a gRNA targeting the gene along with Cas9 endonuclease mRNA were injected into the fertilized egg of zebrafish at the single-cell stage. The gRNA leads the Cas9 endonuclease to break the double strand at a desired specific sequence in the genome, finally, the repair system tries to repair the breakage but during the process, some unwanted change like insertion or deletion is added. For the in vitro transcription of gRNA, the specific sequence has to be cloned into a suitable plasmid. The oligos *insra*_CRISPR1_Fwd: TAGGTTGGGGAACAGGTCACTG, *insra*_CRISPR1_gen_Rev: GCTGAAGTCGCCGTTGATAG, *insrb*-CRISP3-for: TAGGAGTTGACGGTGGTGTATC and *insrb*-CRISP3-rev: AAACGATACACCACCGTCAACT were ordered & supplied from Thermofischer Scientific and dissolved with autoclaved MiliQ water to get a solution which was stored in -20°C. This solution was used to anneal for cloning in plasmids. The following protocol was used for annealing of the oligos in a 0.2ml PCR tube:

2µl *insra*_CRISPR1_Fwd
2µl *insra*_CRISPR1_Rev
2µl NEB buffer 3
14µl MilliQ water
The tube was incubated in a thermal cycler with the following protocol:
95°C for 5 minutes
Cool down to 50°C at 0.1°C/second
50°C for 10 minutes
Cool down to 4°C at 1°C/second
Incubate at 4°C.

2.2.2.2 Restriction digestion and ligation of annealed oligos

The annealed oligos were then ligated into the pUC19 plasmid. A protocol was adopted and modified by Dr. Sandra Cramer-Stoll. The protocol was as follows:

1µl of annealed oligos
400ng pUC19 plasmid
1µl NEB buffer 3
1µl T4 DNA Ligase buffer
0.5µl BsmBI
0.3µl BglII
0.3µl SalI
0.5µl T4 DNA Ligase
5.4µl of MilliQ water to make the total volume 10µl.

The tube was incubated with the following temperature in a thermal cycler:
37°C for 60 minutes, 16°C for 45 minutes
Repeated 3 times
37° for 30 minutes
55°C for 30 minutes
80°C for 15 minutes
Incubate at 4°C forever or until the sample is removed

2.2.2.3 Transformation of the plasmid into E. coli

The ligated plasmid containing the desired oligos was then transferred to *E. coli* (strain DH5α). For this 50µl of E. coli stock was placed on ice for thawing. The ligated plasmid mixture was added into the tube, stirred gently, and left for 20 minutes on ice. After that, the tubes were incubated at 42°C for 90 seconds in heat blocks and then kept for another 90 seconds on ice. 1ml of LB medium was added into the tube and incubated at 37°C and 200rpm for 45 minutes in a shaker. The LB with bacteria was then centrifuged for 5 minutes at 4°C and 6000rpm. Then the supernatant was thrown away and the layer was resuspended and spread onto an LB agar plate containing ampicillin. The plate was then incubated at 37°C overnight. After overnight incubation, single colonies were picked to inoculate 3ml LB medium with ampicillin in a tube and incubated overnight at 37°C and 200 rpm. The next morning Bacterial culture was collected and plasmids were isolated using Illustra PlasmidPrep Mini spin kit according to the supplied protocol. For each sample 60-100ng of

plasmid DNA was sent to Eurofins for sequencing. The plasmids containing the desired nucleotide were then retransformed and maxi prep was using Qiagen maxi prep kit.

2.2.2.4 Preparation of CRISPR gRNA and Cas9 mRNA

pUC19 plasmid containing the desired sequence was linearized using the BamHI-HF restriction enzyme. For linearization 1-3µg of DNA was incubated at 37°C for overnight with 1-2µl of restriction enzyme and 10% volume of buffer. Plasmids were then purified by PCR purification kit according to the protocol provided by manufacturer Qiagen. In vitro transcription with this cleaned Insra, Insrb, and control DNA was done by T7 Megashortscript kit and mMESSAGE MACHINE kit was used for Cas9. TurboDnase was used to kill the DNA after incubation for 4 hours. Then RNA was purified using MiRNeasy mini and RNeasy mini kit using protocol from the manufacturer and stored at -80°C.

2.2.2.5 Injection of CRISPR gRNA into zebrafish eggs

CRISPR gRNA and mRNA for Cas9 were then injected into the eggs of zebrafish. gRNA was diluted in 0.1M KCL solution to a concentration of 150 pg/nL and mixed with Cas mRNA which was diluted to 200pg/nL. 1 nL of this mixture was then injected into the cell of the single cell stage of eggs. After 4-6 hours, eggs were sorted out and unfertilized eggs were removed. As a control, gRNA without target sequence from empty pT7 plasmid was taken. To check the efficiency, injected embryos were collected and then sent for sequencing.

2.2.2.6 Genomic DNA extraction from zebrafish embryo

For determination of the mutation, genomic DNA from the embryos was extracted. For this, zebrafish 48/72 hpf embryos were anesthetized with .003% Tricaine and individually taken into 0.2µl PCR tubes. 20µl of lysis buffer was added into each tube and was incubated at 98°C for 10 minutes, 55°C for 4 hours to overnight, then 55°C for an hour and finally 98°C for 10 minutes again. After the first 98°C incubation, 10µl of proteinase K was added into each tube and after incubation at 55°C for more than 4 hours, the tubes were flicked with fingers so that the undigested part of the embryos were dissolved properly. Finally, the tubes were cooled down and stored at -20°C.

2.2.2.7 Amplification of the genomic DNA

Before the sequencing to detect the changes caused by CRISPR the genomic DNA extracted from embryos were amplified with specific primers. For *insra* gene the primers *insra*_CRISPR1_gen_for and *insra*_CRISPR1_gen_rev and for *insrb* gene *insrb*_CRISPR3_gen_for and *insrb*_CRISPR3_gen_rev primers were used to amplify the specific region. The master mix containing DNA for the PCR was as follows.

Genomic DNA	2µl
Forward Primer	2µl
Reverse primer	2µl
Green Taq mix	12.5µl
H_2O	6.5µl
Total	25µl

The reaction mixture was incubated on the thermal cycler as per following sequence:

Insra		Insrb	
95°C	5 minutes	95°C	5 minutes
95°C	30 seconds	95°C	30 seconds
60°C	30 seconds	66°C	30 seconds
72°C	45 seconds	72°C	45 seconds
72°C	10 minutes	72°C	10 minutes
4°C	forever	4°C	forever

The PCR amplified sequence was then run on an already prepared 1% agarose gel submerged in TAE buffer in an electrophoresis chamber. Ethidium bromide (1:20000) was added to the agarose gel to visualize the nucleotides under ultraviolet (UV) light in a specific chamber. If the desired band is visualized under UV light thus amplification of the desired part of the sequence is proved, the PCR product is purified using a PCR cleanup mini kit. For each sample, the purified DNA was mixed with forward primer and sent to Eurofins laboratory for sequencing.

2.2.2.8 Isolation of mRNA from zebrafish larvae

RNA extraction was done using the RNeasy mini kit from Qiagen and the protocol supplied with the kit was followed. Zebrafish larvae at 96hpf were anesthetized with 0.003% tricaine

and collected in a 1.5mL tube. With a micropipette, the liquid was pipetted up and down a few times to destroy the yolk sack. After that, it was centrifuged at 4°C for 5 minutes. The supernatant was discarded. 700µL RLT lysis buffer premixed with 7µL β-mercaptoethanol was added to the larvae. The tissue was kept on ice for 30 minutes. And disrupted using a 1mL plastic syringe and 20G needle three to four times in between. After that, the whole lysate was centrifuged for 3 min at 4°C and the supernatant was discarded. At the next step, 700µL of 70% ethanol was added, mixed by pipette, and taken in a supplied mini spin column placed in a 2mL collection tube. This column was spun for 15s at 10000rpm at 4°C the flow-through was discarded. Then 700µL RW1 buffer was used and centrifuged with the same setting as the last step. At the next step 500µL RPE buffer was added and spin for 15s at 10000rpm at 4°C the flow-through was discarded. This step was then repeated once more. Then the spin column was placed on a 2mL collection tube and centrifuged at full speed for 1 minute to dry the membrane. Later on, the dried spin column was placed on a 1.5mL collection tube, 20-30µL of RNase-free water was added directly to the column and centrifuged at 10000rpm for 1 minute to elute the RNA. The concentration of the RNA was then measured in a spectrometer and used for a further procedure or stored at -80°C.

2.2.2.9 cDNA preparation

cDNA was prepared from the extracted RNA from zebrafish larvae. For this, a maxima first strand cDNA synthesis kit was used and the supplied protocol was followed. The protocol was optimized for 1µg of RNA and the generated cDNA was stored at -20°C.

2.2.2.10 Real-time quantitative PCR (qPCR)

A Real-Time qPCR experiment was performed for analyzing the gene expression in mutants and wt zebrafish larvae. For this experiment, Roche LightCycler® 480 was used which detects the expression of the gene using specific probes. Primers for our gene of interest *insra*_for_1, *insra*_rev_1, *insrb*_for_1, *insrb*_rev_1, *β-actin*_for_1, *β-actin*_rev_1 was designed using Roche Universal Probe Library (https://lifescience.roche.com/en_de/articles/Universal-ProbeLibrary-System-Assay-Design.html). The source of zebrafish gene transcripts was the Ensembl database (https://www.ensembl.org/index.html) and ordered from ThermofishcerScientific. As a

reference gene to compare against, β-actin was used as a housekeeping gene or control. SensiFAST™ SYBR® No-ROX Kit was used as PCR master mix. For the PCR, the gene, master mix, and primer were mixed in the following amount:

Primer Mix	2µL
SensiFAST™ SYBR® No-ROX Kit	10µL
cDNA + water-Mixture (20ng of DNA)	8µL
Total	20 µl

The PCR reaction was run in the thermal cycler with the following steps:

Step	Temperature	Time (seconds)	Cycles
Denaturation	95	10 seconds	
Annealing	60	30 seconds	45
Elongation	72	1 second	

The real-time qPCR was calculated using following method:

$$\text{Ratio of expression level} = \frac{\text{Amount of target gene}}{\text{Amount of housekeeping gene}}$$

2.2.2.11 Preparation of protein lysate

Protein lysate was prepared from mutants and wild type control 96hpf zebrafish embryo for biochemical analysis and experiments. At first 45-50 anesthetized 96hpf zebrafish embryos were taken in a 1.5ml tube. The embryos were then mixed & resuspended using a pipette and centrifuged at 14000rpm for 5 minutes at 4°C to get rid of the yolk. The supernatant was discarded, embryos were resuspended in 100µl NP40 buffer and incubated for 30 minutes. Then embryos were homogenized with a syringe. After that, it was left for another 5 minutes on ice. The lysate was then centrifuged at 14000rpm for 5 minutes at 4°C, the supernatant was collected and stored at -20°C for further use.

2.2.2.12 Quantification of protein in the lysate

The protein amount in the lysate was quantified to ensure that all the samples should have the same amount of protein. The method adopted was BCA protein assay and it was performed using Pierce BCA protein assay kit. This working reagent (WR) was prepared by mixing 50 parts of BCA reagent A with 1 part of BCA reagent B (50:1, Reagent A: B). WR was prepared for 24 samples as 18 was for 9 standard curves and 6 was for 3 samples. A 96 well plate was taken and 25µl of each standard or sample was taken twice in two wells. After that 200µl of this WR was added into each well. For the standard curve, wells were named as A, B, C, D, E, F, G, H, and I final BSA concentration subsequently was 2000, 1500, 1000, 750, 500, 250, 125, 25, and 0 µg/mL. For samples, the wells were named J, K, and L. The 96well plate was covered with aluminum and incubated at 37°C for 30 minutes. Then the plate was taken in a spectrophotometer and absorbance was measured at 562nm. The standard curve was fitted with the absorbance from well A to I and the standard curve was used to determine the concentration of protein in well J, K, and L.

2.2.2.13 Western Blot

Western Blot was done to detect Insr protein in Insra and Insrb mutants' embryos against WT embryos. The lysates prepared before were diluted as per concentration so that were mixed with 5x Laemmle buffer and boiled at 95°C for 5 minutes in a heat block. After that, the lysates were loaded into a 10% SDS gel. The SDS gel was prepared with the following chemicals:

1.5M Tris/HCL pH = 8.8
1.5M Tris/HCL pH = 6.8
dH_2O
10%SDS
10% APS
TEMED

This SDS gel was submerged in a tank filled with running buffer and ran with 90V for 2 hours. After this step, the gel was incubated in the tank while attached to a nitrocellulose membrane to transfer the protein from the gel to the membrane. Then the protein in the membrane was

blocked by soaking the membrane in 5% milk powder dissolved in .05% PBST for 1 hour. After the soaking, the membrane was washed three times with .05% PBST. Then it was cut into two pieces and one part was incubated with anti-Insr antibody (1:200) and the other part was incubated with anti-β-actin overnight at 4°C with gentle movement. The next day the parts of the membrane were again washed with 0.5% PBST three times each 5 minutes. Then it was incubated in anti-goat secondary antibody dissolved in 0.5% PBST (1:1000) for 1 hour at room temperature. After this, the membrane was again washed in 0.5% PBST for 3 times 5 minutes each and then visualized by enhanced chemiluminescence detection and the signal was analyzed in Intas GelPro analyzer.

2.2.2.14 Organ preparation and Immunohistochemistry

Fishes were euthanized with 0.025% tricaine solution for organ harvesting. The fishes were decapitated and the head was taken into ice cold PBS buffer. The body was cut open on the ventral side and fixed on a cold PBS filled agarose plate with a needle. The liver and muscle tissues were removed with tweezers, taken into a 1.5mL tube, remaining water was sucked away and immediately frozen in liquid nitrogen. The body of the fish with the kidney was then taken into a 2mL tube filled with 4% PFA-PBS/.1%DMSO solution and left at 4°C overnight. The next day several steps were taken before they were embedded in paraffin. The steps were:

First day:	70% Ethanol	2 x 15 minutes
	70% Ethanol	kept at overnight at 4°C & no movement
Second Day:	80% Ethanol	2 x 15 minutes
	90% Ethanol	2 x 15 minutes
	96% Ethanol	3 x 15 minutes
	99% Ethanol	3 x 15 minutes

These steps were performed on a saw rocker.

	Xylol	3 x 5 minutes

This step was performed under a hood.

Paraffin was kept liquid in a 62°C incubator. The dehydrated kidney was then transferred to a square-shaped rubber cast and embedded in paraffin. These paraffin embedded kidneys

were cut with a microtome (Leica HistoCore Multicut) at a thickness of 4µm, dried, and mounted for staining procedure. For Periodic Acid Schiff (PAS) staining the following steps were done. The first step including incubation in distilled water is to rehydrate the samples. The second step is for the staining procedure specifically.

Rehydration:

Tissue Clear (Xylene substitute)	10 minutes
Tissue Clear (Xylene substitute)	10 minutes
99% Ethanol	5 minutes
96% Ethanol	5 minutes
70% Ethanol	5 minutes
Distill Water	5 minutes
Distill Water	5 minutes

Staining procedure:

1% Periodic acid	10 minutes
Distill water	Rinse
Schiff's reagent	20 minutes
Sulfurous water	3x 2 minutes
Washing under water	5 minutes
Haematoxylin	5 minutes
coloring	5 minutes
70% Ethanol	1 minute
96% Ethanol	3x 1 minute
Tissue clear	3x 1minute
Acetic acid n-butyl ester store	until covered

The staining was done in Leica ST5010 Autostainer and sections were then fixed by covering under glass slides and coverslips in Leica CV5030 Fully Automated Glass Coverslipper. The glass slides were checked in and photos were taken by a scanner (Olympus).

2.2.2.15 Software

Images from agarose gel electrophoresis were taken using IntasGelcapture. For measurement of the in vivo pronephros, Leica LAS Version 4.8 is used. Analysis and quantification of embryonic and adult retinal vasculature were done using GIMP2, Leica LAS V4.8, and ImageJ software. For Statistical analysis and graph generation, GraphPad prism 7 was used.

2.2.2.16 statistical test

All statistical analysis was carried out using Graphpad prism 6.0. On the graphs, the data were plotted with mean ± SEM (standard error of the mean). For comparison among groups and to assay the statistical significance, one-way ANOVA was performed for variance within the group and Dunnette's multiple comparison test for unpaired comparison with wt was performed. The student's t-test was used for comparison between two groups. $P \leq 0.05$; was used to show any significant difference among comparable groups. * $P \leq 0.05$, ** $P \leq 0.01$, *** $P \leq 0.001$ was used to differentiate three levels of significance.

3. Result

3.1 *insra*$^{-/-}$ and *Insrb*$^{-/-}$ zebrafish grow to adulthood without morphological alteration and produce nonfunctional proteins

For this research project, insulin receptor a (*insra*) and insulin receptor b (*insrb*) mutant were generated in zebrafish using the CRISPR/Cas9 genome editing technique (Chang *et al.*, 2013; Jao, Wente, & Chen, 2013) The CRISPR gRNA was designed using the sequence available on ensemble (*insra*: ENSDART00000008302.6 and *insrb*: ENSDART00000105823.6). The sequence CAGTGACCTGTTCCCCAA on exon 2 in the *insra* gene was targeted and for *insrb*, the target sequence was GATACACCACCGTCAACTCCACCT in exon 3 (Fig: 3.1.1).

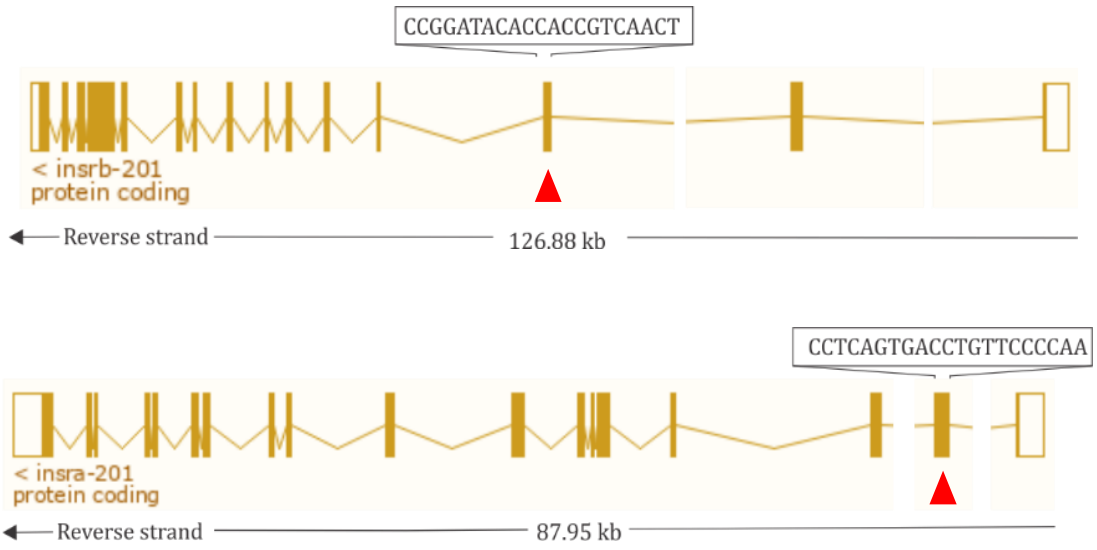

Figure 3.1.1. Generation of *insra*$^{-/-}$ and *insrb*$^{-/-}$ mutant zebrafish using CRISPR/Cas technique. The binding site of the *insra*-CRISPR gRNA in exon 2 and *insrb*-CRISPR gRNA in exon 3 [graphic illustration of intron and exon has been taken and modified from the Ensembl database].

The mutation in F0/F1/F2 generation was verified by the Sanger sequencing method and the sequences were analyzed using the electropherogram (Fig 3.1.2 B and 3.1.2 C). At F1 generation, 2 different types of mutation were found in the *insra* gene: (1) 2 base deletion

with 1 base exchange in *Tg(fli1:EGFP)* transgenic fish line and (2) 8 base deletion with 10 base insertion in *Tg(wt1b: EGFP)* transgenic fish line (Fig 3.1.2 A).

In the *insrb* gene, 4 different types of mutations were found at the F1 generation and 2 genotypes were selected for further experiments. Those are (1) 2 base insertion with 22 base deletion, (2) 1 base insertion with 32 base deletion (Fig 3.1.2 B).

A

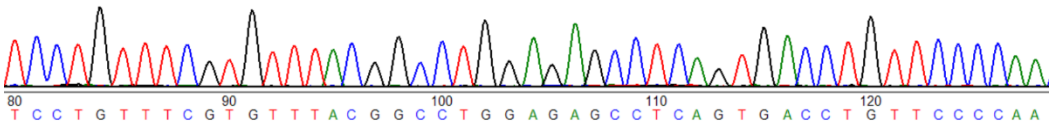

insra gene sequence in wt

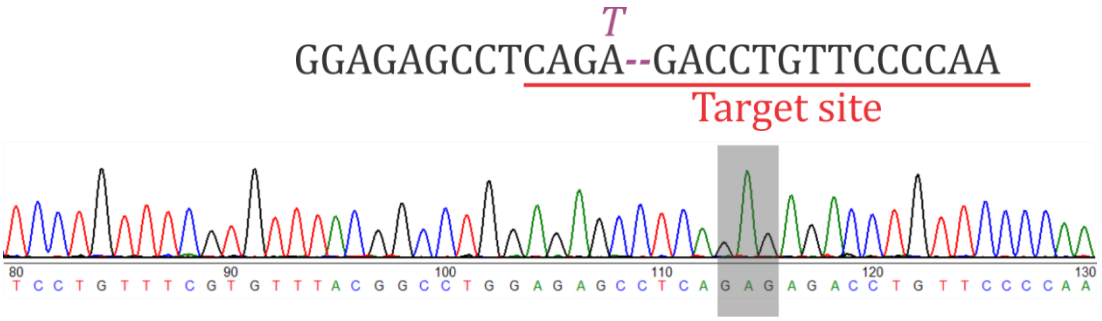

TG(*fli1:EGFP*): 2 base insertion + 1 base exchange

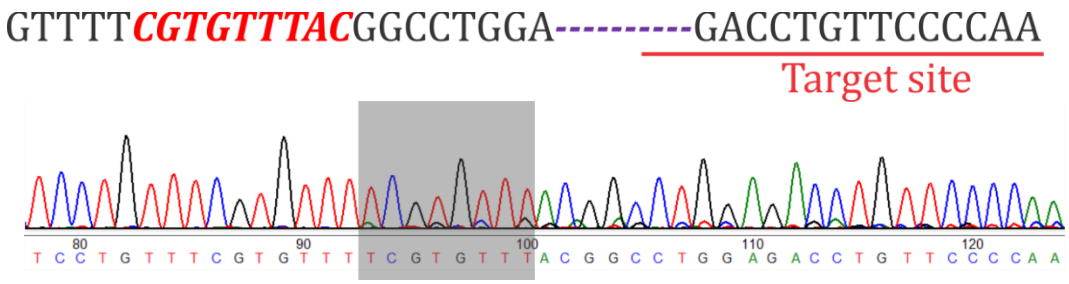

TG(*Wt1B:EGFP*): 10 base insertion + 8 base deletion

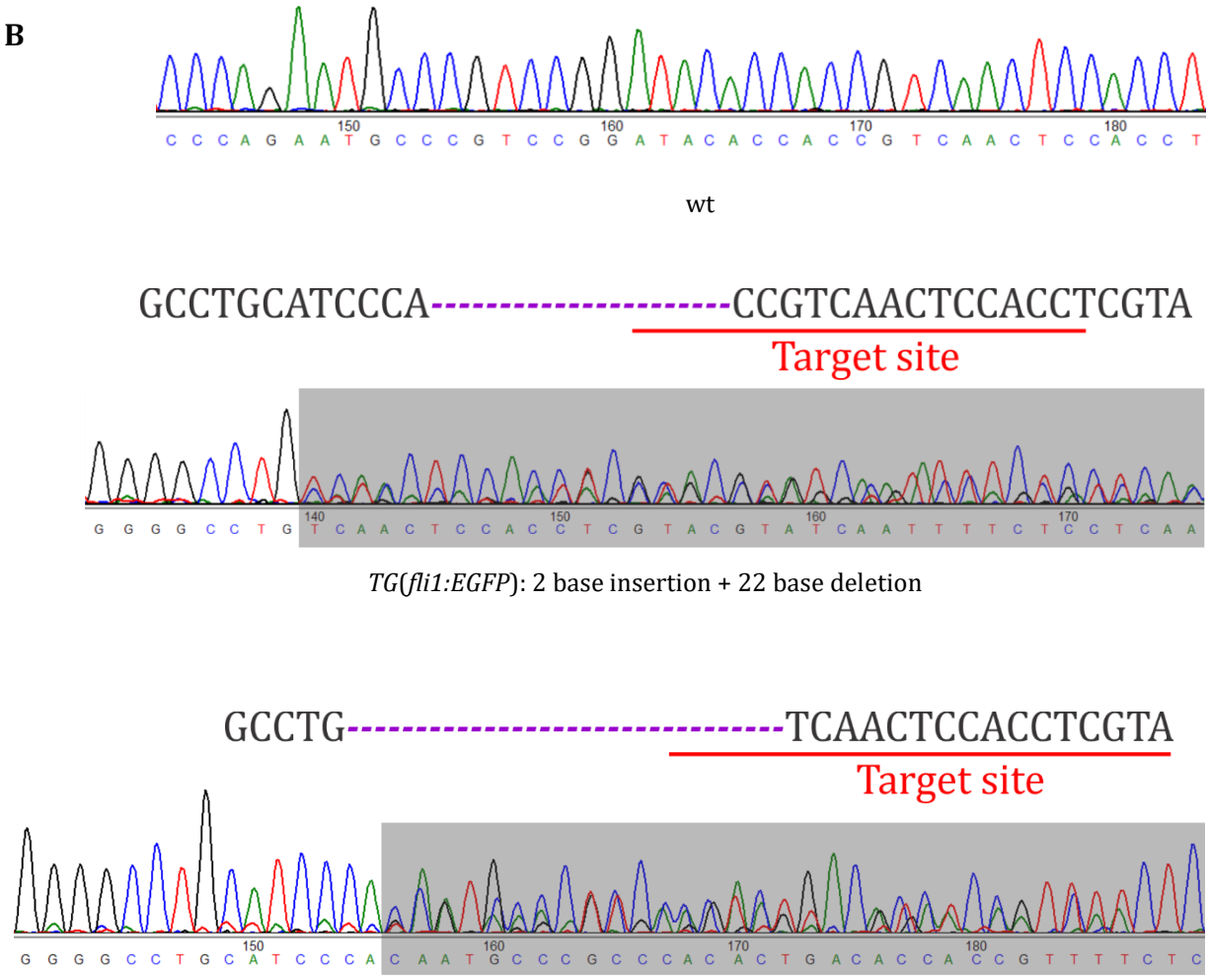

Figure 3.1.2. Generation of *insra*$^{-/-}$ and *insrb*$^{-/-}$ mutant zebrafish using CRISPR/Cas technique. (A) The electropherogram is showing the mutations in the genome of *insra*$^{-/-}$ zebrafish. the first one is the sequence of the *insra* gene of wt zebrafish. the second electropherogram shows 1 base exchange + 2 base deletion in the genome of *TG*(*fli1:EGFP*) zebrafish which is marked with a grey rectangle. 10 base insertion + 8 base deletion for *Tg(Wt1B:EGFP*). 1st electropherogram is from wt, 2nd is from *insra*$^{-/-}$ *Tg*(*fli1*:EGFP), and 3rd is for *insra*$^{-/-}$ *Tg(Wt1B:EGFP)* embryo. (B) The mutation found in the genome of *insrb*$^{-/-}$ zebrafish embryo. *insrb*$^{-/-}$ has four different types of mutation (2 base insertion + 22 base deletion, 32 base deletion + 1 base insertion). 1st graphic is for wt and 2nd is for *insrb*$^{-/-}$ *Tg*(*fli1:EGFP*) mutants.

The Insra primary sequence consists of 1353 amino acids (aa) and the *insra*$^{-/-}$ sequence analysis shows that frameshift mutation leading to the premature stop codon produces the

peptide with the size of 98aa and 103aa in two transgenic lines. The primary sequence of the Insrb protein is 1348aa, while in mutants it is shortened to 318aa-329aa. A tetrabasic protein cleavage site can be found at positions 733-736aa in Insra and 730-733aa in Insrb. Upon cleavage of the zebrafish Insr, an α-subunit and a β-subunit are created. The reactive tyrosine kinase domain which has the potential ATP binding site at 1001-1028aa for Insra and 996-1023aa for Insrb, are located in this β-subunit. That means Insra and Insrb produced in these mutants do not contain the active site and are nonfunctional. To confirm the generation of mutants, I have run Western Blot with an anti-Insr antibody. Here, both *insra*$^{-/-}$ and *insrb*$^{-/-}$ mutants showed a much weaker protein band compared to wt animals (Fig 3.1.3 A). As the polyclonal antibody binds against both the Insr in zebrafish, total nullification of the band was not possible hence only the weakening of the band could be visualized. This was due to the absence of one of the two insulin receptor proteins in respective mutants.

Upon knockout of Insr, I have seen that *insra*$^{-/-}$ and *insrb*$^{-/-}$ can grow up to adulthood without showing any morphological changes. Fig 3.1.3 B shows zebrafish larvae from three different genotypes at 96hpf. *insra*$^{-/-}$ and *insrb*$^{-/-}$ mutants reach adulthood without any problems and there was no aberration in fecundity too.

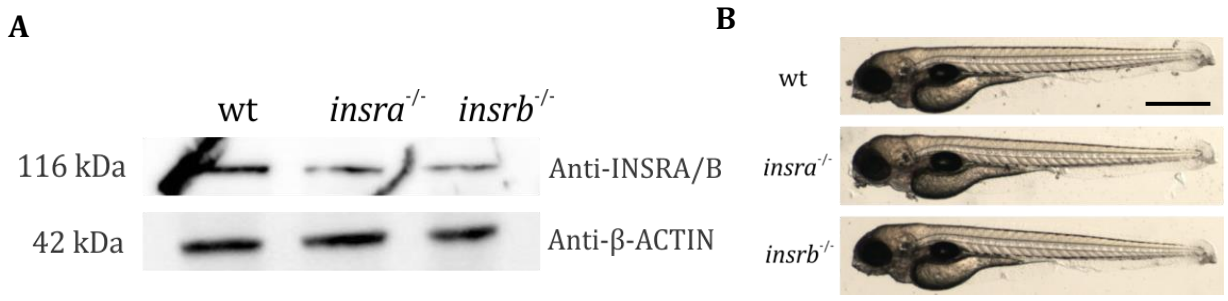

Fig 3.1.3 (A) Representative western blot done with lysates from 96hpf old Zebrafish larvae by anti Insra-b antibody shows the reduction of signals of *insra*$^{-/-}$ and *insrb*$^{-/-}$ Knockout animals. β-actin was used as the loading control. (B) *insra*$^{-/-}$ and *insrb*$^{-/-}$ mutants show no morphological changes at 96hpf in mutant larvae when compared with wt. wt = *insra*$^{+/+}$/*insrb*$^{+/+}$. The black scale bar represents 1mm in length.

In my experiment, I have found the genotypes of the mutants follow the rules of Mendelian statistics. The ratio of the mutants, wt:heterozygous:homozygous was 1:2:1 (Fig 3.1.4 A). I

have intercrossed double heterozygous fishes (*insra*$^{+/-}$/*insrb*$^{+/-}$) but found that double knockout (*insra*$^{-/-}$/*insrb*$^{-/-}$) fish cannot live after the juvenile stage (3.1.4 B). In conclusion, we created *insra*$^{-/-}$ and *insrb*$^{-/-}$ mutants that produce nonfunctional Insra and Insrb proteins. These mutants are morphologically similar to wt and can reach adulthood without any drastic hindrance. For this research project, 1-48 hpf old zebrafish are marked as the embryo and 48hpf-120hpf old are marked as larvae.

As the preliminary effect of *insr* knockout is seen on the glucose level, whole body glucose value was measured after the generation of mutants. I did not observe any change in total glucose (whole-body glucose) in the wt, *insra*$^{-/-}$ and *insrb*$^{-/-}$ larvae at 96hpf (Fig 3.1.4 C).

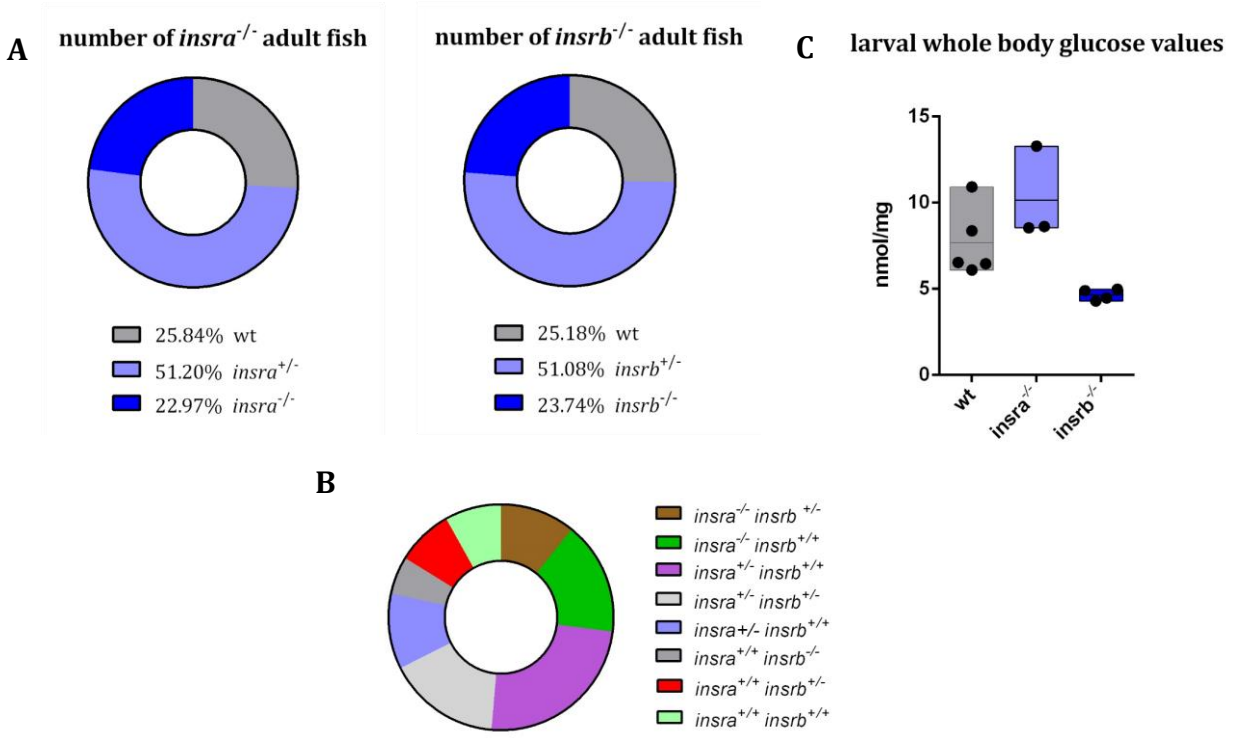

Figure 3.1.4: Ratio of adult fish with different genotypes and total glucose was measured in larvae. A) the ratio of wt:heterozygous:homozygous follow the Mendelian theory of genetics. The total number of fish was 209 for the *insra*$^{-/-}$ and 139 for the *insrb*$^{-/-}$. B) There was no alteration of total glucose values in *insra*$^{-/-}$ and *insrb*$^{-/-}$ 96hpf larvae. Each measurement consists of 45-50 larvae. n=5 for wt, n=3 for *insra*$^{-/-}$ and n=4 for *insrb*$^{-/-}$. C) the ratio of mutant larvae while crossing *insra*$^{+/-}$ and *insrb*$^{+/-}$ fish. The total number of larvae genotyped was 37.

3.2 *insra*$^{-/-}$, but not *insrb*$^{-/-}$ have a higher number of hyperbranches in the trunk

Vasculogenesis and angiogenesis are basic processes for the formation of new blood vessels. Vasculogenesis is the differentiation of angioblasts into endothelial cells & de novo formation of primitive vascular network and angiogenesis is the growth of new capillaries from present blood vessels (Kolte *et al*, 2016; Risau, 1997). Trunk axial vessel formation in different developing vertebrates is resembled by zebrafish vasculogenesis (K Jörgens & Kroll, 2012; Kristina Jörgens et al., 2015; Z. Liu & Liu, 2012). Of all the angiogenic vessels formed in all vertebrates including zebrafish, the intersegmental vessel (ISV) of the trunk is among the first. When there is a sprout of cells originating from an ISV, it is counted as an ectopic sprout and when the ectopic sprout is long and connects itself to another ISV, it is counted as a hyperbranch (Fig 3.2 A).

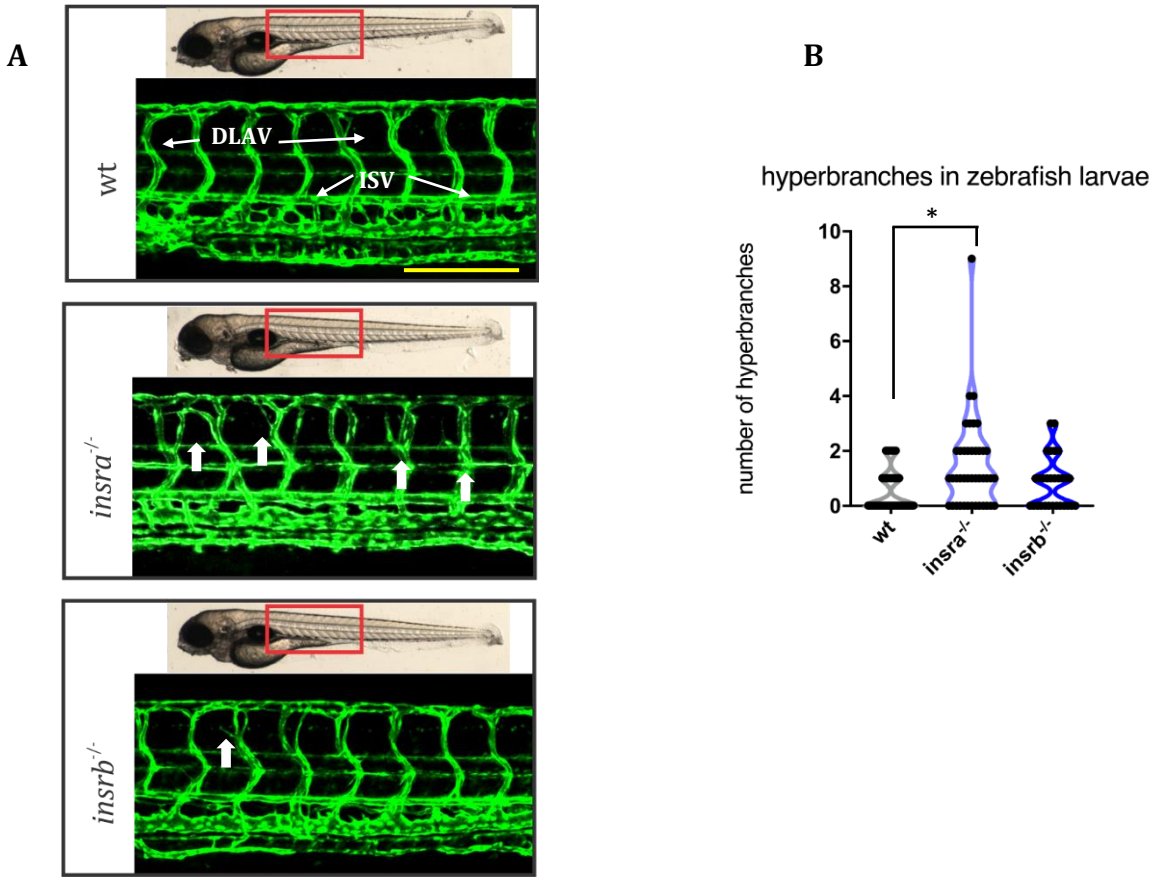

Figure 3.2: Insra depletion can alter the trunk vascular development of zebrafish but Insrb does not. (A) Vascular structure from wt, *insra*$^{-/-}$ and *insrb*$^{-/-}$ zebrafish larvae where the dorsal longitudinal anastomotic vessel (DLAV) and ISV are marked. B) Quantification and statistical analysis show that

there was a higher number of sprouts and hyperbranches in *insra*$^{-/-}$ larvae but not in *insrb*$^{-/-}$ larvae. ISV = intersegmental vessel, DLAV = dorsal longitudinal anastomotic vessel. Then number of larvae: wt = 48, *insra*$^{-/-}$ n=48, *insrb*$^{-/-}$ n=48. For statistical analysis, one-way ANOVA is used and significance is denoted as *P<0.05; the graph represents mean ± SEM for each genotype. The white scale bar represents 200µm in length.

I have quantified the aberration in wt and mutant larvae and saw that the number of ectopic sprouts and hyperbranches are higher in *insra*$^{-/-}$ larvae but not in *insrb*$^{-/-}$ (Fig 3.2 B).

3.3 Diameter of hyaloid-retinal vessels was increased in the *insra*$^{-/-}$ and *insrb*$^{-/-}$ larvae

In the previous experiment, I have observed trunk vasculature was altered in the *insra*$^{-/-}$. As the patterning of hyaloid retinal vessels has similarities in mechanism compared to the trunk vessels in zebrafish (Gore *et al*. 2012), we wanted to check if loss of Insr has any effect on the retinal vascular development. The portion of retinal blood vessels internal to the eye is defined as hyaloid vessels (Isogai, Horiguchi, & Weinstein, 2001) and at 60hpf first hyaloid vessels are can be seen as tightly attached to the lens (Alvarez *et al*, 2007). I have isolated the hyaloid vessels from the eyes of 120hpf zebrafish larvae (Fig 3.3 A) using the protocol described in (Jung *et al.,* 2016) and found that both the *insra*$^{-/-}$ and *insrb*$^{-/-}$ mutant larvae, the vessel diameter is significantly increased in the hyaloid vessels of the mutants (Fig 3.3 B).

A

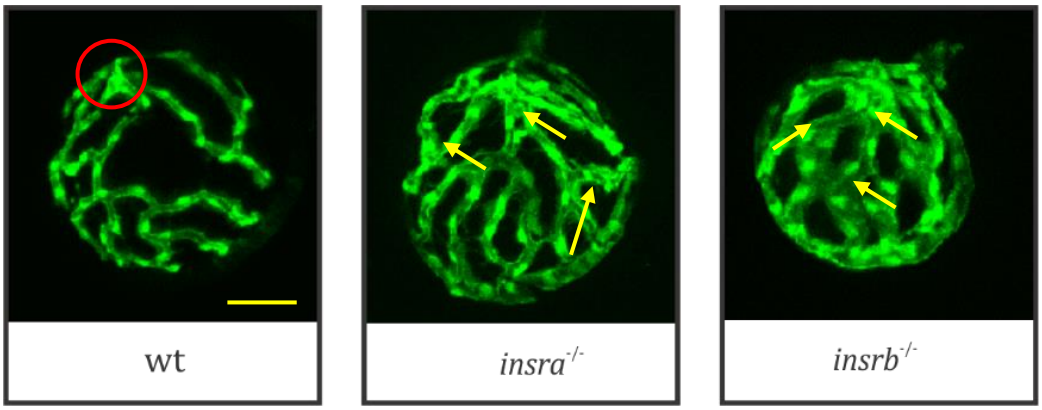

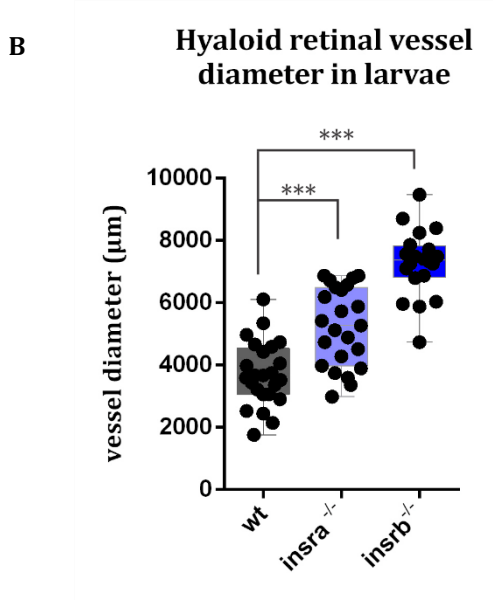

Figure 3.3: Hyaloid-retinal vessels diameter is increased in *insr* mutants. (A) The hyaloid vessels isolated from wt, *insra*$^{-/-}$ and *insrb*$^{-/-}$ larvae. The diameter of hyaloid vessels was measured at locations proximal to the optic disk shown by the red circle. The white scale bar represents 20µm. (B) The thickness of the vessel diameter and number of branches are higher in the *insra*$^{-/-}$ and *insrb*$^{-/-}$ retina. For each lens, the vessel diameter was measured three times and calculated using ImageJ software. wt represents genotype *insra*$^{+/+}$/*insrb*$^{+/+}$.; wt n= 23, *insra*$^{-/-}$ n = 21 and *insrb*$^{-/-}$ n= 22. For statistical analysis, one-way ANOVA is used, and significance is denoted as ***P<0.001; the graph represents mean ± SEM for each genotype.

Interestingly, there was no apparent change in the *insrb*$^{-/-}$ trunk vasculature but among the three groups, *insrb*$^{-/-}$ shows the highest diameter in the hyaloid vessels followed by *insra*$^{-/-}$ (Fig: 3.3 B).

3.4 Early-stage pronephros are not affected in *insr* zebrafish mutants.

There has been no change in the glucose values in the KO larvae but there was an aberration in the trunk vasculature in *insra*$^{-/-}$ larvae. Moreover, changes were also found in the hyaloid vessels of both the *insra*$^{-/-}$ and *insrb*$^{-/-}$. Nephropathy is a major microvascular complication, so I have investigated the effect on the kidney of mutant zebrafish too. The kidney in animals consists of a functional unit named the nephron. During the early stages of zebrafish, it has

Pronephros which is the simplest form of the kidney, instead of full form. Pronephros forms during embryogenesis and is the functional kidney during the larval stage of zebrafish (Vize *et al*, 2002; Drummond & Davidson, 2016). At 48hpf there is a single pronephros that filters the liquid in the zebrafish embryonic body and measurement of the structure such as the neck length, glomerular length, and glomerular width of the pronephros, as well as the functional assay of zebrafish pronephros at 48hpf, can indicate pronephros function (Sharma *et al*, 2016).

The loss of Insra or Insrb did not lead to any remarkable change in pronephros structure at early stage zebrafish (Fig 3.4.1 B). The glomerular neck length, glomerular width, and glomerular length was measured (marked in red ring Fig: 3.4.1 A wt)

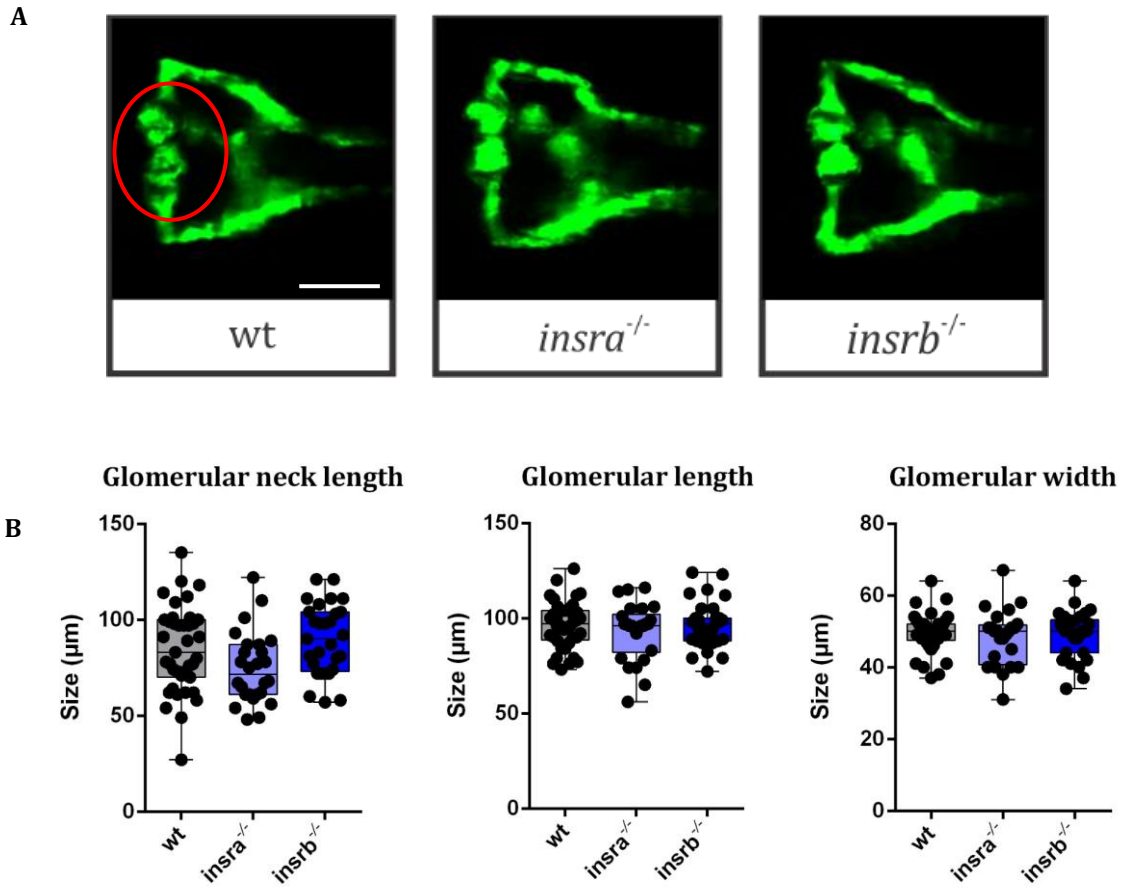

Figure 3.4.1: Pronephros from zebrafish embryo at 48hpf are not altered in *insra*$^{-/-}$ and *insrb*$^{-/-}$ embryo. (A) There were no visible abnormalities found in the pronephros of wt, *insra*$^{-/-}$ and *insrb*$^{-/-}$ zebrafish embryo. (B) The neck length, glomerular length, and glomerular width were quantified in

insra$^{-/-}$ and *insrb*$^{-/-}$ transgenic *Tg(wt1b:EGFP)* embryo but there was no apparent change among those. wt n= 41, *insra*$^{-/-}$ n = 26 *insrb*$^{-/-}$ n = 35. The white scale bar represents 50µm.

I have also performed a functional assay of kidney damage by injecting Texas Red® labeled Dextran in zebrafish embryo's heart at 72hpf, and fluorescence loss was measured at three time points: 1-hour post-injection (hpi), 24 hpi, and 48hpi (3.4.2 A). A high fluorescence loss resembles an albuminuria-like phenotype that represents an affected pronephros. This would elucidate any further functional abnormality, such as albuminuria or proteinuria, which is an early sign of diabetic nephropathy and can predict the progression of damage to the kidney (Berhane *et al*. 2011; Gnudi *et al*. 2016). In this experiment, I have not seen any change among wt or *insra*$^{-/-}$ or *insrb*$^{-/-}$ zebrafish embryos (Fig 3.4.2 B).

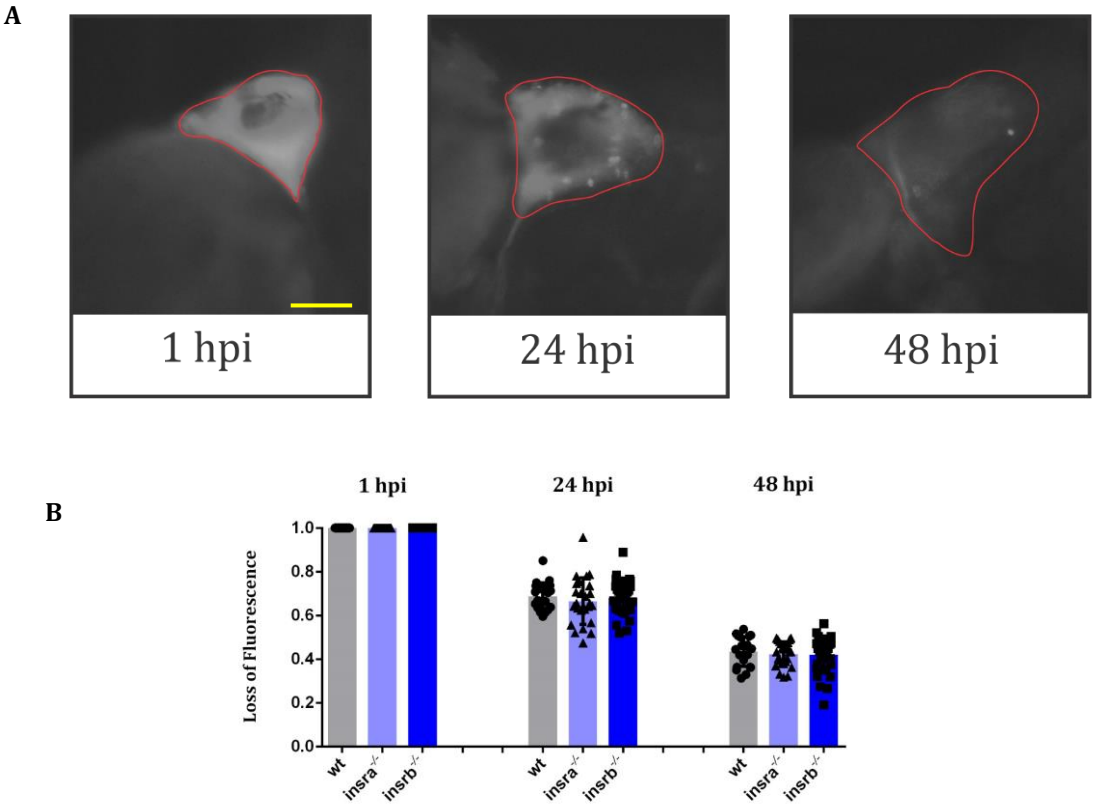

Figure 3.4.2: There was no alteration in the function of pronephros found in *insra*$^{-/-}$ and *insrb*$^{-/-}$. (A) Images of embryo heart injected with Texas Red® Labelled dextran after 1hpi, 24 hpi, and 48 hpi. The red encircled area is the heart after injection. The white scale bar represents 200µm in length. (B) There was no difference in a percentage loss of fluorescence from the embryonic heart of *insra*$^{-/-}$ and

insrb$^{-/-}$. For statistical analysis, one-way ANOVA is used, and; the bar graph represents mean ± SEM for each genotype.

3.5 Loss of Insr can lead to increased saturated and unsaturated fatty acids during early stages

In zebrafish, Insra and Insrb have different albeit some overlapping functions and previous research showed that regulation of several enzymes was affected in *insra*$^{-/-}$ and *insrb*$^{-/-}$ zebrafish larvae. So I wanted to investigate if there are any changes in the fatty acid content of primary metabolites in the mutants. Metabolomics analysis was done using the FAME-GC-MS technique in the mutant larvae at 96hpf. Most of the saturated, unsaturated fatty acids and cholesterol are increased in *insra*$^{-/-}$ and *insrb*$^{-/-}$ mutant larvae (Fig 3.5.1). C14:0 (Myristic acid), C16:0 (Palmitic acid), C18:0 (Stearic acid), C22:0 (Behenic acid), and C24:0 (Lignoceric acid) has been increased in the mutants (Fig: 3.5.1).

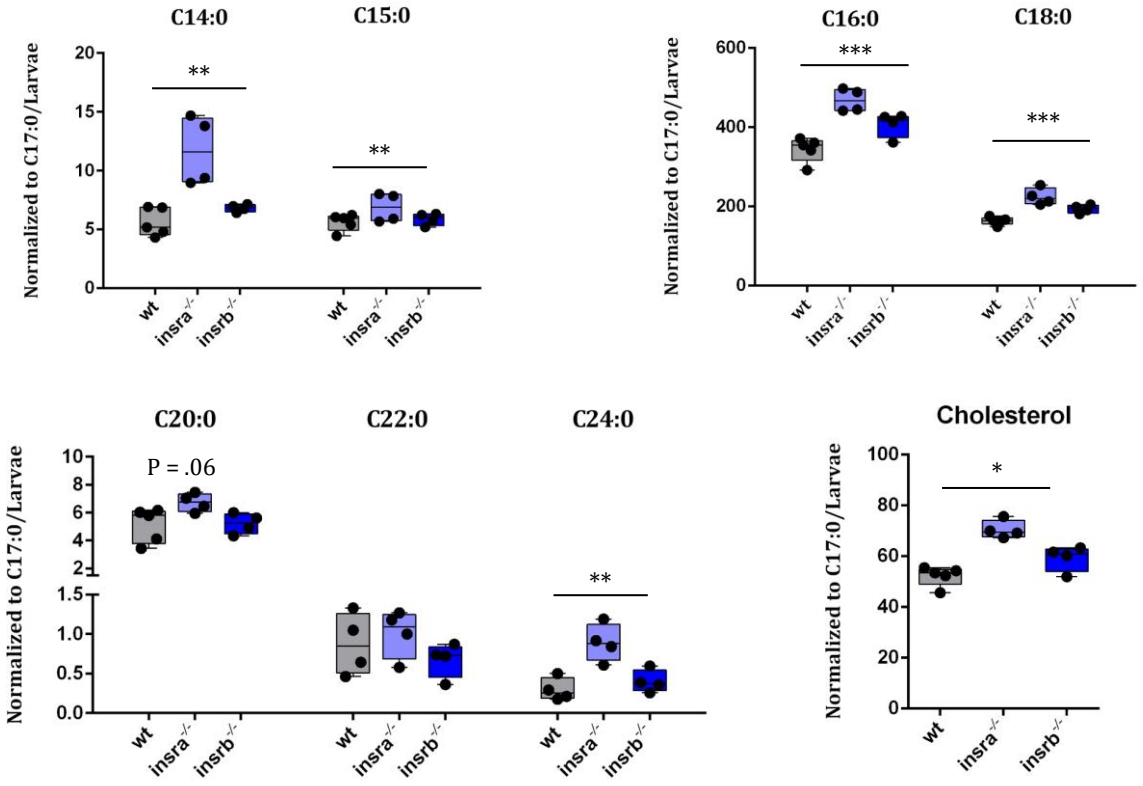

Figure 3.5.1: Loss of insr leads to increased saturated fatty acid and cholesterol content. A Semi-targeted GC-MS-analysis technique was used to determine the fatty acids in zebrafish larvae. The

calculated value was normalized to C17:0/larvae. wt = *insra*$^{+/+}$/*insrb*$^{+/+}$, wt n=5, *insra*$^{-/-}$ 4, *insrb*$^{-/-}$ n=4 readings, each readings contained 48-52 larvae. For statistical analysis, one-way ANOVA is used and significance is denoted as *P<0.05, **P<0.01, ***P<0.001; the graph represents mean ± SEM for each genotype.

Among unsaturated fatty acids, I have found that ω-3, ω-6, and ω-9 fatty acids (Eicosapentaenoic acid, Docosahexaenoic acid, Cervonic acid, Linoleic acid, Arachidonic acid, Oleic acid) have increased in the mutants (Fig 3.5.2).

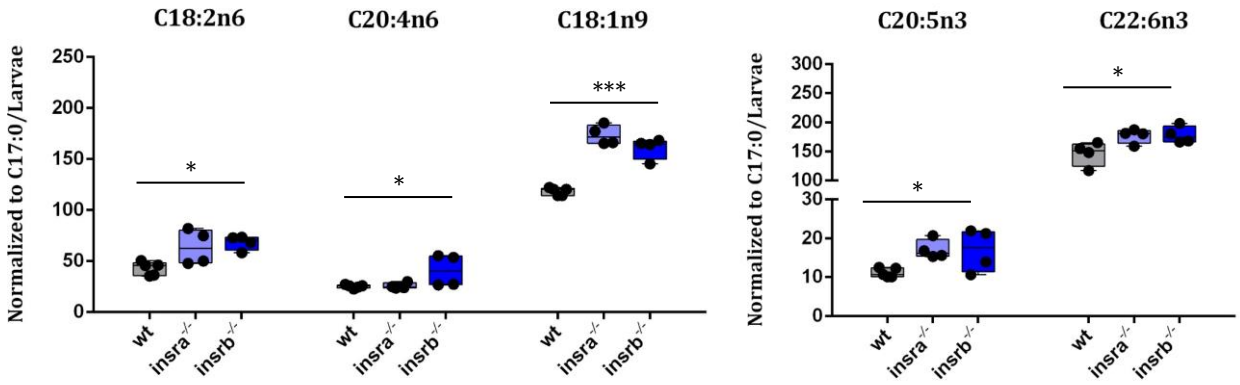

Figure 3.5.2: Unsaturated fatty acids are increased in *insra*$^{-/-}$ and *insrb*$^{-/-}$ larvae. FAME-GC-MS techniques were used for metabolomics analysis. The calculated value was normalized to C17:0/larvae. wt n=5, *insra*$^{-/-}$ 4, *insrb*$^{-/-}$ n=4 readings, each readings contained 48-52 larvae. For statistical analysis, one-way ANOVA is used, and significance is denoted as *P<0.05, ***P<0.001; the graph represents mean ± SEM for each genotype.

insulin signaling modulates not only glucose metabolism, but also regulates mRNA translation and protein synthesis among other functions (Riehle & Abel, 2016). I have analyzed if there was any alteration of primary metabolite in *insra*$^{-/-}$ and *insrb*$^{-/-}$ mutant larvae. Using the same method as the previous experiment, Among several amino acid contents and metabolites of glucose oxidation analyzed, I found that the amount of glycine and citric acid is higher in only *insra*$^{-/-}$ but not in *insrb*$^{-/-}$. but the rest of the amino acids and primary metabolites were not changed in any of the mutants (Fig 3.5.3).

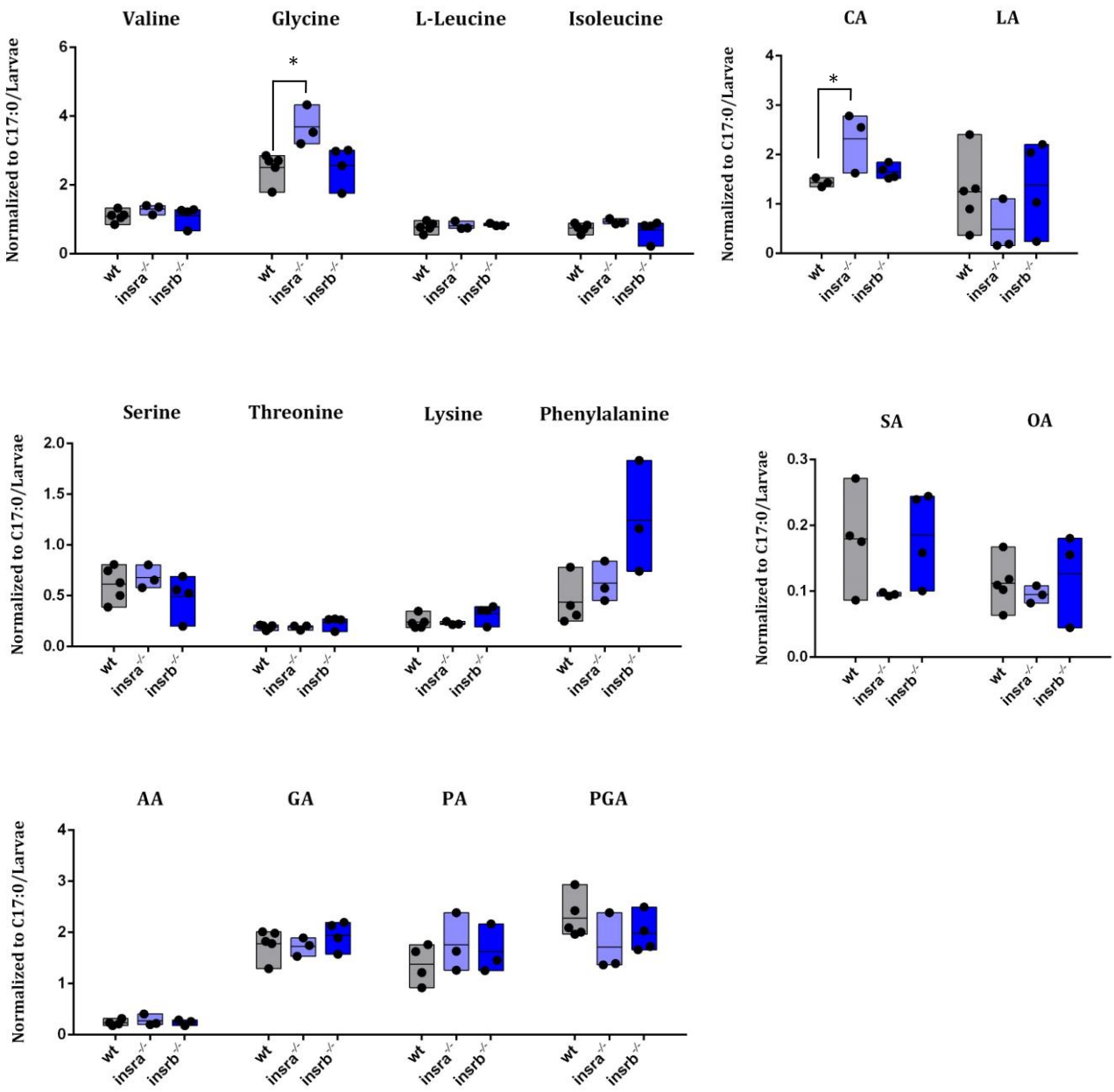

Figure 3.5.3: Depletion of insra and insrb leads to alteration in glycine and citric acid content but no other primary metabolites. wt = *insra*$^{+/+}$/*insrb*$^{+/+}$, wt n=5, *insra*$^{-/-}$ 4, *insrb*$^{-/-}$ n=4 readings, each readings contained 48-52 larvae. For statistical analysis, one-way ANOVA is used, and significance is denoted as *P<0.05; the graph represents mean value ± SEM for each genotype. FAME-GC-MS techniques were used for metabolomics analysis and the calculated value was normalized to

C17:0/larvae. CA = Citric acid; LA = Lactic acid; SA = Succinic acid; OA = Oxalic acid; AA = Aspartic acid; GA = Glutamic acid PA = Phosphoric acid; PGA = Pyroglutamic acid.

With these experiments, it has been shown that fatty acid metabolism is altered in zebrafish larvae. The alteration is higher in *insra*$^{-/-}$ compared to *insrb*$^{-/-}$. Among primary metabolites, glycine and citric acid were increased only in *insra*$^{-/-}$, however other primary metabolites and amino acids remain unchanged in *insra*$^{-/-}$ and *insrb*$^{-/-}$.

3.6 *insra*$^{-/-}$ adult fish has elevated fasting high blood glucose and fatty liver upon overfeeding

So far, generation of *insra*$^{-/-}$and *insrb*$^{-/-}$ zebrafish has been done but there was no increase in total glucose at 96hpf. As Insr function is impaired, I wanted to verify if extra food intake can have any effect on the glycemic level. Therefore, 4 months old *insra*$^{-/-}$ mutant were fed for 8 weeks with three times the normal amount of food (Oka *et al*., 2010). I found that the fasting glucose value was higher in the overfed (OF) *insra*$^{-/-}$ mutant compared to the control group of fish (wt normalfed/ NF) fish (Fig 3.6.1 A). In addition, upon overfeeding, both wt and *insra*$^{-/-}$ fishes have gained weight and increased in size. Although, both OF counterparts had a significant increase in body weight compared to their NF fishes, the weight increase in wt OF was higher than in *insra*$^{-/-}$ OF (Fig 3.6.1 B & C). I have also observed that *insra*$^{-/-}$ mutant overfed fishes had fatty liver (Fig 3.6.1 C).

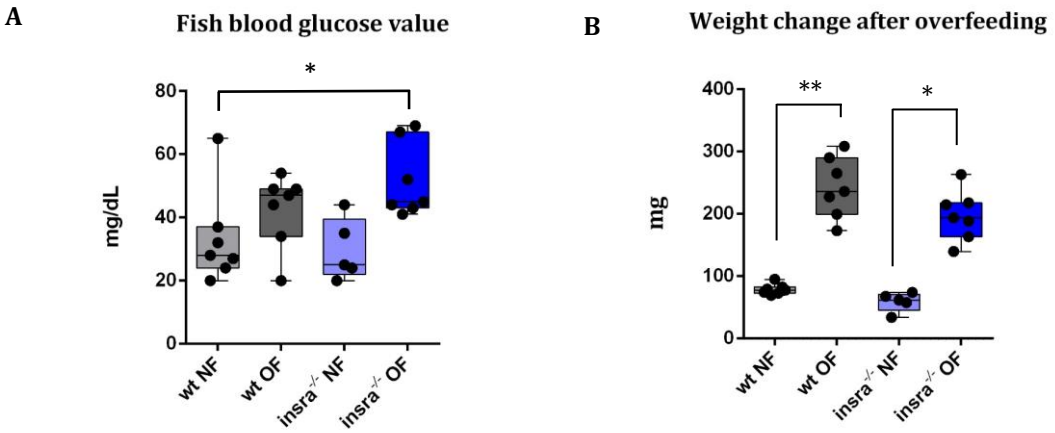

C

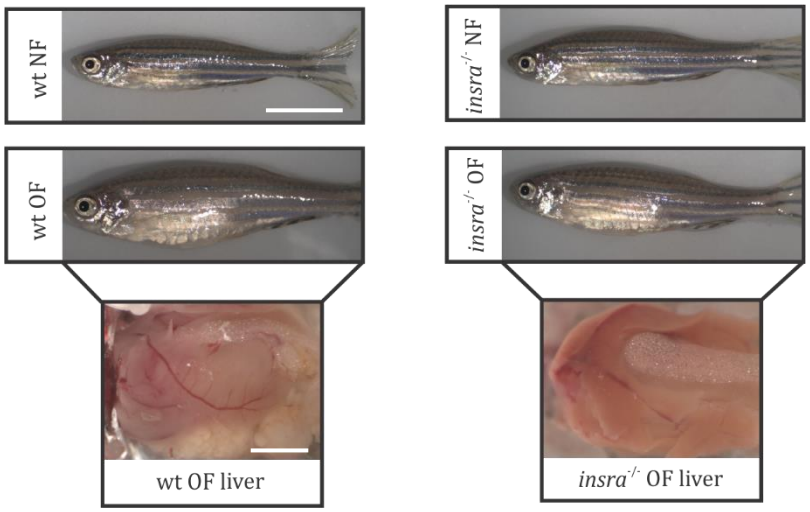

Figure 3.6.1: Overfeeding leads to fasting hyperglycemia in *insra*$^{-/-}$ fishes. (A) fasting hyperglycemia was seen after 8 weeks of overfeeding in wt and *insra*$^{-/-}$ fishes. (B) The weight of the fish is increased after overfeeding. C) Images of wt and *insra*$^{-/-}$ fishes after 4 months of Normalfeeding and Overfeeding. The scale bar represents 5mm in length. Liver of wt NF and *insra*$^{-/-}$ OF fish. The liver from *insra*$^{-/-}$ mutant fish has higher fat content thus more orange coloration based on observation under a bright field microscope. wt represents genotype *insra*$^{+/+}$/*insrb*$^{+/+}$; wt NF n= 7, wt OF n= 7, *insra*$^{-/-}$ NF n = 5, and *insra*$^{-/-}$ OF n = 7. For statistical analysis, one-way ANOVA is used, and significance is denoted as *P<0.05, **P<0.01; the graph represents mean ± SEM for each genotype. NF: normalfed, OF: overfed. The upper white scale bar with the whole fish represents 500µm in length. The scale bar on the liver picture represents 100µm in length.

For the overfeeding and subsequent phenotypic analysis, only *insra*$^{-/-}$ fish were selected based on two reasons. The first is the evidence of hyperglycemia and fatty liver in other fish with a mutation in the *insra* gene (Riddle *et al*., 2018). Secondly, in the early stage, in *insra*$^{-/-}$ larvae, whole body glucose values of *insra*$^{-/-}$ were higher than *insrb*$^{-/-}$ even though both were not higher than wt. Moreover, I have found higher metabolic alteration compared to the *insrb*$^{-/-}$. In summary, loss of Insra and Insrb does not result in hyperglycemia in the early stages but overfeeding can create glycemic stress which leads to fasting high blood sugar in *insra*$^{-/-}$ fishes.

3.7 Higher ectopic sprouting is seen in over-fed *insra*$^{-/-}$ retina and in normal-fed *insrb*$^{-/-}$ retina

Loss of Insra and Insrb affects the hyaloid-retinal vasculature during the larval stage. The vessel's diameter was higher in mutants at 120hpf. The abnormalities of the hyaloid vessels that are seen during the early stages can also be present in the adult stages (Jung *et al*., 2016; Wiggenhauser *et al*., 2020). So I have isolated the retina of *insra*$^{-/-}$ and *insrb*$^{-/-}$ fish and observed them under a confocal microscope (3.7.1 A & B).

As in the previous section, I have explained why only *insra*$^{-/-}$ fish were used to investigate the effect of overfeeding. Subsequently, isolation of retinal vessels and analysis was done with the retina from wt and *insra*$^{-/-}$ with NF and OF treatment. However, for *insrb*$^{-/-}$ fish, I have selected only the normalfed fish (3.7.1 B). The background of this selection process is the phenotype observed during the early stage. The hyaloid vessels diameter was increased in *insrb*$^{-/-}$ so I suspected that the retina of *insrb*$^{-/-}$ fish would be affected without any hyperglycemic stress.

A

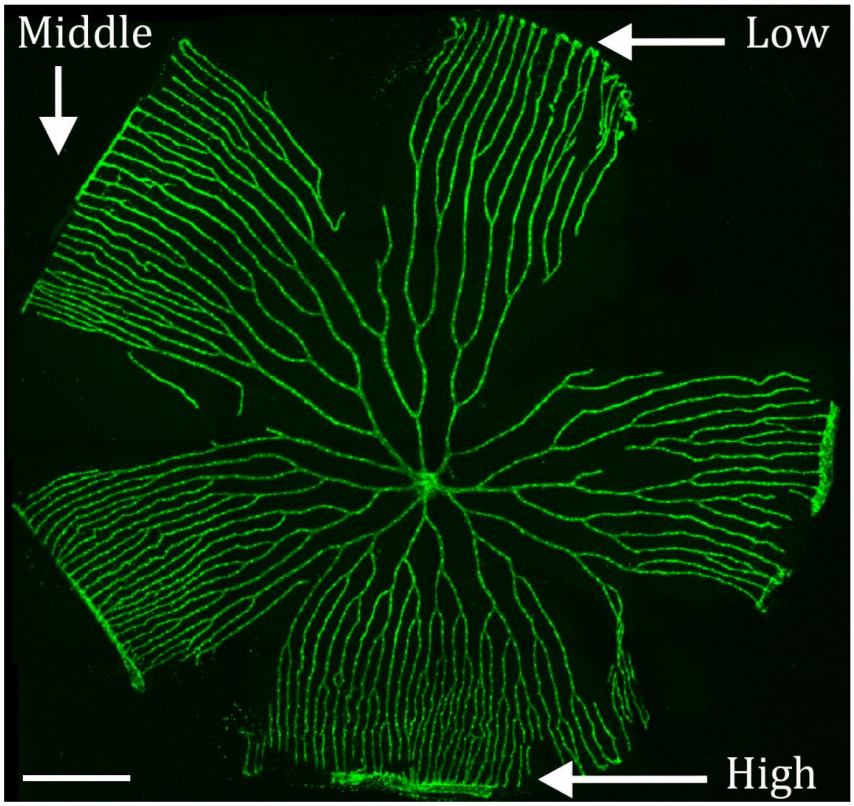

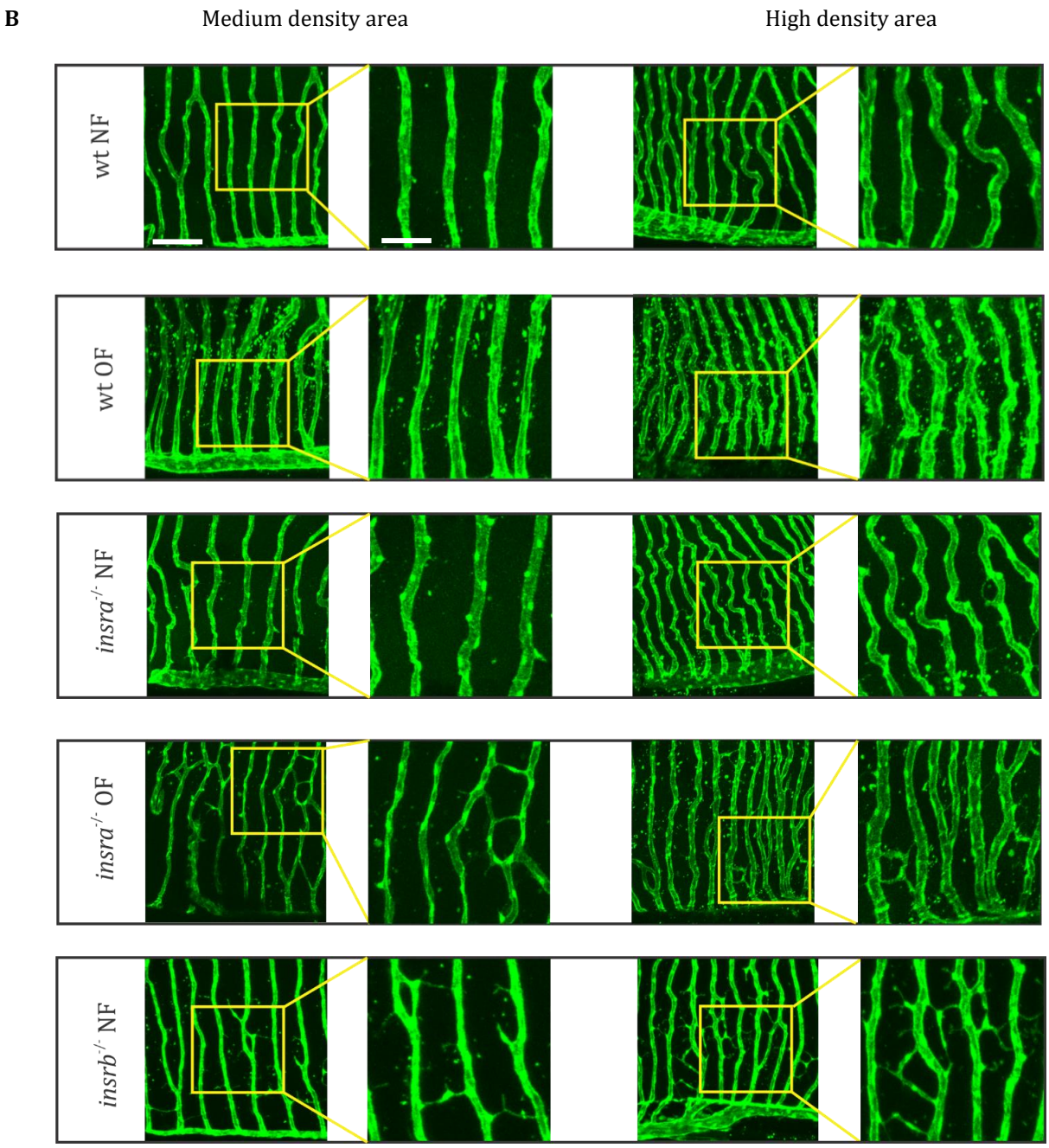

Figure 3.7.1: Higher number of retinal blood vessel sprouts were seen in over-fed *insra*$^{-/-}$ fish and normal-fed *insrb*$^{-/-}$ fish. (A) The whole vasculature of a single retina from *Tg(fli1:EGFP)* when isolated and spread on a coverslip. There are three different zones in each retina depending on the density of vessels: High, middle, and low. The white scale bar represents 350µm in length (B) For quantification, each retinal region was divided into 350µm squares. In each retina, there is a low, middle, and high-density region of vessels. The images of the squares are from the high and middle dense region from

fish of different genotypes. The white scale bar in the left represents 100µm and the scale bar in the zoomed image represents 50µm.

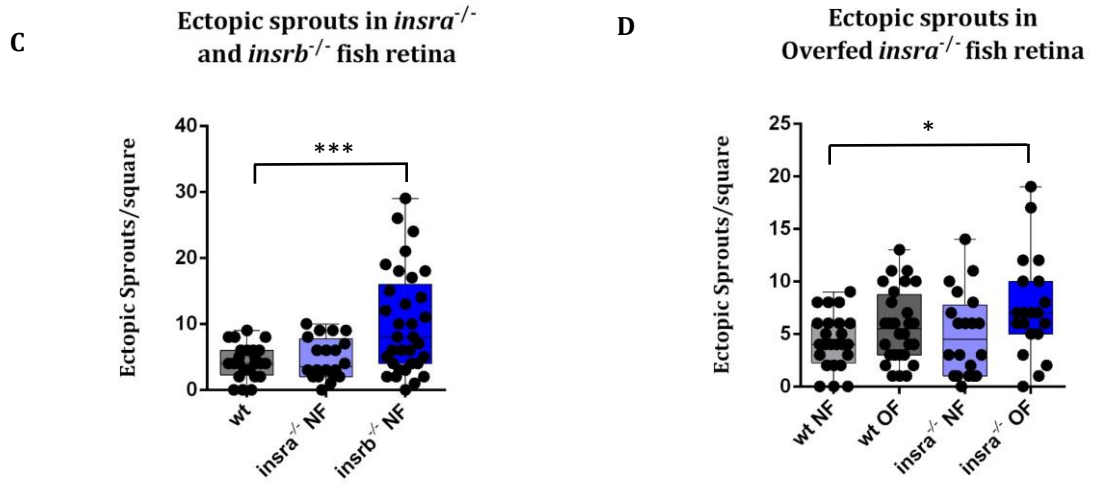

3.7.1 (C) Under a normal feeding regime, there is a higher number of sprouts in the *insrb*$^{-/-}$ fish retina but no change is found in the *insra*$^{-/-}$ retina. (D) Overfeeding leads to higher sprouting in the *insra*$^{-/-}$ retina. Here, wt represents genotype *insra*$^{+/+}$/*insrb*$^{+/+}$; number of fishes wt NF n= 7, wt OF n= 7, insra$^{-/-}$ NF n = 5 and *insra*$^{-/-}$ OF n = 7, *insrb*$^{-/-}$ n=4 . For statistical analysis, one-way ANOVA is used and significance is denoted as *P<0.05, ***P<0.001; the graph represents mean ± SEM for each genotype.

3.8 Symptoms like early stage kidney disease were seen in the kidney of Insra depleted over-fed zebrafish

pronephros morphology and function were not affected by the depletion of Insra and Insrb in the developmental stage of zebrafish. Along with that, since DKD is often not diagnosed until the late stage, to analyze if there is any effect of insulin receptor depletion on adult fish, I have performed histological analysis on the kidney from wt and *insra*$^{-/-}$ fish both in normalfed and overfed states. Besides several markers like urinary albumin, serum creatinine, and GFR measurement as signs of DKD, pathological analysis is widely accepted as the only tool for estimation of renal damage (Sharma *et al*., 2013; Suarez *et al*. 2013). For this analysis, I have adopted Periodic Acid-Schiff (PAS) staining method. However, I have not

found a visible pattern of changes among the glomerular structure in the wt or the mutant fishes regardless they were overfed or not (Fig 3.8.1).

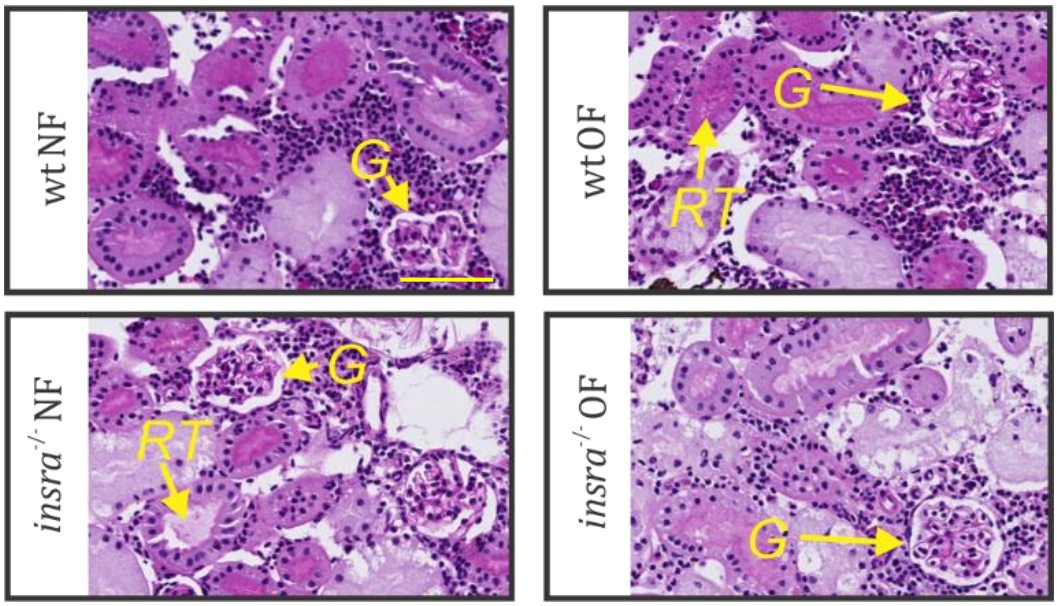

Fig 3.8.1: knocking out *insra* and hyperglycemia due to overfeeding in those mutants does not alter the glomerular structure. This figure shows the PAS stained thin sections of adult zebrafish kidneys both from NF and OF groups. The glomerular or renal tubular structure was not affected in control or mutant fish. Here, G indicates glomerulus, T indicates tubules. NF: normalfed, OF: overfed. The yellow scale bar represents 50µm.

Although PAS staining provides the possibility for histological analysis of the kidney but the analysis of ultrastructure is not possible. In the case of the severely affected kidney, glomerulosclerosis can be identified by the PAS staining method but in the early stages of kidney disease where some lesions are characterized by thickening of the glomerular basement membrane (GMB) can only be identified by electron microscopy analysis (Suarez *et al*. 2013). Reminding this point of view, I have analyzed the electron microscopy images of zebrafish kidneys from wt and *insra*$^{-/-}$ fish taken by Christoph Tabler. There was no change observed in the ultrastructure of wt fish kidney and overfeeding for 8 weeks does not affect it too. However, GBM structure in the kidney in the OF *insra*$^{-/-}$ fish was affected. (Fig 3.8.2).

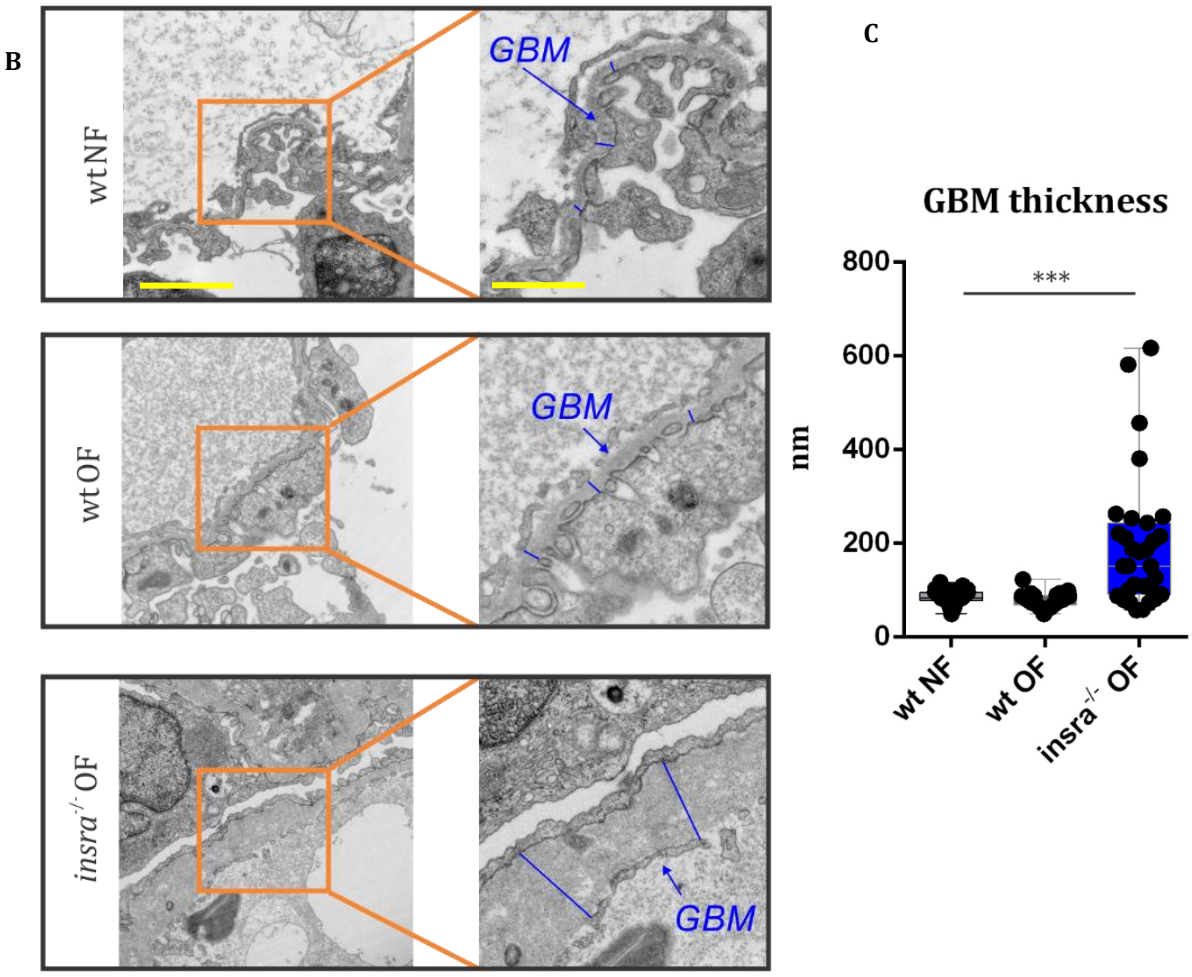

Figure 3.8.2. Kidneys of *insra*$^{-/-}$ OF fish are affected by GBM thickening when they are overfed. (A) The glomerular basement membrane structure of zebrafish kidney. Glomerular structure from insra$^{-/-}$ OF and the GBM was thickened. wt represents genotype *insra*$^{+/+}$/*insrb*$^{+/+}$, NF: normalfed, OF: overfed. GBM: glomerular basement membrane. The yellow scale bar on the left represents 250nm and on the zoomed image represents 500nm, the number of glomeruli analyzed per group was 12. For the analysis, EM images of several glomeruli from the kidney were taken and thickness was measured. The mean value of each glomerulus was taken and final statistical analysis was done with these mean GBM thickness values.

Even though zebrafish kidneys can regenerate after acute kidney injury (Sander & Davidson, 2014), I wanted to investigate the extent of the damage caused by insulin resistance. For this experiment, *insra*$^{-/-}$ NF fish were not selected for EM imaging. Due to the reduced availability

of the electron microscope and sample processing, we had to select only three groups of fish. Based on the condition and other phenotypes after overfeeding, *insra*$^{-/-}$NF fish kidney was excluded. For the same reason, the experiment on *insrb*$^{-/-}$ adult fish was not done.

3.9 Fatty acid content is increased in muscles but not in liver of overfed *insra*$^{-/-}$ fishes

I have seen that most of the saturated and unsaturated fatty acids are increased in *insra*$^{-/-}$ and *insrb*$^{-/-}$ mutant larvae at 96hpf. Moreover, I have observed that the liver from overfed mutant fish has more fat accumulation in the liver when I observe them under a microscope. I have performed an analysis of the metabolites of the liver and muscle tissue collected from wt and *insra*$^{-/-}$ fish.

The analysis was done using the FAME-GC-MS technique and livers from 3 fishes were used in each group. I have not seen any significant changes among wt fishes regardless of the feeding. Interestingly, there was consistency in the other three groups for fatty acid content but with the *insra*$^{-/-}$ OF fish, I have seen higher saturated fatty acid content in specific fish. The deviation among the fishes was higher than in other fish groups (Fig 3.9.1).

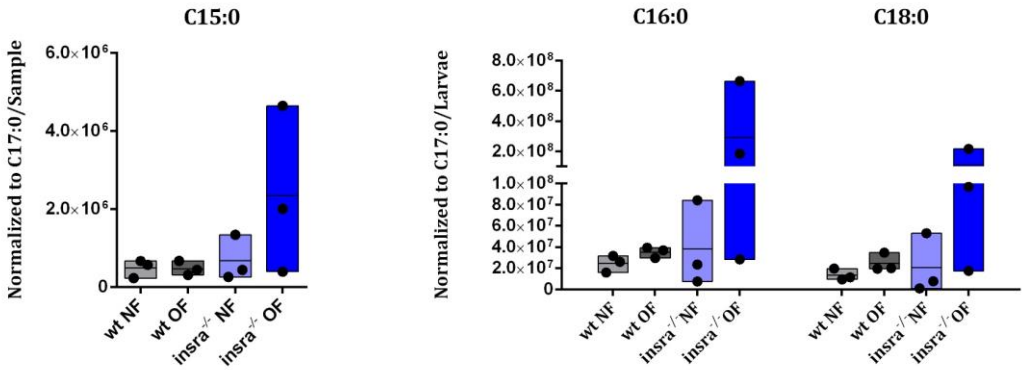

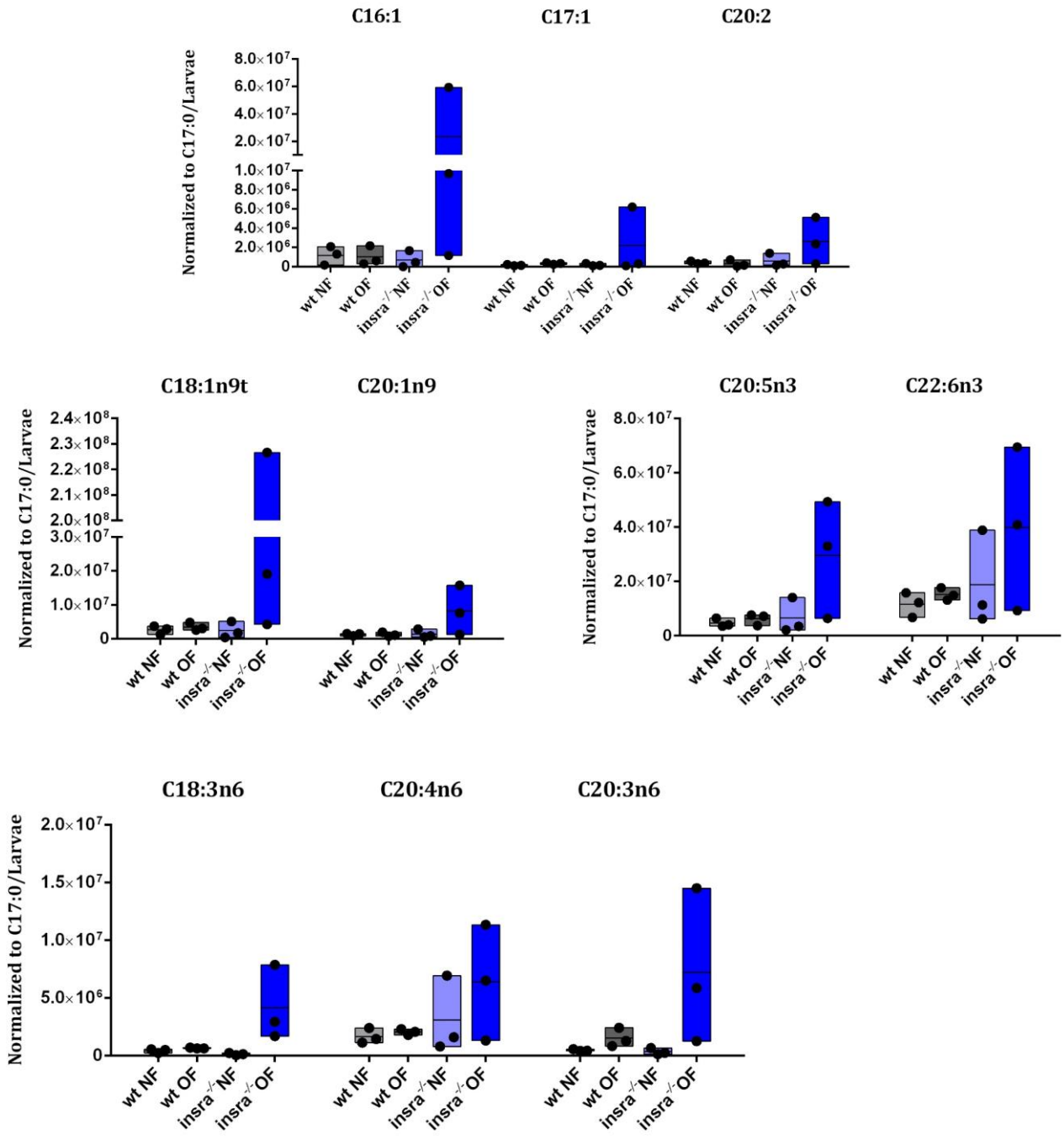

Figure 3.9.1: Overfeeding can increase fatty acid content in *insra*$^{-/-}$ zebrafish liver. In the graph, NF= Normal fed, OV = Overfed. *insra*$^{+/+}$ NF n =3, *insra*$^{+/+}$ OF n = 3, *insra*$^{-/-}$ NF n = 3, *insra*$^{-/-}$ OF n=3 readings, the graph represents mean value of fatty acid content ± SEM for each genotype. Livers were isolated from euthanized zebrafish and immediately preserved in liquid nitrogen for metabolomics analysis where the FAME-GC-MS technique was used. The calculated amount was then normalized to C17:0/sample.

I have also analyzed fatty acid content in the skeletal muscle tissues collected from the same four groups of fish and found that several saturated and polyunsaturated acids are increased in *insra*$^{-/-}$ fish. (Fig 3.9.2).

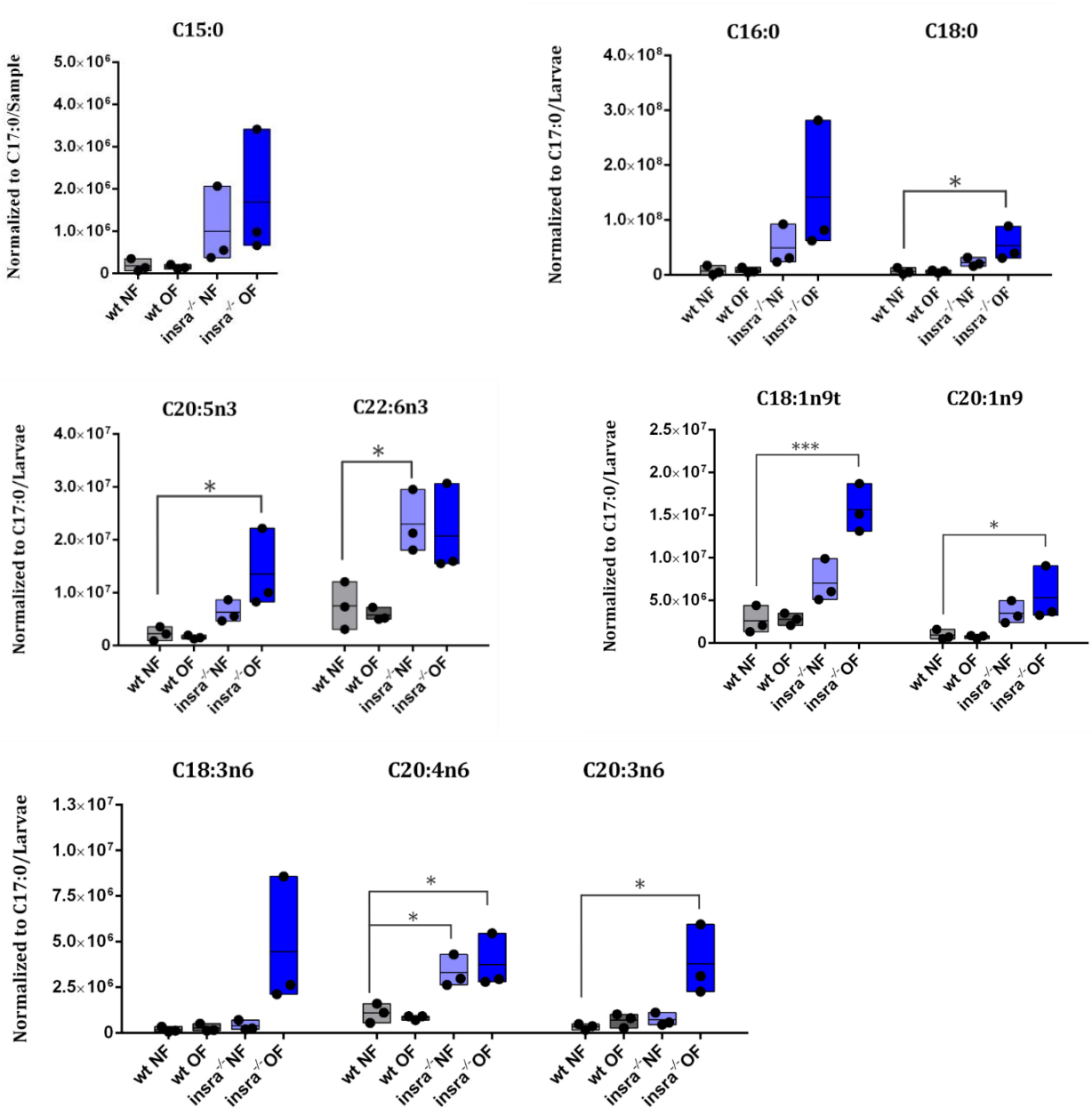

Figure 3.9.2: Overfeeding can increase fatty acid content in insra$^{-/-}$ zebrafish skeletal muscle. In the graph, NF= Normal fed, OV = Overfed. *insra*$^{+/+}$ NF n =3, *insra*$^{+/+}$ OF n = 3, *insra*$^{-/-}$ NF n = 3, *insra*$^{-/-}$ OF n=3 readings. For statistical analysis, one-way ANOVA is used, and significance is denoted as *P<0.05,

**P<0.01, ***P<0.001; the graph represents mean ± SEM for each genotype. Livers were isolated from euthanized zebrafish and immediately preserved in liquid nitrogen for metabolomics analysis where the FAME-GC-MS technique was used. The calculated amount was then normalized to C17:0/sample.

4. Discussion

This study was carried out to characterize the abnormalities created by the knockout of insulin receptors (*insra* and *insrb*) in zebrafish. The major outcomes from this study are summarized below:

i) There were no changes in the morphology in *insra* and *insrb* mutants during early and adult stages, hence, no compensation for gene knockouts.

ii) No change was found in whole body glucose in mutant zebrafish larvae, however overfeeding led to fasting hyperglycemia in adult *insra*$^{-/-}$ fish.

iii) Knockout of insra and insrb resulted in retinal vessel thickening in early stages.

iv) Increased ectopic sprouts were observed in *insrb*$^{-/-}$ adult fish under NF conditions, whereas, only OF *insra*$^{-/-}$ fishes showed similar outcomes.

v) Depletion of insulin receptors does not affect the early developing kidneys in the zebrafish embryo. But overfeeding can lead to GBM thickening which is considered an early stage of nephropathy.

vi) Metabolic pathways were altered, such as high fatty acid and cholesterol are observed in *insr* mutant zebrafish larvae and adult fish muscle tissues.

4.1 Depletion of Insr doesn't cause hyperglycemia in the early stage but overfeeding leads to high fasting blood glucose in *insra*$^{-/-}$ fish

Type 2 diabetes (T2D) consists of 95% of the diabetics in the world and insulin resistance is the hallmark of T2D. Not only the underlying pathway to T2D, but insulin resistance itself is also considered a disease denoted as either resistance syndrome A, syndrome X, Donohue Syndrome, Rabson Mendenhall syndrome, or leprechaunism which can be caused by the biallelic mutations in the insulin receptor gene (Falik Zaccai *et al*., 2014). Infants with a mutation in the insulin receptor gene have been found before with hyperglycemia, severe

growth retardation, and physiological deformities (Rojek *et al*., 2021; Saltiel & Kahn, 2012; Wertheimer *et al*., 1993).

Previously *insr* knockout (KO) mice have been generated, both general and tissue-specific to investigate the physiological impact of Insr depletion. Those research elucidated glucose homeostasis, fatty acid composition, weight changes, and physiological properties in mice (Hernandez-Ono *et al*., 2005, Michael MD *et al*., 2000, Kim *et al*., 2000). Furthermore, research on *insr* KO zebrafish also showed several changes in the regulation of enzymes involved in metabolism including glycolysis and gluconeogenesis (Gong *et al.*, 2018; B. Y. Yang *et al.*, 2018). Mutation in the insulin receptor gene in the cavefish population also causes physiological changes compared to their river-adapted population (Riddle *et al*., 2018). Keeping all these data on insulin receptors in various species in mind and the advantage of having transgenic zebrafish, the focus of this research is to investigate the impact of the loss of insulin receptors in the development of microvascular complications.

The physiological conditions of *insr* mutants vary among species. There have been reported cases of 5 homozygous null *Insr* mutations in humans and all of them had severe intrauterine growth retardation, while in mice there is only slight (~10%) retardation (Biddinger & Kahn, 2006; Kitamura, Kahn, & Accili, 2003a; Rojek *et al.*, 2021) which suggest that relationship of insulin signaling with the growth of the fetus is varied among species. In one instance, an one year old child with deletion of both alleles of insulin receptor gene has been found alive, however, there has been no update on the condition of that child afterward reported (Wertheimer *et al*., 1993). Nonetheless, according to our experiment, in *insra*$^{-/-}$ and *insrb*$^{-/-}$ there has been no symptoms of physiological and morphological abnormalities at their early stages (on day 2, 3, 4, and 5) and develop normally into adulthood when kept and fed with normal fish feed such as *Artemia salina* and commercial fish flakes. *Ins*$^{+/-}$ mice do not suffer from any severe physiological change but *insr*$^{-/-}$ mice develop symptoms like ketoacidosis, skeletal muscle hypertrophy and die within 7 days after birth. Similar to the *insr*$^{-/-}$ mice double knockout *insra*$^{-/-}$/*insrb*$^{-/-}$ generated from *insra*$^{+/-}$ crossing with *insrb*$^{+/-}$ fish also does not survive beyond the juvenile stage. This outcome is also coherent with the observation on doubt mutant zebrafish by Gong *et al*., 2018. However, they observed heart

cardiac defects in the *insra*$^{-/-}$/*insrb*$^{-/-}$ during the developmental phase which were not investigated during this project.

In mammals, 70-90% of oral glucose load is disposed to the skeletal muscle. Interestingly, Muscle-specific *insr* KO mice are euglycemic and do not develop glucose intolerance (Bruning et al. 1998). A similar scenario is also seen in fat cell-specific *insr* KO mice. fat cell-specific *insr* knockout protects against insulin resistance syndrome in mice and lives longer compared to control mice. Although glucose transportation in hepatocytes is not insulin-dependent and is not through GLUT-4 like skeletal muscle rather during fed state (Rui, 2014), liver cell-specific Insr knockout shows mild fasting hyperglycemia but strong impaired glucose tolerance. This happens rather because of the insulin-sensitive nature of the hepatocytes in maintaining the blood glucose and fatty acid oxidation through gluconeogenesis and lipogenesis (Bazotte, *et al*., 2014; Kitamura *et al*., 2003a) and not because of insulin-dependent glucose transport. The *insr* KO in β-cells elucidates some autoendocrine action of the insulin hormone too. β-cell specific KO mice have normal fasting and fed blood sugar levels, however, they develop altered glucose tolerance at the age of two months which deteriorates as they grow older. These mice are smaller compared to their control counterpart at the age of 4 months Kulkarni *et al.,* 1999).

Along with the variation of glucose levels in tissue-specific mice models, It is reported that *insra*$^{-/-}$ and *insrb*$^{-/-}$ zebrafish have higher glucose than their wt counterpart and among the three groups, *insra*$^{-/-}$ had the highest glucose content (B. Yang *et al*., 2017). However, I have found the *insra*$^{-/-}$ and *insrb*$^{-/-}$ glucose content to be completely normal. For my experiments, the *insra*$^{-/-}$ and *insrb*$^{-/-}$ were generated in Tg(*fli1:EGFP*) and Tg(*Wt1B:EGFP*) transgenic line while the mutants reported by Yang *et al*., 2018 were in Wild-type (AB). There has been no research conducted on the difference of insulin signaling on transgenic lines versus non-transgenic lines in zebrafish, so I suspect it is not because of the transgenic line of zebrafish used for this experiment rather the way glucose measurement is performed. Yang *et al*. measured by collecting part of two larvae and merged it to use as a single test sample. Whereas I have created a pool of 45-50 mutant larvae as one sample and measured the glucose values accordingly. As I have previously mentioned that *insra*$^{+/-}$ mice have normal physiology and do not develop hyperglycemia (Wertheimer *et al*., 1993) so having two genes

for insulin receptors in zebrafish might have contributed to maintaining glucose even without overexpression of the genes in knockout conditions.

Depletion of Insra and Insrb leads to postprandial high glucose in adult fishes and a decrease of the enzyme involved in glycolysis such as *hkdc1, gck, aldoaa, pklr,* and *gpia.* The glucose level is higher in *insra*$^{-/-}$ than in *insrb*$^{-/-}$ fish and the decrease of glycolytic enzymes in *insra*$^{-/-}$ are also higher than in *insrb*$^{-/-}$ fish (B. Y. Yang *et al*., 2018). However, in my experiments, I have not measured the postprandial blood glucose as the focus of the research is to investigate the microvascular complications and these complications are majorly late-onset diseases. Instead, keeping the published data in mind, I opted for 8 weeks of an overfeeding regime (as described in Oka *et al.*, 2010) in *insra*$^{-/-}$. The idea was to challenge the control of blood glucose in mutants which might lead to microvascular complications.

Overfeeding for 8 weeks leads to fasting high glucose in *insra*$^{-/-}$ fish while the normalfed *insra*$^{-/-}$ fish were not hyperglycemic. In a normal fed condition, one Insr can facilitate glucose entrance into cells, overfeeding results in a glycemic challenge that cannot be met by one single Insr. Zebrafish from wt and *insra*$^{-/-}$ both groups gained weight after overfeeding regime, whereas the gain of weight in wt was higher compared to the mutants. This finding was in contrast to the findings by Riddle et al., 2018 in insulin-resistant cavefish but similar to the findings in mammals. Overfed *insra*$^{-/-}$ fish has also fatty liver that is similar to the insulin-resistant cavefish and infant with a null mutation in the *insr* gene (Aspiras *et al*., 2015, Rojek et al., 2021). Tissue-specific knockout can have different physiological properties in animals based on gender such as neuronal insulin receptor KO mice showing varied properties between female and male mice. Female mice have increased body weight and food intake compared to their male counterpart (Bruning *et al*., 2000), however, in *insr* KO zebrafish, there have not been such variations based on sexes marked in my experiments.

So far, *insr* KO zebrafish carry similarities with tissue-specific insr KO mice and some The experiment with overfeeding on mutants was done with only *insra*$^{-/-}$ fish because of several reasons. The first one was a reference to the observation on cavefish which has a mutation in the *insra* gene and the second was the unavailability of *insrb*$^{-/-}$ mutants.

4.2 *insr* knockout leads to metabolic alteration in zebrafish

In addition to playing a role in glucose transport, insulin signaling regulates several metabolic functions in the body through different pathways (Brownlee, 2005). Insulin signaling in the liver promotes gluconeogenesis and suppress lipolysis which helps in balancing glucose level in the bloodstream. Furthermore, Insulin resistance leads to de novo lipogenesis by inhibiting the hypoglycemic effects of insulin, via activation of sterol regulatory element-binding protein (SREBP1) (Winters *et al*., 2020). The survivability of infants suffering from null insulin receptors is severely low and there has not been much data on the changes of the metabolites in the bloodstream, nor enough data available in *insr*$^{-/-}$ mice because of their early death (within 72h) with ketoacidosis. However, striking variations in TG level and free fatty acid levels are seen among different tissue-specific knockout mice. Neuron-specific insr KO in mice leads to 30% higher serum triglycerides. Interestingly, adipocyte-specific KO mice have decreased serum TG levels with unchanged free fatty acid in the serum. Whereas muscle-specific insr KO mice have 38% increased whole-body fat and 53% increased epididymal fat pad weight while 43% increase in serum triglycerides and a 16% increase in free fatty acids. Hepatocyte-specific insr KO mice have decreased rates of hepatic triglyceride secretion but serum albumin levels are decreased by half.

Changes in different metabolites happen along with the passing of time in zebrafish embryos [4, 8, 12, 24, 48 hpf] (Y. Huang *et al*., 2013). Zebrafish being teleost fish also has a well-developed lipid metabolism system like mammals which starts developing at 24hpf (Fraher *et al*., 2016). Yolk sacks full of lipids provide nutrition for up to 5 days in the zebrafish embryo and thus can change the way lipid is metabolized during early days. Nearly one-fourth of lipid species increases from 0 to 24 hpf, including cholesterol, phospholipids, triglycerides, cholesterol esters, ceramides, and other less abundant lipids (Fraher *et al*., 2016; Quinlivan & Farber, 2017) and at 4 dpf, multiple cell types required for lipid digestions are differentiated active (Wallace *et al*., 2005). Furthermore, enzymes involved in lipid processing such as elongases, phospholipases are active in zebrafish's early stages. as insulin signaling modulates downstream metabolic pathways such as glycolysis, gluconeogenesis, lipolysis, etc. knocking out the *insr* gene would naturally affect these processes. Enzymes of

glycolysis have been downregulated while enzymes catalyzing gluconeogenesis have been upregulated in the *insra*$^{-/-}$ and *insrb*$^{-/-}$ zebrafish larvae. Transcriptome analysis shows that like larvae, gluconeogenic enzymes like glucose-6-phosphatase catalytic subunit 1a (*g6pca.1*) and phosphofructokinase muscle a (*pfkma*) is upregulated whereas glycolytic genes glucokinase (gck), Lactate dehydrogenase A (*ldha*), Triosephosphate isomerase (*tpi1a*), Hexokinase (*hkdc1*), Pyruvate kinase for liver and RBC (*pklr*) has been downregulated (B. Yang *et al*., 2017).

Till now, studies were done by measurements of TG or fatty acids in serums or organs but a specific assessment of metabolites has not been investigated. Several Saturated, Monounsaturated, Polyunsaturated fatty acid, and cholesterol content has been increased in the mutant larvae and the highest increase was seen in the *insra*$^{-/-}$.

Not just during the developmental stage, this metabolic discrepancy is also seen in adult stages. fatty acid content especially unsaturated fatty acids are increased in the skeletal muscles of *insra*$^{-/-}$ overfed fish. Nonetheless, neither saturated nor unsaturated fatty acids were changed in the livers collected from *insra*$^{-/-}$ fish even though fatty livers were identified under light microscopes. Metabolite analysis in *db/db* and *ob/ob* mice shows an increase of diverse lipid classes including fatty acids, fatty alcohols after two weeks of feeding (Giesbertz *et al.*, 2015) though there was only mild hyperglycemia in *ob/ob* mice. Two out of three patients suffering from type 2 diabetes often have nonalcoholic fatty liver disease (NAFLD) and in those NAFLD patients, often the free fatty acids (FFAs) are remarkably increased (Khan *et al*., 2019). There can be one explanation for the higher fatty acids in skeletal muscles; I assume the accumulation of lipids in the muscle might be the result of decreased fatty acid clearance from the liver.

However downregulation of lipogenic enzymes in *insra*$^{-/-}$ fish but not in *insrb*$^{-/-}$ fish. As in the previous sections I described that the changes of metabolites have been investigated only in OF *insra*$^{-/-}$ but not in *insrb*$^{-/-}$ fish, the investigation of the effect of overfeeding in liver and muscle can elucidate more on the levels of fatty acids in the organs off the *insrb*$^{-/-}$ fish.

Along with TG, free fatty acids and glucose level, amino acids, and other metabolites are also changed in patients with T2D, branched-chain amino acids: Valine, leucine, and isoleucine is

up to 2 times higher than healthy persons (Guasch-Ferré *et al*., 2016, Roberts *et al.,* 2014). However, no change in these three marker amino acids is changed in the mutants larvae. Glycine is a non-essential amino acid that is involved in the conjugation of bile acids (BAs), which are required for lipid absorption, digestion, and cholesterol homeostasis regulation. In patients with obesity and T2D, plasma glycine concentration is lower than in healthy persons (Okekunle *et al*., 2017). Glycine levels in plasma collected from *ob/ob* and *db/db* mice are also lower than the wt mice (Giesbertz *et al.,* 2015). However, my findings are in contrast with the findings in mice and patients as in *insra*$^{-/-}$ larvae, glycine levels are higher whereas, in *insrb*$^{-/-}$, it is relatively unchanged. My assumption would be the cellular machinery might increase glycine production to compensate for reduced PKB/Akt signaling as Protein kinase B/mTOR1 (PKB) signaling is modulated by glycine availability (Sun *et al*. 2016).

Pyruvates produced in the glycolysis converted into acetyl-coA in the mitochondria take part in the citric acid cycle produces ATP. Citrate is produced in mitochondria from pyruvate is also interconvertible with isocitrate. An alternative pathway of citrate production is through the glutamine-dependent pathway (Icard *et al*., 2021). Among primary metabolites analyzed, citric acid was increased in *insra*$^{-/-}$ larvae. As in the insulin resistance state, with the rate of glycolysis gone down, this increase of citrate is possibly through acetyl-CoA generated from the breakdown of fatty acid which I have found to be abundant in mutant larvae (Lunt & Vander Heiden, 2011).

Some metabolites in diabetes and NAFLD patients are considered as biomarkers of disease progression. Some data I have found is similar to the findings in human patients, however, some are in contrast. Further investigation on this could help us understand more if there are some new parameters in the insulin resistance state or specific to fish metabolism.

4.3 Loss of Insr leads to vascular abnormalities in early and adult stages retina

In patients with diabetes or insulin resistance syndrome, disease progression in organs such as the retina, kidney, and peripheral organs often starts with the vascular system and associated cells. One of many, vascular damages plays a role as the background of diabetic

macular edema and proliferative retinopathy (Pemp *et al*. 2013). Gradually progressive alterations of the microvasculature in the retina can be used to characterize retinopathy in diabetes patients (Hammes, *et al.*, 2011). Moreover, microcirculatory dysfunction is proposed to have a role in peripheral nerve dysfunction too, moreover, endoneurial capillary density is often increased in diabetics compared to healthy persons, suggesting that capillary density plays in developing nerve ischemia (Feldman *et al*., 2019, Kim *et al*., 2012). These studies prove that in all the subsequent complications of diabetes, the vascular system has been affected.

Zebrafish have been used as a model organism for developmental and vascular research because of their ease of editing genes, early development of functional organs, well developed transgenic lines with transparency through which observation is possible (Heckler & Kroll, 2017; Middel, Hammes, & Kroll, 2021). In this project, I have used all these advantages to observe the impact of depletion of Insra and Insrb in the vasculature of zebrafish larvae in the trunk and retina. Vasculogenesis is defined as the de novo formation of the vascular network and the growth of new capillaries from existing blood vessels is regarded as angiogenesis which develops through sprouting (Cimpean and Raica, 2021). The primitive vasculature is initially formed by vasculogenesis but subsequent vessels are formed via angiogenesis (Gore et al., 2012). ISVs of the trunk form very early in all vertebrates and Dorsal Longitudinal Anastomotic Vessels (DLAV) formation arises from Dorsal Aorta (DA) and Posterior Cardinal Vein (PCV) (Isogai *et al*., 2001).

Hyperglycemia is touted as an effector of vasculogenesis and angiogenesis. High glucose leads to methylglyoxal formation which eventually increases the VEGF signaling and vascular malformation in zebrafish (Jörgens *et al*., 2015). Moreover, incubation in glucose solution leads to thickening of hyaloid vessels in zebrafish which could be reversed by anti-VEGF therapy as reported by Jung *et al*. As I described before in the previous section, in the *insra*$^{-/-}$ and *insrb*$^{-/-}$ larvae I have not observed any hyperglycemia, however loss of Insra results in increased hyperbranches in the ISVs but the loss of Insrb does not.

In zebrafish trunk and retinal vasculature, developmental processes have structurally some similarities as both involve endothelial cells and several factors like vascular endothelial

growth factor among others (Gore *et al.*, 2012). Mutation in the PlexinD1 receptor gene can affect both the trunks and the retinal vasculature which proves that trunk vasculature are not so different from than retina (Alvarez *et al*., 2009). Diabetic retinopathy is currently categorized based on the presence of vascular (and closely associated) lesions and the absence or presence of neovascularization. In addition to neovascularization, Changes in retinal vessel thickness are an important parameter in determining the state of Macular Edema in patients who have had diabetes for a long time. It is considered a pathological trait in patients suffering from diabetic eye disease Dilatation of retinal arterioles has been observed in the early stages of diabetic retinopathy (Ajaz *et al*., 2019). Retinal thickness has also been reported to change in patients with long-term DM and retinopathy (Wiemer *et al.*, 2008). Moreover, narrowing of retinal arterioles in T2D patients can lead to a reduction of diabetic retinopathy (Pederson *et al*. 2014).

Insra and Insrb depleted zebrafish larvae has similar phenotypes despite normal total glucose level. Hyaloid retinal vessel diameter was higher in the *insr* mutants and interesting to mention that the thickness was highest in *insrb*$^{-/-}$ larvae. Wiggenhauser et al., 2020 reported that zebrafish suffering from hyperglycemia due to ablation of Pdx1 has thicker hyaloid vessels and increased branches in the early stages. In *pdx1*$^{-/-}$ larvae, the proliferative diabetic retinopathy mimicking phenotype arises from increased nitric oxide signaling and VEGF expression. This phenotype can be rectified through the usage of inhibitors of nitric oxide synthase (NOS) and anti-VEGF therapy. NOS inhibitors can reduce the thickness of the vessel whereas anti-VEGF therapy can reduce branching. Recently published data by Qi et al., 2021 also shows that zebrafish larvae have higher branching in the hyaloid retinal vessel when injected with morpholino that blocks *insr* expression.

A recent study has shown that small diameters of retinal arterioles in patients with diabetes mellitus during childhood may predict the development of diabetes mellitus later in life (Broe *et al*. 2014). Besides the short term effect, the exposure to glucose solution also has long term implications as incubated zebrafish embryos during the early embryonic stage (3hpf-5dpf) can lead to higher retinal vessel sprouts in the adult stage (Singh *et al.*, 2019) which means the abnormalities seen can be carried to the later stage of life. So keeping the outcome of these studies, I have investigated the retinal vessels in *insra*$^{-/-}$ and *insrb*$^{-/-}$fishes.

Under normal feeding conditions, there were higher ectopic sprouts in *insrb*$^{-/-}$ fish. in *insra*$^{-/-}$ fish, no such change in the retina of the normalfed fish was seen, however overfeeding can lead to change in *insra*$^{-/-}$ fish. interestingly, hyaloid vessel diameter was highest in *insrb*$^{-/-}$ larvae followed by *insra*$^{-/-}$, and in *insrb*$^{-/-}$ adult fishes, no hyperglycemic stress or external factor was needed for the abnormalities to appear whereas for *insra*$^{-/-}$, only overfeeding leads to such an aberration.

higher sprouting in the retina of *pdx1*$^{-/-}$fish in adult stages which have postprandial hyperglycemia is also seen (Wiggenhauser *et al.*, 2020) and *glo1*$^{-/-}$ knockout zebrafish develop insulin resistance with hyperglycemia and also show similar phenotypes (Lodd *et al.*, 2019). Further research needs to be done to see, in the case of insulin resistance, it is carried over from early stage to adult or dedicatedly because of metabolic alteration.

There might be several possible reasons behind this hyaloid retinal phenotype. *insra*$^{-/-}$ and *insrb*$^{-/-}$ larvae might be due to the rather than hyperglycemia derived neovascularization. Insulin promotes vasodilation by increasing the production and bioavailability of nitric oxide in the vascular endothelium (Muniyappa & Shazene Yavuz, 2013). Interestingly opposite action of insulin signaling exists too as insulin induces secretion of endothelin-1 stimulating vasoconstriction (Muniyappa, *et al*., 2009). Insulin signaling modulates Akt/PI3K dependent and Ras/MAPK dependent downstream pathways. In the case of insulin resistance, the PI3K pathway is impaired but not the Ras/MAPK pathway (Jiang *et al*., 1999, Cusi *et al.* 2000). MAPK dependent cell proliferation pathway might be activated which results in angiogenesis in the trunk and retina. Knocking out of Insr leads to an increase in the expression of *igf-1* receptor. Igf-1 has a role in ocular neovascularization, that is why overexpression might result in the retinal vascular phenotypes seen in Insr devoid zebrafish. The involvement of eNOS in vascular formation can be another pathway that takes place through acylation. acylation of the enzyme by the myristate and palmitate is necessary for targeting the protein to localize (Michel, 1999). Myristic acid and Palmitic acid are significantly increased in insra and insrb zebrafish which might play a role in eNOS function and vessel dilation. Overall, with this experiments I have found that insr KO can affect trunk vasculature and increase of the diameter of retinal hyaloid vasculature albeit with varying degree in *insra*$^{-/-}$ and *insrb*$^{-/-}$ zebrafish.

4.4 Overfeeding can create preliminary-stage nephropathy phenotypes in *insra*$^{-/-}$ fish

Diabetic nephropathy (DN) affects 30% of T1D and 40% of T2D patients and is characterized by functional and structural changes in the kidney (O'Shaughnessy *et al.,* 2017, Alicic *et al*., 2017). To detect DN and to identify nephropathy progress, Invasive methods like staining with renal biopsies and non-invasive like albuminuria, and glomerular filtration rate (GFR) measurements have been widely adopted (Papal *et al*. 2010, Fox *et al*., 2012). During the early stage of DKD, GFR decline or albuminuria is often undetected and this stage is called the silent period (Najafian B, Mauer M. 2012). Nephropathy in diabetic patients develops gradually and thickening of the glomerular basement membrane (GBM) is the first structural change (Alicic et al., 2017). The GBM is composed of laminin, nidogen, heparin sulfate proteoglycans, and type IV collagen is a major functional part of the glomerular filtration barrier (Miner, 1999; Miner, 2012). GBM thickening is followed by endothelial fenestration, mesangial matrix expansion, and loss of podocytes foot processes. hyperglycemia dictates the mesangial cells to proliferate and produce matrix by activating VEGF and TGF-β (Ziyadeh et al., 2000).

Insulin resistance is implicated in the development of DN, by creating hyperglycemia or by modulating other signaling pathways (Gnudi *et al.*, 2016). Hyperglycemia can affect the kidney by generating ROS, increased oxygen demand in the renal cortex, downregulation of thrombomodulin, and activated protein C leading to endothelial dysfunction (Bock *et al*., 2013, Zeni *et al.*, 2017). Podocytes specific *insr* KO mice develop albuminuria, glomerulosclerosis, excessive matrix generation, and thickening of GBM without high glucose which proves that there are other mechanisms involved (Welsh *et al*., 2016). Insulin resistance also creates higher salt sensitivity leading to hypertension and renal function decline (Trevisan, R. *et al.* 1998; Vedovato, M. *et al*. 2004). For this project, I have analyzed the kidney (pronephros) phenotypes in developing and adult insulin-resistant zebrafish.

In hyperglycemic zebrafish embryos, the morphological structure of pronephros is altered, albuminuria-like phenotypes are seen and dystrophy of the podocytes foot processes is seen according to a study done by Sharma *et al.* 2016. However, I did not see any alteration in the morphological or functional change in the pronephros of *insra*$^{-/-}$ or *insrb*$^{-/-}$ during the early

stage. Further research needs to be done to investigate if this is due to the lack of hyperglycemia or the signaling process mediated by Insr is different in zebrafish podocytes.

As in the early developmental stage, insulin resistance does not affect the pronephros so I have investigated the effect of overfeeding on the kidney of *insra*$^{-/-}$ fish. There was no apparent glomerulosclerosis in the kidneys of wt and *insra*$^{-/-}$ fish regardless of the feeding procedure. However, electron microscopy revealed the presence of GBM thickening which was unidentified by PAS staining proving that early-stage phenotypes can only be detected by electron microscopy theorized by Davis *et al*. 2019. I assume that the extent of final damage to the glomerulus in wt NF and wt OF fish kidneys was not high because of regeneration and thus not identified (Sander & Davidson, 2014; Zhou *et al*., 2010). But in the case of *insra*$^{-/-}$ OF fish, exposure to high blood glucose for a longer period leads to higher damage, and kidney injury was identified by EM images.

Staining with Previous studies on animal models for diabetic nephropathy including mice have produced ambiguous phenotypes because no diabetic models can perfectly resemble nephropathy in humans (Betz *et al*., 2016, Azushima *et al*., 2017). There has not been a stark difference between T1D or T2D diabetic mice, among T1D models, Akita mice provide a closer resemblance to human nephropathy which includes kidney structure alterations, renal hypertrophy, and mesangial matrix expansion (Gurley *et al*., 2006). *db/db* or *ob/ob* mice suffer from obesity and hyperglycemia and the kidney is affected by mesangial expansion and albuminuria but without glomerulosclerosis (Chatzigeorgiou *et al*., 2009).

As in the corresponding result section, I have explained the reason for not investigating the kidneys of *insrb*$^{-/-}$. Further investigation using PAS staining and EM technique should be used with the *insrb*$^{-/-}$ fish to understand more about the development of kidney disease in zebrafish. Single nucleotide polymorphism in ELMO1 is associated with DKD, so research on ELMO1 expression in *insra*$^{-/-}$ and *insrb*$^{-/-}$ could help find out why some fishes are affected whereas others are not from the same genotype. (Doria, 2010, Sharma *et al*. 2016). Furthermore, gene expression analysis and further research could be done to find out more about DN in zebrafish.

5 Conclusion and outlook

Insulin resistance is the underlying physiology of patients suffering from T2D and further develop microvascular complications in the late stages. With my thesis I have analyzed the effect of loss Insr and if a microvascular complication arises due to insulin resistance in zebrafish. the findings are summarized in Fig 4.1.

The reason for normal glycemic level in *insra*$^{-/-}$ and *insrb*$^{-/-}$ despite IR depletion should be studied further. The next step might be to analyze the insulin like growth factors 1 and 2 (igf 1, igf2) and their role in the *insr* depleted state. Metabolite content is altered in *insr* mutant larvae. However, in adult fish, the measurement was done in *insra*$^{-/-}$ fish. Metabolite analysis in *insrb*$^{-/-}$ fish could reveal more details on the variations of underlying pathways. Furthermore, targeted metabolite analysis in the brain could be suggested as the brain responds differently compared to other organs like the liver and skeletal muscle.

While maintaining a euglycemic state, *insra*$^{-/-}$ zebrafish larvae show higher vascular sprouting in the trunk which I did not see in *insrb*$^{-/-}$ larvae. The hyaloid vessels of the retina in both the mutants are affected. VEGF-A and NO are touted as mediators of angiogenesis and are increased in the hyperglycemic state in zebrafish (Qi et al., 2021; Wiggenhauser et al., 2020). Further research on VEGF-A and NO in insulin-resistant euglycemic states could be investigated. Insulin resistance is often accompanied by hyperinsulinemia in the late stage (Dylan *et al*. 2019). Studies on hyperinsulinemia and its correlation with *igf1r/igf2r* could provide some indication on triggering angiogenesis. This data might provide a framework for research on the different processes for vascular patterning on the trunk and retina.

Overfeeding of *insra*$^{-/-}$ fish has a detrimental effect on blood glucose homeostasis, vascular formation, and kidney internal structure. But the effects in *insrb*$^{-/-}$ fish have not been yet analyzed. The next step of this research should be to observe the effect in *insrb*$^{-/-}$ under the overfeeding regime. Regulation of several genes is implicated in microvascular complications. The role of potential candidate genes like ELMO1 analysis in *insr* mutants might provide the background of the variation among fishes.

My research on *insr* knockout zebrafish shows several abnormalities and phenotypes which will help to understand how insulin resistance is related to diabetic complications. Prospects

can include IR mutant zebrafish as an animal model for disease/phenotype-based drug trials. Drugs against hyperglycemia have been effective in reducing phenotype even in patients with glycemic control. In the end, it can be speculated that the outcome of this research can help to discover pathways that affect diabetic patients. The future of this study includes the translation of the research in patients and finding out the possible mechanism of late stage complications in patients suffering from diabetes.

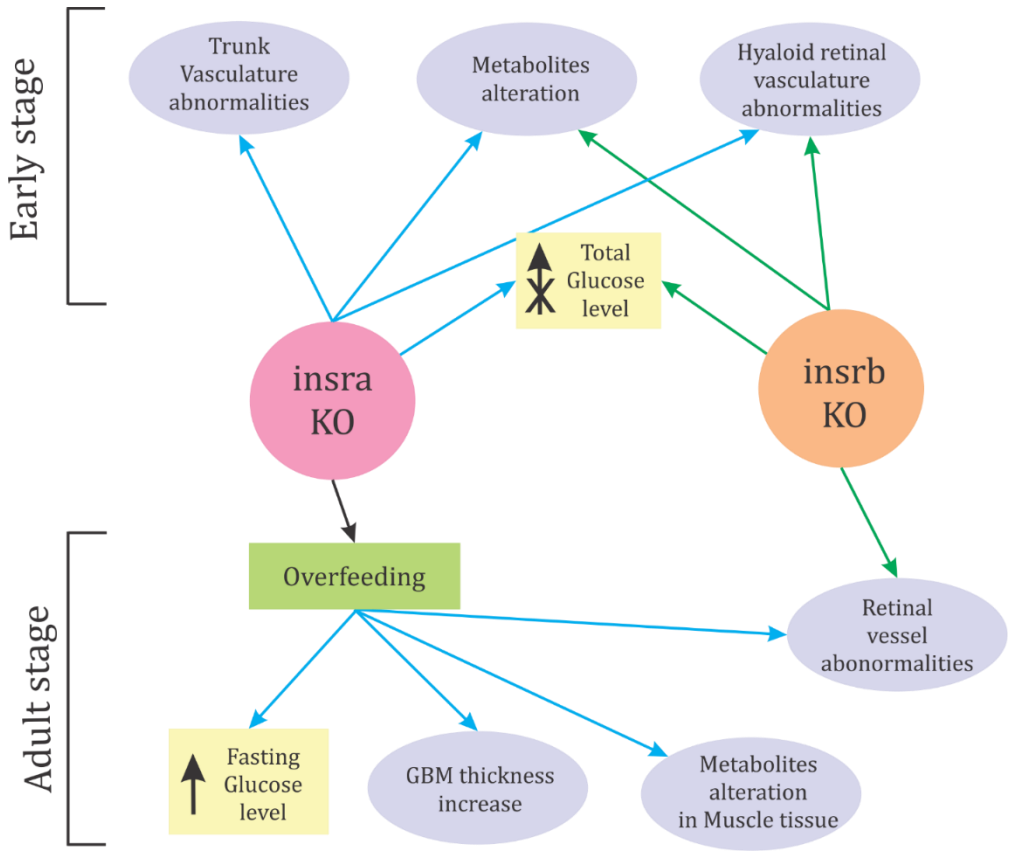

Figure 4.1: Effect of loss of Insr in zebrafish during early and adult stages. Knockout of *insra* and *insrb* leads to vascular damage in the retina and metabolic shift which can also be seen in insra adult fish after overfeeding. KO = Knockout.

5. List of Abbreviations

	°C	Degree Celsius
	µl	Microliter
	µm	Micrometer
	µM	Micromolar
	%	Percentage
A	ACE	Angiotensin-Converting-Enzyme
	ACE inhibitor	Angiotensin-Converting-Enzyme inhibitor
	ADP	Adenosine diphosphate
	AGE	Advanced glycation end product
	Amp	Ampicillin
	approx.	Approximately
	Arg	Arginine
	Asn	Asparagine
	Asp	Aspartate/aspartic acid
	ATP	Adenosine triphosphate
B	bp	Base pairs
	BSA	Bovine serum albumin
C	C14:0	Myristic acid
	C15:0	Pentadecanoic acid
	C16:0	Palmitic acid
	C16:1	Palmitoleic acid
	C18:0	Stearic acid
	C18:1n9	Oleic acid.

	C18:2n6	Linoleic acid
	C18:3n6	Gamma-Linoleic acid
	C20:0	Arachidic acid
	C20:2	Eicosadienoic acid
	C22:0	Behenic acid;
	C20:4n6	Arachidonic acid;
	C20:5n3	Eicosapentaenoic acid
	C22:6n3	Cervonic acid;
	C24:0	Lignoceric acid;
	$CaCl_2$	Calcium Chloride
	Cas9	CRISPR associated protein 9
	cDNA	Complementary deoxyribonucleic acid
	cm	Centimeter
	Co	Control
	CRISPR	Clustered regularly-interspaced short palindromic repeats
	CrisprCon	CRISPR Con gRNA
	Cys	Cysteine
D	Del	Deletion
	DHAP	Dihydroxyacetone phosphate
	DM	Diabetes Mellitus
	DN	Diabetic nephropathy
	DNA	Deoxyribonucleic acid
	dNTP	equal molar mix of the deoxy-nucleotides dATP, dCTP, dGTP and dTTP
	dpf	Days post fertilization
	DR	Diabetic retinopathy
	DT	Distal tubule

E	E. coli	Escherichia coli
	EDTA	EhylenDiamine-TetraAcetic acid
	EGFP	Enhanced Green Fluorescent Protein
	EM	electron Microscopy
	ESRD	End-Stage Renal Disease
	et al.	and others
F	fli	Friend leukemia integration1
G	G	Glomerulus
	g	Gram
	GBM	Glomerular Basement Membrane
	GC	Genetic compensation
	GC-MS	Gas chromatography-mass spectrometry
	GEF	Guanine nucleotide Exchange Factor
	GFB	Glomerular Filtration Barrier
	GFP	Green Fluorescent Protein
	Gln	Glutamine
	Glo1	Glyoxalase1
	Glu	Glutamic acid
	GLUT	Glucose transporter
	Gly	Glycine
	gRNA	Guide RNA
	GWAS	Genome wide association studies
H	h	Hours
	H_2O	Water

	HCL	Hydrochloric acid
	His	Histidine
	HMIT	H+/myoinositol transporter
	hpf	Hours post fertilization
	hpi	Hours post injection
	HPLC	High performance liquid chromatography
	Hz	Hertz
I	Igf1	Insulin like growth factor 1
	Igf1r	Insulin like growth factor 1 receptor
	Ile	Isoleucine
	Indel	Insertion and deletion
	INL	Inner nuclear layer
	IPL	Inner plexiform layer
	IR	Insulin receptor
K	kb	Kilo bases
	KCl	Potassium chloride
	kDa	Kilo Dalton
L	l	Liter
	LB	Lysogeny broth
	LC-MS/MS	Liquid chromatography-tandem mass spectometry
	Leu	Leucine
	Lys	Lysine
M	M	Molar
	Met	Methionine

	MG	Methylglyoxal
	mg	Milligram
	min	Minutes
	ml	Millilitre
	mM	Millimolar
	mmol	Millimol
	MO	Morpholino
	mRNA	Messenger RNA
N	n	Number of samples
	NaCl	Sodium chloride
	NADP(H)	Nicotinamide adenine dinucleotide phosphate
	NCBI	National Center for Biotechnology Information
	NF	Normal feeding
	nl	Nanoliter
	nm	Nanometre
	nmol	Nanomole
	NO	Nitric Oxide
	NOS	Nitric oxide synthase
	ns	Not Significant
O	OF	Overfeeding
	O_2	Oxygen
P	p	p-value (probability)
	PAM	Protospacer adjacent motif
	PAS	Periodic acid Schiff
	PBS P	hosphate buffered saline

	PCR	Polymerase chain reaction
	pdx1	Pancreatic and duodenal homeobox 1
	PFA	Paraformaldehyde
	Phe	Phenylalanine
	PKC	Protein kinase C
	pmol	Picomol
	Pro	Proline
	PT	Proximal tubule
	PTU	Phenylthiourea
Q	qPCR	Quantitative Real time polymerase chain reaction
R	RNA	Ribonucleic acid
	ROS	Reactive oxygen species
	rpm	Rounds per minute
	RT-PCR	Reverse transcription polymerase chain reaction
S	SD	Standard deviation
	SEM	Standard error of Mean
	SDS	Sodium dodecyl sulfate
	Ser	Serine
T	t	Extension time
	T	Annealing time
	TCA	Tricarboxylic acid
	Tg	Transgenic
	Thr	Threonie
	Tris	Tris-aminomethan
	Tyr	Tyrosine

U	UPLC-MS	Ultraperformance liquid chromatography-mass spectrometry
V	Val	Valine
	VEGF	Vascular endothelial growth factor
W	w/v	Weight/volume
	wt1b	Wilms tumor gene1b

6. Appendix

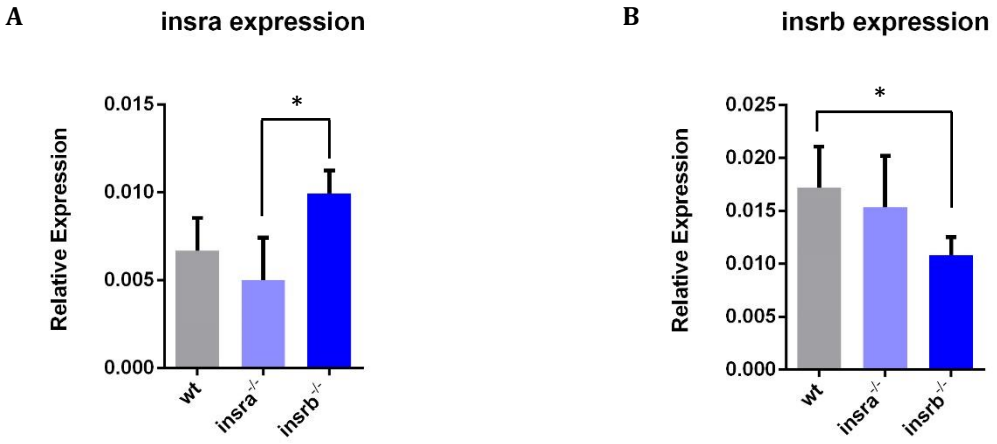

Figure: Expression of insra and insrb gene in insra$^{-/-}$ and insrb$^{-/-}$ zebrafish larvae compared to wt (insra$^{+/+}$/insrb$^{+/+}$). A) Insra gene is seen to be increased in insrb$^{-/-}$ mutant. B) There was no change observed in the expression of the insrb gene in any mutants or wt. The number of experiment/qPCR runs is n=4. cDNA produced from obtained mRNA at 96 hpf. For statistical analysis, one-way ANOVA is used and significance is denoted as *P<0.05, the graph represents mean ± SEM for each genotype.

The name of the fatty acids from the legends:

C14:0 = Myristic acid; C15:0 = Pentadecanoic acid; C16:0 = Palmitic acid; C18:0 = Stearic acid; C20:0 = Arachidic acid; C22:0 = Behenic acid; C24:0 = Lignoceric acid. C20:5n3 = Cis-5, 8, 11, 14, 17 Eicosapentaenoic acid / Timnodonic acid; C22:6n3 = Cis-4, 7, 10, 13, 16, 19 Docosahexaenoic acid / Cervonic acid; C18:2n6 = Cis-9, 12 Octadecadienoic acid / Linoleic acid; C20:4n6 = Cis-5, 8, 11, 14 Eicosatetraenoic acid / Arachidonic acid; C18:1n9 = Cis-9 Octadecenoic acid / Oleic acid.

5. References

Ahlqvist, E., Van Zuydam, N. R., Groop, L. C., & McCarthy, M. I. (2015). The genetics of diabetic complications. *Nature Reviews Nephrology*, *11*(5), 277–287.

Aiello Lloyd Paul. (2005). Angiogenic pathways in diabetic retinopathy. *N Engl J Med*; 353: 839–41.

Ajaz, A., Aliahmad, B., Sarossy, M., & Kumar, D. K. (2019). Relation Between Retinal Vasculature and Retinal Thickness in Macular Edema. *2019 41st Annual International Conference of the IEEE Engineering in Medicine and Biology Society (EMBC)*, 5593–5596.

Albers, J. W., & Pop-Busui, R. (2014). Diabetic Neuropathy: Mechanisms, Emerging Treatments, and Subtypes. *Curr Neurol Neurosci Rep*, 1.

Albers JW, Herman WH, Pop-Busui R, et al. Effect of prior intensive insulin treatment during the Diabetes Control and Complications Trial (DCCT) on peripheral neuropathy in type 1 diabetes during the Epidemiology of Diabetes Interventions and Complications (EDIC) study.

Alicic, R. Z., Rooney, M. T., & Tuttle, K. R. (2017). Diabetic kidney disease: Challenges, progress, and possibilities. *Clinical Journal of the American Society of Nephrology*, *12*(12), 2032–2045.

Alpers CE, Hudkins KL. (2011). Mouse models of diabetic nephropathy. *Curr Opin Nephrol Hypertens* 20: 278–284.

Alvarez, Y., Astudillo, O., Jensen, L., Reynolds, A. L., Waghorne, N., Brazil, D. P., … Kennedy, B. N. (2009). Selective inhibition of retinal angiogenesis by targeting PI3 kinase. *PLoS ONE*, *4*(11), 1–10.

Anca Maria Cimpean and Marius Raica (2021). Historical Overview of In Vivo and In Vitro Angiogenesis Assays. Methods Mol Biol. 2021;2206:1-13.

Andreas Eisenreich, Ulrike Leppert (2017). Update on the Protective Renal Effects of Metformin in Diabetic Nephropathy. *Current Medicinal Chemistry*. Volume 24 , Issue 31

, 2017.

Arar NH, Freedman BI, Adler SG, et al. Heritability of the severity of diabetic retinopathy: the FIND- Eye study. Invest Ophthalmol Vis Sci 2008;49:3839–3845

Artunc, F., Schleicher, E., Weigert, C., Fritsche, A., Stefan, N., & Häring, H. U. (2016). The impact of insulin resistance on the kidney and vasculature. *Nature Reviews Nephrology*, *12*(12), 721–737.

Aspiras, A. C., Rohner, N., Martineau, B., Borowsky, R. L. & Tabin, C. J. Melanocortin 4 receptor mutations contribute to the adaptation of cavefish to nutrient-poor conditions. *Proc. Natl Acad. Sci.* USA 112, 9668–9673 (2015)

Avogaro, A., & Fadini, G. P. (2019). Microvascular complications in diabetes: A growing concern for cardiologists. *International Journal of Cardiology*, *291*, 29–35.

Azushima, K., Gurley, S. B., & Coffman, T. M. (2017). Modeling diabetic nephropathy in mice. *Nature Reviews Nephrology*, *14*(1), 48–56.

Bansal V, Kalita J, Misra UK. (2006). Diabetic neuropathy. Postgrad Med J.; 82:95–100.

Bazotte, R. B., Silva, L. G., & Schiavon, F. P. M. (2014). Insulin resistance in the liver: Deficiency or excess of insulin? *Cell Cycle*, *13*(16), 2494–2500.

Berhane AM, Weil EJ, Knowler WC, Nelson RG, Hanson RL (2011) Albuminuria and estimated glomerular filtration rate as predictors of diabetic end-stage renal disease and death. Clin J Am Soc Nephrol 6(10):2444–2451.

Biddinger, S. B., & Kahn, C. R. (2006). From mice to men: Insights into the insulin resistance syndromes. *Annual Review of Physiology*, *68*, 123–158.

Bluher M, Michael MD, Peroni OD, Ueki K, Carter N, et al. 2002. Adipose tissue selective insulin receptor knock- out protects against obesity and obesity- related glucose intolerance. *Dev. Cell* 3:25–38

Bryant, N.J., Govers, R., and James, D.E. (2002). Regulated transport of the glucose transporter GLUT4. *Nat. Rev. Mol. Cell Biol.* 3, 267–277.

Brenner BM, Cooper ME, de Zeeuw D, Keane WF, Mitch WE, Parving HH, Re- muzzi G, Snapinn SM, Zhang Z, Shahin- far S (2001). Effects of losartan on renal and cardiovascular outcomes in patients with type 2 diabetes and nephropathy. *N Engl J Med* 345:861–869.

Breyer MD, Bottinger E, Brosius FC 3rd, Coffman TM, Harris RC, Heilig CW, Sharma K. (2005). Mouse models of diabetic nephropathy. *J Am Soc Nephrol* 16: 27–45.

Brett Drury 1, Robert D Bourke (2011). Short-term intraocular tamponade with perfluorocarbon heavy liquid. *Br J Ophthalmo*l . May;95(5):694-8.

Broe R, Rasmussen ML, Frydkjaer-Olsen U, Olsen BS, Mortensen HB, Hodgson L, et al. Retinal vessel calibers predict long-term microvascular complications in type 1 diabetes. The Dansh Cohort of Pediatic Diabetes 1987 (DCPD1987). *Diabetes.* 2014;63/11:3906–14

Brownlee, M. (2001). Biochemistry and Molecular Cell Biology of Diabetic Complications. *Nature*, *414*(December), 813–820.

Brownlee, M. (2005). The pathobiology of diabetic complications: A unifying mechanism. *Diabetes*, *54*(6), 1615–1625.

Bruning JC, Gautam D, Burks DJ, Gillette J, Schubert M, et al. 2000. Role of brain insulin receptor in control of body weight and reproduction. *Science* 289:2122–25

Caruso, M. A., & Sheridan, M. A. (2011). New insights into the signaling system and function of insulin in fish. *General and Comparative Endocrinology*, *173*(2), 227–247.

Chan YC, Lo YL, Chan ES. (2012). Immunotherapy for diabetic amyotrophy. Cochrane *Database Syst Rev.*; 6 CD006521.

Chang, N., Sun, C., Gao, L., Zhu, D., Xu, X., Zhu, X., … Xi, J. J. (2013). Genome editing with RNA-guided Cas9 nuclease in Zebrafish embryos. *Cell Research*, *23*(4), 465–472.

Chatterjee, S., Khunti, K., & Davies, M. J. (2017). Type 2 diabetes. *The Lancet*, *389*(10085), 2239–2251.

Chatzigeorgiou, A., Halapas, A., Kalafatakis, K. & Kamper, E (2009). The use of animal models in the study of diabetes mellitus. In Vivo 23, 245–258.

Cheung, N., Mitchell, P., & Wong, T. Y. (2010). Diabetic retinopathy. *The Lancet*, *376*(9735), 124–136.

Czech, M.P., and Corvera, S. (1999). Signaling mechanisms that regulate glucose transport. J. Biol. Chem. 274, 1865–1868.

Chua, D. C. Y., & Bakris, G. L. (2006). *Diabetic Nephropathy*. *Clinical Diabetes*.

Chung, S. S. M., Ho, E. C. M., Lam, K. S. L., & Chung, S. K. (2003). Contribution of polyol pathway to diabetes-induced oxidative stress. *Journal of the American Society of Nephrology*, *14*(SUPPL. 3), 233–236.

Cowie, M. R., & Fisher, M. (2020). SGLT2 inhibitors: mechanisms of cardiovascular benefit beyond glycaemic control. *Nature Reviews Cardiology*, *17*(12), 761–772.

Currie, G. (2014). Biomarkers in diabetic nephropathy: Present and future. *World Journal of Diabetes*, *5*(6), 763.

Cusi K, Maezono K, Osman A, Pendergrass M, Patti ME, Pratipanawatr T, DeFronzo RA, Kahn CR, Mandarino LJ. (2000). Insulin resistance differentially affects the PI 3-kinase- and MAP kinasemediated signaling in human muscle. J Clin Invest.; 105:311–20.

Davis, J., Tjipto, A., Hegerty, K., & Mallett, A. (2019). An audit of electron microscopy in the diagnosis of focal segmental glomerulosclerosis: are current pathological techniques missing important abnormalities in the glomerular basement membrane? *F1000Research*, *8*, 1204.

Dronavalli Suma, Irena Duka, George L Bakris. (2008). The pathogenesis of diabetic nephropathy. *Nat Clin Pract Endocrinol Metab*. Aug;4(8):444-52.

Doria, A. (2010). Genetics of Diabetes Complications. *Curr Diab Rep.*, (December).

Dou Huang,1 Marwan Refaat,2 Kamel Mohammedi,3 Amin Jayyousi,4 Jassim Al Suwaidi,5 and Charbel Abi Khalil. (2017). Macrovascular Complications in Patients with Diabetes and Prediabetes. *BioMed Research International Volume* Article ID 7839101, 9 pages

Drummond, B. E., & Wingert, R. A. (2016). Insights into kidney stem cell development and

regeneration using zebrafish. *World J Stem Cells*, *8*(2), 22–31.

Drummond, I. A., & Davidson, A. J. (2016). Zebrafish kidney development. In *Methods in Cell Biology*.

Engerman RL, Kern TS. (1995). Retinopathy in animal models of diabetes. *Diabetes Metab Rev* 11: 109 –120.

Falik Zaccai, T. C., Kalfon, L., Klar, A., Ben Elisha, M., Hurvitz, H., Weingarten, G., … Wertheimer, E. (2014). Two novel mutations identified in familial cases with donohue syndrome. *Molecular Genetics and Genomic Medicine*, *2*(1), 64–72.

Feldman, E. L., Callaghan, B. C., Pop-Busui, R., Zochodne, D. W., Wright, D. E., Bennett, D. L., … Viswanathan, V. (2019). Diabetic neuropathy. *Nature Reviews Disease Primers*, *5*(1).

Filla, L. A., & Edwards, J. L. (2016). Metabolomics in diabetic complications. *Mol Biosyst.*, 1090–1105.

Fisher SJ, Kahn CR. 2003. Insulin signaling is required for insulin's direct and indirect action on hepatic glucose production. *J. Clin. Invest.* 111:463–68

Focal photocoagulation treatment of diabetic macular edema. Relationship of treatment effect to fluorescein angiographic and other retinal characteristics at baseline: ETDRS report no. 19. Early Treatment Diabetic Retinopathy Study Research Group. (1995) *Arch Ophthalmol*; 113: 1144–55.

Fong DS, Aiello LP, Ferris FL 3rd, Klein R. (2004). Diabetic retinopathy. *Diabetes Care*; 27: 2540–53

Forbes, J. M., & Cooper, M. E. (2013). Mechanisms of diabetic complications. *Physiological Reviews*, *93*(1), 137–188.

Fox CS, Matsushita K, Woodward M, Bilo HJ, Chalmers J, Heerspink HJ, Lee BJ, Perkins RM, Rossing P, Sairenchi T, Tonelli M, Vassalotti JA, Yamagishi K, Coresh J, de Jong PE, Wen CP, Nelson RG (2012). Associations of kidney disease measures with mortality and end-stage renal disease in individuals with and without diabetes: a meta-analysis. *Lancet*; 380: 1662-1673

Fraher, D., Sanigorski, A., Mellett, N. A., Meikle, P. J., Sinclair, A. J., & Gibert, Y. (2016). Zebrafish Embryonic Lipidomic Analysis Reveals that the Yolk Cell Is Metabolically Active in Processing Lipid. *Cell Reports*, *14*(6), 1317–1329.

G Viberti (1994). Prognostic significance of microalbuminuria *Am J Hypertens.* Sep;7(9 Pt 2):69S-72S

Gerstein HC, Miller ME, Byington RP, Goff DC Jr, Bigger JT, Buse JB, Cushman WC, Genuth S, Ismail-Beigi F, Grimm RH Jr, Probstfield JL, Simons-Morton DG, Friedewald WT. (2008). Effects of intensive glucose lowering in type 2 diabetes. N Engl J Med 358: 2545–2559.

Giacco, F., & Brownlee, M. (2010). Oxidative stress and diabetic complications. *Circulation Research*, *107*(9), 1058–1070.

Giesbertz, P., Padberg, I., Rein, D., Ecker, J., Höfle, A. S., Spanier, B., & Daniel, H. (2015). Metabolite profiling in plasma and tissues of ob/ob and db/db mice identifies novel markers of obesity and type 2 diabetes. *Diabetologia*, *58*(9), 2133–2143.

Gnudi, L., Coward, R. J. M., & Long, D. A. (2016). Diabetic Nephropathy: Perspective on Novel Molecular Mechanisms. *Trends in Endocrinology and Metabolism*, *27*(11), 820–830.

Gong, Y., Zhai, G., Su, J., Yang, B., Jin, J., Liu, H., … Han, D. (2018). Different roles of insulin receptor a and b in maintaining blood glucose homeostasis in zebrafish. *General and Comparative Endocrinology*, *269*(July), 33–45.

Gore, A. V., Monzo, K., Cha, Y. R., Pan, W., & Weinstein, B. M. (2012). Vascular development in the zebrafish. *Cold Spring Harbor Perspectives in Medicine*, *2*(5), 1–21.

Groop PH, Thomas MC, Moran JL, Wade` n J, Thorn LM, Ma¨ kinen VP, Rosenga° rd-Ba¨ rlund M, Saraheimo M, Hietala K, Heikkila¨ O, Forsblom C, FinnDiane Study Group. (2009). The presence and severity of chronic kidney disease predicts all-cause mortality in type 1 diabetes. *Diabetes* 58:1651-1658.

Guasch-Ferré, M.; Hruby, A.; Toledo, E.; Clish, C.B.; Martínez-González, M.A.; Salas-Salvadó, J.; Hu, F.B. Metabolomics in Prediabetes and Diabetes: A Systematic Review and Meta-analysis. *Diabetes Care* 2016, 39, 833–846

Gurley SB, Clare SE, Snow KP, Hu A, Meyer TW, Coffman TM. (2006). Impact of genetic background on nephropathy in diabetic mice. *Am J Physiol Renal Physiol* 290: F214 – F222.

Guo Q, Mori T, Jiang Y, et al. Methylglyoxal contributes to the development of insulin resistance and salt sensitivity in Sprague-Dawley rats. *J Hypertens* 2009;27:1664–1671

Haffner SM, Lehto S, Ronnemaa T, Pyorala K, Laakso M. (1998). Mortality from coronary heart disease in subjects with type 2 diabetes and in nondiabetic subjects with and without prior myocardial infarction. *N Engl J Med* 339: 229–234.

Hammes, H. P. (2018). Diabetic retinopathy: hyperglycemia, oxidative stress, and beyond. *Diabetologia*, *61*(1), 29–38.

Hammes, H. P., Du, X., Edelstein, D., Taguchi, T., Matsumura, T., Ju, Q., … Brownlee, M. (2003). Benfotiamine blocks three major pathways of hyperglycemic damage and prevents experimental diabetic retinopathy. *Nature Medicine*, *9*(3), 294–299.

Hammes, H. P., Feng, Y., Pfister, F., & Brownlee, M. (2011). Diabetic retinopathy: Targeting vasoregression. *Diabetes*, *60*(1), 9–16.

Hammes, H. P., Lemmen, K. D., & Bertram, B. (2020). Diabetic Retinopathy and Maculopathy. *Experimental and Clinical Endocrinology and Diabetes*, *128*.

Heckler, K., & Kroll, J. (2017). Zebrafish as a model for the study of microvascular complications of diabetes and their mechanisms. *International Journal of Molecular Sciences*, *18*(9), 1–9.

Heng, L. Z., Comyn, O., Peto, T., Tadros, C., Ng, E., Sivaprasad, S., & Hykin, P. G. (2013). Diabetic retinopathy: Pathogenesis, clinical grading, management and future developments. *Diabetic Medicine*, *30*(6), 640–650.

Hernandez-Ono A, Zhang Y-L, Chiang J, Moon B, Kahn CR, et al. 2005. Lipoprotein metabolism in the liver insulin receptor knockout (LIRKO) mouse: critical role of insulin signaling in the regulation of very low density lipoprotein (VLDL) secretion. *Diabetes* 54(Suppl. 1):A2 (Abstr.)

Hietala K, Forsblom C, Summanen P, Groop PH (2008). Heritability of proliferative diabetic retinopathy. *Diabetes*;57:2176–2180.

Hirai FE, Tielsch JM, Klein BE, Klein R. (2003).Ten-year change in vision-related quality of life in type 1 diabetes: Wisconsin epidemiologic study of diabetic retinopathy. *Ophthalmology* 118: 353–358, 2011.

Hovind, P., Rossing, P., Tarnow, L., Smidt, U. M., & Parving, H. H. (2001). Progression of diabetic nephropathy. *Kidney International*, *59*(2), 702–709.

Howe, K., Clark, M. D., Torroja, C. F., Torrance, J., Berthelot, C., Muffato, M., … Stemple, D. L. (2013). The zebrafish reference genome sequence and its relationship to the human genome. *Nature*, *496*(7446), 498–503.

Hruz, P.W., and Mueckler, M.M. (2001). Structural analysis of the GLUT1 facilitative glucose transporter (review). *Mol. Membr. Biol*. 18, 183–193

Huang, P., Zhu, Z., Lin, S., & Zhang, B. (2012). Reverse Genetic Approaches in Zebrafish. *Journal of Genetics and Genomics*, *39*(9), 421–433.

Huang, Y., Harrison, M. R., Osorio, A., Kim, J., Baugh, A., Duan, C., … Lien, C. L. (2013). Igf Signaling is Required for Cardiomyocyte Proliferation during Zebrafish Heart Development and Regeneration. *PLoS ONE*, *8*(6).

Hwang, W. Y., Fu, Y., Reyon, D., Maeder, M. L., Tsai, S. Q., Sander, J. D., … Joung, J. K. (2013). Efficient genome editing in zebrafish using a CRISPR-Cas system. *Nature Biotechnology*, *31*(3), 227–229.

Icard, P., Coquerel, A., Wu, Z., Gligorov, J., Fuks, D., Fournel, L., … Simula, L. (2021). Understanding the central role of citrate in the metabolism of cancer cells and tumors: An update. *International Journal of Molecular Sciences*, *22*(12), 1–19.

Isogai, S., Horiguchi, M., & Weinstein, B. M. (2001). The vascular anatomy of the developing zebrafish: An atlas of embryonic and early larval development. *Developmental Biology*, *230*(2), 278–301.

James W. Albers, Rodica Pop-Busui (2014). Diabetic Neuropathy: Mechanisms, Emerging

Treatments, and Subtypes. *Curr neurol Neurosciene reports.*

Jao, L. E., Wente, S. R., & Chen, W. (2013). Efficient multiplex biallelic zebrafish genome editing using a CRISPR nuclease system. *Proceedings of the National Academy of Sciences of the United States of America*, *110*(34), 13904–13909.

Jiang Y, Thakran S, Bheemreddy R, Ye E-A, He H, Walker RJ, Steinle JJ. (2014). Pioglitazone normalizes insulin signaling in the diabetic rat retina through reduction in tumor necrosis factor α and suppressor of cytokine signaling 3. *J Biol Chem.*; 289(38):26395–405.

Jiang, Z. Y., Lin, Y. W., Clemont, A., Feener, E. P., Hein, K. D., Igarashi, M., … King, G. L. (1999). Characterization of selective resistance to insulin signaling in the vasculature of obese Zucker (fa/fa) rats. *Journal of Clinical Investigation*, *104*(4), 447–457.

Joost, H.-G., & Thorens, B. (2009). The extended GLUT-family of sugar/polyol transport facilitators: nomenclature, sequence characteristics, and potential function of its novel members. *Molecular Membrane Biology*, *7688*(769440770).

Jorge L. Gross, M., Mirela J. DE Azevedo, M., Sandra P. Silveiro, M., LU´IS HENRIQUE CANANI, M., MARIA LUIZA CARAMORI, M., & THEMIS ZELMANOVITZ, M. (2005). Diabetic nephropathy: Diagnosis, prevention and treatment. *Diabetes Care 28:176–188, 2005*, *28*(1), 176–188.

Jörgens, K, & Kroll, J. (2012). Zebrafish: A Model for understanding. *Exp Clin Endocrinol Diabetes*, *120*, 186–187.

Jörgens, Kristina, Stoll, S. J., Pohl, J., Fleming, T. H., Sticht, C., Nawroth, P. P., … Kroll, J. (2015). High tissue glucose alters intersomitic blood vessels in zebrafish via methylglyoxal targeting the VEGF receptor signaling cascade. *Diabetes*, *64*(1), 213–225.

Jung, S. H., Kim, Y. S., Lee, Y. R., & Kim, J. S. (2016). High glucose-induced changes in hyaloid-retinal vessels during early ocular development of zebrafish: A short-term animal model of diabetic retinopathy. *British Journal of Pharmacology*, *173*(1), 15–26.

K J Schjoedt 1, P Jacobsen, K Rossing, F Boomsma, H H Parving (2005). Dual blockade of the

renin-angiotensin-aldosterone system in diabetic nephropathy: the role of aldosterone *Horm Metab Res* Apr;37 Suppl 1:4-8

Kawanami, D., Takashi, Y., & Tanabe, M. (2020). Significance of metformin use in diabetic kidney disease. *International Journal of Molecular Sciences*, *21*(12), 1–16.

Khan, R. S., Bril, F., Cusi, K., & Newsome, P. N. (2019). Modulation of Insulin Resistance in Nonalcoholic Fatty Liver Disease. *Hepatology*, *70*(2), 711–724.

Kim, H., Kim, J. J. & Yoon, Y. S. Emerging therapy for diabetic neuropathy: cell therapy targeting vessels and nerves. Endocr. Metab. Immune Disord. *Drug Targets* 12, 168–178 (2012).

Kim JK, Michael MD, Previs SF, Peroni OD, Mauvais-Jarvis F, (2000). Redistribution of substrates to adipose tissue promotes obesity in mice with selective insulin resistance in muscle. *J. Clin. Invest*. 105:1791–97

Kim SJ, Equi R, Bressler NM. (2007). Analysis of macular edema after cataract surgery in patients with diabetes using optical coherence tomography. *Ophthalmology* ; 114: 881–89.

Kimmel, C. B., Ballard, W. W., Kimmel, S. R., Ullmann, B., & Schilling, T. F. (1995). Stages of embryonic development of the zebrafish. *Developmental Dynamics*, *203*(3), 253–310.

Kitamotoa, T., Sakuraid, K., Lee, E. Y., Yokoteb, K., Accilic, D., & Miki, T. (2017). Distinct roles of systemic and local actions of insulin on pancreatic b-cells. *Physiology & Behavior*, *176*(3), 139–148.

Kempen JH, O'Colmain BJ, Leske MC, Haffner SM, Klein R, Moss SE, Taylor HR, Hamman RF (2004) The prevalence of diabetic retinopathy among adults in the United States. *Arch Ophthalmol* 122: 552–563.

Klein R. (2008). Epidemiology of Diabetic Retinopathy. In: Diabetic Retinopathy. Duh E, ed. Totowa: Humana Press.

Klein R, Knudtson MD, Lee KE, Gangnon R, Klein BE. (2008).The Wisconsin Epidemiologic Study of Diabetic Retinopathy: XXII the twenty-fi ve-year progression of retinopathy in

persons with type 1 diabetes. *Ophthalmology* ; 115: 1859–68.

Kluding PM, Pasnoor M, Singh R, et al. (2012). The effect of exercise on neuropathic symptoms, nerve function, and cutaneous innervation in people with diabetic peripheral neuropathy. *J Diabetes Complicat*; 26:424–429.

Kitamura, T., Kahn, C. R., & Accili, D. (2003a). Insulin Receptor Knockout Mice. *Annual Review of Physiology*, *65*, 313–332.

Kitamura, T., Kahn, C. R., & Accili, D. (2003b). INSULIN RECEPTOR KNOCKOUT MICE. *Annu. Rev. Physiol*, *65*, 313–332.

Krishna Rakesh Sharma, Karl Heckler, Sandra J Stoll Jan-Luuk Hillebrands, Katharina Kynast , Esther Herpel, Stefan Porubsky, Marlies Elger, Boris Hadaschik, Karen Bieback, Hans-Peter Hammes, Peter P Nawroth, Jens Kroll (2016). ELMO1 protects renal structure and ultrafiltration in kidney development and under diabetic conditions. *Sci Rep* Nov 16;6:37172.

Kitt Falk Petersen , Sylvie Dufour, David B Savage, Stefan Bilz, Gina Solomon, Shin Yonemitsu, Gary W Cline, Douglas Befroy, Laura Zemany, Barbara B Kahn, Xenophon Papademetris, Douglas L Rothman, Gerald I Shulman (2007). The role of skeletal muscle insulin resistance in the pathogenesis of the metabolic syndrome. *Proc Natl Acad Sci USA*; 104: 12587–94.

L.Joshi, R., Lamothe, B., Cordonnier, N., Mesbah, K., Monthioux, E., Jamil, J., & Bucchini, D. (1996). Targeted disruption of the insulin receptor gene in the mouse results in neonatal lethality, *20*(17), 6269–6275.

Laing SP, Swerdlow AJ, Slater SD, Burden AC, Morris A, Waugh NR, Gatling W, Bingley PJ, Patterson CC (2003). Mortality from heart disease in a cohort of 23,000 patients with insulin-treated diabetes. *Diabetologia* 46: 760–765.

Leak TS, Perlegas PS, Smith SG, et al. Variants in intron 13 of the ELMO1 gene are associated with diabetic nephropathy in African Americans. *Ann Hum Genet* 2009;73:152–159.

Lee -J-J, Wang P-W, Yang I-H, Huang H-M, Chang C-S, Wu C-L, Chuang J-H. (2015). High-fat

diet induces toll-like receptor 4-dependent macrophage/microglial cell activation and retinal impairment. I*nvest Ophthalmol Vis Sci*.; 56(5):3041–50.

Lee, T. M., Chang, N. C., & Lin, S. Z. (2017). Dapagliflozin, a selective SGLT2 Inhibitor, attenuated cardiac fibrosis by regulating the macrophage polarization via STAT3 signaling in infarcted rat hearts. *Free Radical Biology and Medicine*, *104*(September 2016), 298–310.

Lewis EJ, Hunsicker LG, Bain RP, Rohde RD (1993). The effect of angiotensin-convert- ing-enzyme inhibition on diabetic ne- phropathy: the Collaborative Study Group. *N Engl J Med* 329:1456–1462.

Lewis EJ, Hunsicker LG, Clarke WR, Berl T, Pohl MA, Lewis JB, Ritz E, Atkins RC, Rohde R, Raz I (2001). Renoprotective effect of the angiotensin-receptor antag- onist irbesartan in patients with ne- phropathy due to type 2 diabetes. *N Engl J Med* 345:851–860.

Lieschke, G. J., & Currie, P. D. (2007). Animal models of human disease: Zebrafish swim into view. *Nature Reviews Genetics*, *8*(5), 353–367.

Lim, A. K. H. (2014). Diabetic nephropathy – Complications and treatment. *International Journal of Nephrology and Renovascular Disease*, *7*, 361–381.

Liu, S., Li, X., Yang, J., Zhu, R., Fan, Z., Xu, X., … Liu, M. (2019). Misfolded proinsulin impairs processing of precursor of insulin receptor and insulin signaling in β cells. *FASEB Journal*, *33*(10), 11338–11348.

Liu, Z., & Liu, F. (2012). Cautious use of fli1a:EGFP transgenic zebrafish in vascular research. *Biochemical and Biophysical Research Communications*, *427*(1), 223–226.

Lodd, E., Wiggenhauser, L. M., Morgenstern, J., Fleming, T. H., Poschet, G., Büttner, M., … Kroll, J. (2019). The combination of loss of glyoxalase1 and obesity results in hyperglycemia. *JCI Insight*, *4*(12).

Louvi A, Accili D, Efstratiadis A. (1997). Growth-promoting interaction of IGF-II with the insulin receptor during mouse embryonic development. Dev. Biol. 189:33–48

Madan A, Penn JS. (2003) Animal models of oxygen-induced retinopathy. *Front Biosci* 8:

d1030 –1043.

Malmberg, K., Rydén, L., Wedel, H., Birkeland, K., Bootsma, A., Dickstein, K., … Waldenström, A. (2005). intense metabolic control by means of insulin in patients with diabetes mellitus and acute myocardial infarction (DIGAMI 2): Effects on mortality and morbidity. *European Heart Journal*, *26*(7), 650–661.

Mario, T., Thomas, A., & Wilhelm, S. (2010). Handbook of Experimental Pharmacology: Preface. *Handbook of Experimental Pharmacology*, *195*, 209–226.

Martin, C. L., Albers, J. W. & Pop-Busui, R. (2014).Neuropathy and related findings in the diabetes control and complications trial/epidemiology of diabetes interventions and complications study. *Diabetes Care* 37, 31–38.

Mathis D, Vence L, Benoist C. (2001). Beta-Cell death during progression to diabetes. *Nature* 414: 792–798.

McKinney MC, Weinstein BM. (2008). Using the zebrafish to study vessel formation. *Methods Enzymol* 444: 65–97.

Michael MD, Kulkarni RN, Postic C, Previs SF, Shulman GI, et al. 2000. Loss of insulin signaling in hepatocytes leads to severe insulin resistance and progressive hepatic dysfunction. *Mol. Cell* 6:87– 97

Michel, T. (1999). Targeting and translocation of endothelial nitric oxide synthase. *Brazilian Journal of Medical and Biological Research*, *32*(11), 1361–1366.

Middel, C. S., Hammes, H. P., & Kroll, J. (2021, May 25). Advancing Diabetic Retinopathy Research: Analysis of the Neurovascular Unit in Zebrafish. *Cells*. NLM (Medline).

Miner, J. H. (1999). Renal basement membrane components. *Kidney International*, *56*(6), 2016–2024.

Miner, J. H. (2012). The Glomerular Basement Membrane. *Exp Cell Res.*, *21*, 973–978.

Mora-Fernández, C., Domínguez-Pimentel, V., de Fuentes, M. M., Górriz, J. L., Martínez-Castelao, A., & Navarro-González, J. F. (2014). Diabetic kidney disease: From physiology

to therapeutics. *Journal of Physiology*, *592*(18), 3997–4012.

Morales, E. E., & Wingert, R. A. (2017). Zebrafish as a model of kidney disease. *Results and Problems in Cell Differentiation*, *60*, 55–75.

Morrish N, Wang S, Stevens L, Fuller J, Keen H. Mortality and causes of death in the WHO Multinational Study of Vascular Disease in Diabetes. *Diabetologia*. 2001 Sep 1; 44 (Suppl 2):S14– S21. 2001

Muniyappa, R., Iantorno, M., & Quon, M. J. (2009). An Integrated View of Insulin Resistance and Endothelial Dysfunction, *37*(3), 1–24.

Muniyappa R, Yavuz S. (2012). Metabolic Actions of Angiotensin II and Insulin: A Microvascular Endothelial Balancing Act. *Mol Cell Endocrinol.* 378(1–2):59–69.

Muniyappa, R., & Shazene Yavuz. (2013). Metabolic Actions of Angiotensin II and Insulin: A Microvascular Endothelial Balancing Act. *Mol Cell Endocrinol.*, *378*(1), 59–69.

NHANES. 2007-2008 questionnaires, datasets, and related documentation. Atlanta (GA): Centers for Disease Control, National Center for Health Statistics; accessed 2018 Jun 29.https://wwwn.cdc.gov/nchs/nhanes/continuousnhanes/default.aspx?BeginYear=2007.

Najafian B, Mauer M (2012) Morphologic features of declining renal function in type 1 diabetes. *Semin Nephrol* 32:415–422.

Noemi Lois , Rachel V McCarter , Christina O'Neill , Reinhold J Medina , Alan W Stitt (2014). Endothelial progenitor cells in diabetic retinopathy. *Front Endocrinol* (Lausanne). Apr 9;5:44

O'Shaughnessy MM, Hogan SL, Poulton CJ, Falk RJ, Singh HK, Nickeleit V, Jennette JC (2017) Temporal and demographic trends in glomerular disease epidemiology in the southeastern United States, 1986–2015. *Clin J Am Soc Nephrol CJASN* 12:614–62

Oka, T., Nishimura, Y., Zang, L., Hirano, M., Shimada, Y., Wang, Z., … Tanaka, T. (2010). Diet-induced obesity in zebrafish shares common pathophysiological pathways with mammalian obesity. *BMC Physiology*, *10*(1).

Okekunle, A.P.; Li, Y.; Liu, L.; Du, S.; Wu, X.; Chen, Y.; Li, Y.; Qi, J.; Sun, C.; Feng, R. Abnormal circulating amino acid profiles in multiple metabolic disorders. *Diabetes Res. Clin. Pract*. 2017, 132, 45–58.

Papale M, Di Paolo S, Magistroni R, Lamacchia O, Di Palma AM, De Mattia A, Rocchetti MT, Furci L, Pasquali S, De Co- smo S, Cignarelli M, Gesualdo L. Urine proteome analysis may allow noninvasive differential diagnosis of diabetic nephropathy. Diabetes Care 2010; 33: 2409-2415

Papasani, M. R., Robison, B. D., Hardy, R. W., & Hill, R. A. (n.d.). Early developmental expression of two insulins in zebrafish (Danio rerio).

Parichy, D. M., Elizondo, M. R., Mills, M. G., Gordon, T. N., & Raymond, E. E. (2009). Normal Table of Post-Embryonic Zebrafish Development: Staging by Externally Visible Anatomy of the Living Fish. *Dev Dyn.*, *238*(12), 2975–3015.

Parving H-H, Andersen AR, Smidt UM, PA Svendsen: (1983). Early aggressive antihypertensive treatment reduces rate of decline in kidney function in diabetic nephropathy. *Lancet* 1:1175–1179

Patel A, MacMahon S, Chalmers J, Neal B, Billot L, Woodward M, Marre M, Cooper M, Glasziou P, Grobbee D, Hamet P, Harrap S, Heller S, Liu L, Mancia G, Mogensen CE, Pan C, Poulter N, Rodgers A, Williams B, Bompoint S, de Galan BE, Joshi R,Travert F. (2008) Intensive blood glucose control and vascular outcomes in patients with type 2 diabetes. *N Engl J Med* 358: 2560–2572.

Pedersen L, Jeppesen P, Knudsen ST, Poulsen PL, Bek T. Improvement ofmild retinopathy in type 2 diabetic patients corre- lates with narrowing of retinal arterioles. A prospective observa- tional study. *Graefes Arch Clin Exp Ophthalmo*l. 2014;252/10: 1561–7

Pemp B, Cherecheanu AP, Garhofer G, Schmetterer L. Calculation ofcentral retinal artery diameters from non-invasive ocular haemo- dynamic measurements in type 1 diabetes patients. *Acta Ophthalmol.* 2013;91/5:e348–52

Peng, J. (2019). Gene redundancy and gene compensation: An updated view. *Journal of Genetics and Genomics*, *46*(7), 329–333.

Pernicova, I., & Korbonits, M. (2014). Metformin-Mode of action and clinical implications for diabetes and cancer. *Nature Reviews Endocrinology*, *10*(3), 143–156.

Perrone RD, Madias NE, Levey AS. Serum creatinine as an index of renal function: new insights into old concepts. *Clin Chem* 1992; 38: 1933-1953

Pezzolesi MG, Katavetin P, Kure M, et al. Confirmation of genetic associations at ELMO1 in the GoKinD collection supports its role as a susceptibility gene in diabetic nephropathy. Diabetes 2009;58:2698–2702. [PubMed: 19651817] •• Extension of the findings of association between variants at the ELMO1 genes and diabetic nephropathy to Europen Whites. The paper shows how information about candidate genes can be extracted from GWA studies.

Phillips, J. B., & Westerfield, M. (2014). Zebrafish models in translational research: Tipping the scales toward advancements in human health. *DMM Disease Models and Mechanisms*, *7*(7), 739–743.

Photocoagulation treatment of proliferative diabetic retinopathy. Clinical application of Diabetic Retinopathy Study (DRS) findings, DRS Report Number 8. The Diabetic retinopathy Study Research Group (1981). *Ophthalmology* ; 88: 583–600.

Qi, H., Schmöhl, F., Li, X., Qian, X., Tabler, C. T., Bennewitz, K., … Kroll, J. (2021). Reduced Acrolein Detoxification in akr1a1a Zebrafish Mutants Causes Impaired Insulin Receptor Signaling and Microvascular Alterations. *Advanced Science*, *2101281*, 1–15.

Quinlivan, V. H., & Farber, S. A. (2017). Lipid uptake, metabolism, and transport in the larval zebrafish. *Frontiers in Endocrinology*, *8*(NOV), 1–11.

Rabbani N, Godfrey L, Xue M, et al. Glycation of LDL by methylglyoxal increases arterial atherogenicity: a possible contributor to increased risk of cardiovascular disease in diabetes. *Diabetes* 2011;60:1973–1980

Rask-Madsen C, King GL. (2010). Kidney complications: factors that protect the diabetic vasculature. Nat Med; 16:40–41

Reidy, K., Kang, H. M., Hostetter, T., & Susztak, K. (2014). Molecular mechanisms of diabetic

kidney disease. *Journal of Clinical Investigation*, *124*(6), 2333–2340.

Reiter CEN, Wu X, Sandirasegarane L, Nakamura M, Gilbert KA, Singh RSJ, Fort PE, Antonetti DA, Gardner TW. (2006). Diabetes reduces basal retinal insulin receptor signaling: reversal with systemic and local insulin. *Diabetes*. 55(4):1148–56.

Rewers M, Ludvigsson J. (2016). Environmental risk factors for type 1 diabetes. *Lancet*; 387: 2340–48

R Trevisan, D Bruttomesso, M Vedovato, S Brocco, A Pianta, C Mazzon, C Girardi, E Jori, A Semplicini, A Tiengo, S Del Prato (1998) Enhanced responsiveness of blood pressure to sodium intake and to angiotensin II is associated with insulin resistance in IDDM patients with microalbuminuria. *Diabetes* 47, 1347–1353.

Rhodes CJ, White MF, Leahy JL, Kahn SE. Direct autocrine action of insulin on beta-cells: does it make physiological sense? *Diabetes 2*013;62:2157–63.

Riddle, M. R., Aspiras, A. C., Gaudenz, K., Peuß, R., Sung, J. Y., Martineau, B., … Rohner, N. (2018). Insulin resistance in cavefish as an adaptation to a nutrient-limited environment. *Nature*, *555*(7698), 647–651.

Riehle, C., & Abel, E. D. (2016). Insulin Signaling and Heart Failure. *Circulation Research*, *118*(7), 1151–1169.

Roberts, L.D.; Koulman, A.; Griffin, J.L. Towards metabolic biomarkers of insulin resistance and type 2 diabetes: Progress from the metabolome. *Lancet Diabetes Endocrinol*. 2014, 2, 65–75.

Robinson R, Barathi VA, Chaurasia SS, Wong TY, Kern TS. (2012). Update on animal models of diabetic retinopathy: from molecular approaches to mice and higher mammals. *Dis Model Mech*; 5:444–456

Rojek, A., Wikiera, B., Noczynska, A., & Niedziela, M. (2021). Syndrome of Congenital Insulin Resistance Caused by a Novel INSR Gene Mutation. *Journal of Clinical Research in Pediatric Endocrinology*, *0*(0), 0–0.

Romero-Aroca, P.; Baget-Bernaldiz, M.; Pareja-Rios, A.; Lopez-Galvez, M.; Navarro-Gil, R.;

Verges, R. (2016). Diabetic macular edema pathophysiology: Vasogenic versus inflammatory. *J. Diabetes Res*. 2016, 2156273

Rossing P. (2005). Prediction, progression and prevention of diabetic nephropathy. The Minkowski Lecture. *Diabetologia*. Jan; 49(1):11-9

Rui, L. (2014). Energy Metabolism in the Liver. *Physiology & Behavior*.

Salpeter, S. R., Buckley, N. S., Kahn, J. A. & Salpeter, E. E. (2008) Meta-analysis: metformin treatment in persons at risk for diabetes mellitus. *Am. J. Med*. 121, 149–157 (2008).

Saltiel, A. R., & Kahn, C. R. (2012). Glucose and Lipid Metabolism. *Glucose Homeostasis and Insulin Resistance*, *414*(December), 1–21.

Sander, V., & Davidson, A. J. (2014). Kidney injury and regeneration in zebrafish. *Seminars in Nephrology*, *34*(4), 437–444.

Sarwar N, Gao P, Seshasai SR, Gobin R, Kaptoge S, Di Angelantonio E (2010). Diabetes mellitus, fasting blood glucose concentration, and risk of vascular disease: a collaborative meta-analysis of 102 prospective studies. *Lancet* 375(9733), 2215–2222.

Seth, A., Stemple, D. L., & Barroso, I. (2013). The emerging use of zebrafish to model metabolic disease. *Disease Models & Mechanisms*, *6*, 1080–1088.

Sharma, S. G., Bomback, A. S., Radhakrishnan, J., Herlitz, L. C., Stokes, M. B., Markowitz, G. S., & D'Agati, V. D. (2013). The modern spectrum of renal biopsy findings in patients with diabetes. *Clinical Journal of the American Society of Nephrology*, *8*(10), 1718–1724.

Sheetz, M. J., & King, G. L. (2002). Molecular understanding of hyperglycemia's adverse effects for diabetic complications. *Journal of the American Medical Association*, *288*(20), 2579–2588.

Shimazaki A, Kawamura Y, Kanazawa A, *et al*. Genetic variations in the gene encoding ELMO1 are associated with susceptibility to diabetic nephropathy. *Diabetes* 2005;54:1171–1178

Sima AA, Calvani M, Mehra M, et al. (2005). Acetyl-L-carnitine improves pain, nerve

regeneration, and vibratory perception in patients with chronic diabetic neuropathy: an analysis of two randomized placebo-controlled trials. *Diabetes Care*; 28:89–94.

Singh, A., Castillo, H. A., Brown, J., Kaslin, J., Dwyer, K. M., & Gibert, Y. (2019). High glucose levels affect retinal patterning during zebrafish embryogenesis. *Scientific Reports*, *9*(1), 1–13.

Sinnreich M, Taylor BV, Dyck PJ. (2005). Diabetic neuropathies. Classification, clinical features, and pathophysiological basis. *Neurologist*; 11:63–79.

Smith AG, Singleton JR. (2012). Diabetic neuropathy. Continuum; 18:60–84.

Smith R, Lee C, Charles H, Farber M, Cuncha-Vaz J (1987) Quantification of diabetic macular edema. *Arch Ophthalmol* 105 (2):218–222

Suarez, M. L. G., Thomas, D. B., Barisoni, L., & Fornoni, A. (2013). Diabetic nephropathy: Is it time yet for routine kidney biopsy? *World Journal of Diabetes*, *4*(6), 245.

Sun K, Wu Z, Ji Y, Wu G. (2016). Glycine regulates protein turnover by activating protein kinase B/mammalian target of rapamycin and by inhibiting MuRF1 and atrogin-1 gene expression in C2C12 myoblasts. *J Nutr* 2016; 146:2461–2467.

Suzuma I, Hata Y, Clermont A, et al. (2001). Cyclic stretch and hypertension induce retinal expression of vascular endothelial growth factor and vascular endothelial growth factor receptor-2: potential mechanisms for exacerbation of diabetic retinopathy by hypertension. *Diabetes*: 50: 444–54.

Suzy V Hope, Sophie Wienand-Barnett, Maggie Shepherd , Sophie M King , Charles Fox , Kamlesh Khunti , Richard A Oram , Bea A Knight , Andrew T Hattersley , Angus G Jones , Beverley M Shields (2016) Practical classification guidelines for diabetes in patients treated with insulin: a cross-sectional study of the accuracy of diabetes diagnosis. *Br J Gen Pract*; 66: e315–22.

Tesch GH, Lim AK. (2010). Recent insights into diabetic renal injury from the db/db mouse model of type 2 diabetic nephropathy. *Am J Physiol Renal Physiol* 300: F301–F310.

Tesfaye S, Boulton AJ, Dyck PJ, et al. (2010). Diabetic neuropathies: update on definitions,

diagnostic criteria, estimation of severity, and treatments. *Diabetes Care*; 33:2285–2293.

Tesfaye S, Kempler P. (2005). Painful diabetic neuropathy. *Diabetologia*. 48:805–807.

Thomas NJ, Jones SE, Weedon MN, Shields BM, Oram RA, Hattersley AT. (2018). Frequency and phenotype of type 1 diabetes in the first six decades of life: a cross-sectional, genetically stratified survival analysis from UK Biobank. *Lancet Diabetes Endocrinol*; 6: 122–29

Toto, R. D. (2017). SGLT-2 Inhibition: A Potential New Treatment for Diabetic Kidney Disease? *Nephron*, *137*(1), 64–67.

Toyoshima, Y., Monson, C., Duan, C., Wu, Y., Gao, C., Yakar, S., … LeRoith, D. (2008). The role of insulin receptor signaling in zebrafish embryogenesis. *Endocrinology*.

Tuomi, T., Santoro, N., Caprio, S., Cai, M., Weng, J., & Groop, L. (2014). The many faces of diabetes: A disease with increasing heterogeneity. *The Lancet*, *383*(9922), 1084–1094.

Uthman, L., Baartscheer, A., Bleijlevens, B., Schumacher, C. A., Fiolet, J. W. T., Koeman, A., … Zuurbier, C. J. (2018). Class effects of SGLT2 inhibitors in mouse cardiomyocytes and hearts: inhibition of Na+/H+ exchanger, lowering of cytosolic Na+ and vasodilation. *Diabetologia*, *61*(3), 722–726.

Vedovato, M. et al. (2004) Effect of sodium intake on blood pressure and albuminuria in Type 2 diabetic patients: the role of insulin resistance. *Diabetologia* 47, 300–303

Verma, S., & McMurray, J. J. V. (2018). SGLT2 inhibitors and mechanisms of cardiovascular benefit: a state-of-the-art review. *Diabetologia*, *61*(10), 2108–2117.

Wang X, Desai K, Chang T, Wu L. Vascular methylglyoxal metabolism and the development of hypertension. *J Hypertens* 2005;23:1565–1573

Wanner C, Inzucchi SE, Lachin JM, Fitchett D, von Eynatten M, Mattheus M, Johansen OE, Woerle HJ, Broedl UC, Zinman B; EMPA-REG OUTCOME Investigators: Em- pagliflozin and progression of kidney disease in type 2 diabetes. *N Engl J Med* 2016; 375: 323–334

Weir, M. R. (2016). The kidney and type 2 diabetes mellitus: Therapeutic implications of SGLT2 inhibitors. *Postgraduate Medicine*, *128*(3), 290–298.

Welsh, G. I., Hale, L. J., Eremina, V., Jeansson, M., Maezawa, Y., Pons, D. A., … Saleem, M. A. (2016). Insulin Signaling to the Glomerular Podocyte is Critical for Normal Kidney Function, *12*(4), 329–340.

Wertheimer, E., Lu, S. P., Backeljauw, P. F., Davenport, M. L., & Taylor, S. I. (1993). Homozygous deletion of the human insulin receptor gene results in leprechaunism. *Nature Genetics*, *5*(1), 71–73.

Wiemer, N. G. et al. (2008).The effect of acute hyperglycemia on retinal thickness and ocular refraction in healthy subjects. Graefes Arch. *Clin. Exp. Ophthalmol*. 246, 703–708.

Wiemer, N. G. M., Eekhoff, E. M. W., Simsek, S., Heine, R. J., Ringens, P. J., Polak, B. C. P., & Dubbelman, M. (2008). The effect of acute hyperglycemia on retinal thickness and ocular refraction in healthy subjects. *Graefe's Archive for Clinical and Experimental Ophthalmology*, *246*(5), 703–708.

Wiggenhauser LM, Kohl K, Dietrich N, Hammes HP, Kroll J. (2017). Studying Diabetes Through the Eyes of a Fish: Microdissection, Visualization, and Analysis of the Adult tg*(fli:EGFP)* Zebrafish Retinal Vasculature. *J Vis Exp.* Dec 26;(130):56674.

Wiggenhauser, L. M., Qi, H., Stoll, S. J., Metzger, L., Bennewitz, K., Poschet, G., … Kroll, J. (2020). Activation of retinal angiogenesis in hyperglycemic pdx1$^{-/-}$ zebrafish mutants. *Diabetes*, *69*(5), 1020–1031.

Winters, S. J., Scoggins, C. R., Appiah, D., & Ghooray, D. T. (2020). The hepatic lipidome and hnf4α and shbg expression in human liver. *Endocrine Connections*, *9*(10), 1009–1018.

Wolf, G., Muller, N., Mandecka, A. & Muller, U. A. (2007) Association of diabetic retinopathy and renal function in patients with types 1 and 2 diabetes mellitus. *Clin. Nephrol*. 68, 81–86.

Wood, I. S., & Trayhurn, P. (2003). Glucose transporters (GLUT and SGLT): expanded families of sugar transport proteins. *British Journal of Nutrition*, *89*(1), 3–9.

Yang, B. Y., Zhai, G., Gong, Y. L., Su, J. Z., Peng, X. Y., Shang, G. H., … Xie, S. Q. (2018). Different physiological roles of insulin receptors in mediating nutrient metabolism in zebrafish. *American Journal of Physiology - Endocrinology and Metabolism*, *315*(1), E38–E51.

Yang, B., Zhai, G., Gong, Y., Su, J., Han, D., Yin, Z., & Xie, S. (2017). Depletion of insulin receptors leads to β-cell hyperplasia in zebrafish. *Science Bulletin*, *62*(7), 486–492.

Yau JW, Rogers SL, Kawasaki R, Lamoureux EL, Kowalski JW, Bek T et al. Global prevalence and major risk factors of diabetic retinopathy. *Diabetes Care* 2012; 35: 556–564.

Yilmaz T, Weaver CD, Gallagher MJ, et al. (2009). Intravitreal triamcinolone acetonide injection for treatment of refractory diabetic macular edema: a systematic review. *Ophthalmology*; 116: 902–11.

Y Ohkubo, H Kishikawa, E Araki, T Miyata, S Isami, S Motoyoshi, Y Kojima, N Furuyoshi, M Shichiri (1995) Intensive insulin therapy prevents the progression of diabetic microvascular complications in Japanese patients with non-insulin-dependent diabetes mellitus: a randomized prospective 6-year study. *Diabetes Res Clin Pract.* 28:103–117.

Zang, L., Maddison, L. A., & Chen, W. (2018). Zebrafish as a model for obesity and diabetes. *Frontiers in Cell and Developmental Biology*, *6*(AUG), 1–13.

Zeni, L., Norden, A. G. W., Cancarini, G. & Unwin, R. J. A more tubulocentric view of diabetic kidney disease. J. Nephrol. 30, 701–717 (2017).

Ziegler D, Low PA, Litchy WJ, et al. (2011). Efficacy and safety of antioxidant treatment with alpha-lipoic acid over 4 years in diabetic polyneuropathy: the NATHAN 1 trial. *Diabetes Care;* 34:2054– 2060.

Ziegler D, Reljanovic M, Mehnert H, et al. (1999). α-Lipoic acid in the treatment of diabetic polyneuropathy in Germany: current evidence from clinical trials. *Exp Clin Endocrinol Diabetes.*; 107:421–430.

Ziegler D, Movsesyan L, Mankovsky B, et al. (2009). Treatment of symptomatic polyneuropathy with actovegin in type 2 diabetic patients. Diabetes Care; 32:1479–1484.

Ziyadeh, F. N. et al. Long- term prevention of renal insufficiency, excess matrix gene expression, and glomerular mesangial matrix expansion by treatment with monoclonal antitransforming growth factor beta antibody in db/db diabetic mice. *Proc. Natl Acad. Sci.* USA 97, 8015–8020 (2000).

Zhao HJ, Wang S, Cheng H, Zhang MZ, Takahashi T, Fogo AB, Breyer MD, Harris RC. (2006). Endothelial nitric oxide synthase deficiency produces accelerated nephropathy in diabetic mice*. J Am Soc Nephrol* 17: 2664 –2669.

Zheng S, Noonan WT, Metreveli NS, Coventry S, Kralik PM, Carlson EC, Epstein PN. (2004). Development of late-stage diabetic nephropathy in OVE26 diabetic mice. *Diabetes* 53: 3248 –3257.

Zhou, W., Boucher, R. C., Bollig, F., Englert, C., & Hildebrandt, F. (2010). Characterization of mesonephric development and regeneration using transgenic zebrafish. *American Journal of Physiology - Renal Physiology*, *299*(5), 1040–1047.

Zhou W, Hildebrandt F. (2012). Inducible podocyte injury and proteinuria in transgenic zebrafish. *J Am Soc Nephrol* 2012; 23: 1039-1047